HELSINGIN YLIOPISTO
HELSINGFORS UNIVERSITET
UNIVERSITY OF HELSINKI

Master`s thesis

Department of Geosciences and Geography

Solid Earth Geophysics

Analysis, classification and 3D layer modelling of temperature data at Olkiluoto

Elina Koskela

11/2019

Supervisors:

Ilmo Kukkonen (University of Helsinki)

Risto Kiuru (Geofcon)

UNIVERSITY OF HELSINKI
FACULTY OF SCIENCE
DEPARMENT OF GEOSCIENCES AND GEOGRAPHY
PL 64 (Gustaf Hällströmin katu 2)
00014 University of Helsinki

HELSINGIN YLIOPISTO
HELSINGFORS UNIVERSITET
UNIVERSITY OF HELSINKI

Tiedekunta/Osasto Fakultet/Sektion – Faculty	Koulutusohjelma/Utbildningsprogram– Degree programme
Faculty of Science	Master's programme in Geology and Geophysics

Tekijä/Författare – Author
Elina Anniina Koskela

Työn nimi / Arbetets titel – Title
Analysis, classification and 3D layer modelling of temperature data at Olkiluoto

Opintosuunta /Studieinriktning – Study track
Solid Earth Geophysics

Työn laji/Arbetets art – Level	Aika/Datum – Month and year	Sivumäärä/ Sidoantal – Number of pages
Master's thesis	11/2019	102 + 5 appendices

Tiivistelmä/Referat – Abstract

This study investigates temperature data that Posiva Oy has from the Olkiluoto and ONKALO® sites. The aim of the study was to create a unifying data classification for the existing temperature measurements, give an estimate of the initial undisturbed bedrock temperature and temperature gradient and model the temperature profiles in 3D. The thermal related issues, which the repository will undergo once in operating are significant and have fundamental contribution to the evolution of the repository, creating a need in such a study.

Posiva Oy has temperature data obtained with four main methods; Geophysical drillhole loggings, Posiva flow log (PFL) measurements, thermal properties (TERO) measurements and Antares measurements. The data classification was carried out by creating a platform of quality aspects affecting the measurements. The classification was then applied for all the available data by inspecting the measurement specifics of each configuration and by observing the temperature/depth profiles with WellCad software. According to the specifics of each individual measurement the data was classified into three groups: A= the best data, recommended for further use, and which fulfils all quality criteria, B= data that should be used with reservation and which only partly fulfils quality criteria, and C= unusable data.

Only data that showed no major disturbance within the temperature/depth profile (class A or B) were used in this study. All the temperature/depth data was corrected to the true vertical depth. The initial undisturbed average temperature of Olkiluoto bedrock at the deposition depth of 412 m and the temperature gradient, according to the geophysical measurements, PFL measurements (without pumping), TERO measurements and Antares measurements were found to be 10.93 ± 0.09°C and 1.47°C/100m, 10.85 ± 0.02°C and 1.43°C/100m, 10.60 ± 0.08°C and 1.65°C/100m, and 10.75°C and 1.39°C/100m, respectively.

The 3D layer models presented in this study were generated by using Leapfrog Geo software. From the model a 10.5 – 12°C temperature range was obtained for the deposition depth of 412 – 432 m. The models indicated clear temperature anomalies in the volume of the repository. These anomalies showed relationship between the location of the major brittle fault zones (BFZ) of Olkiluoto island. Not all observed anomalies could be explained by a possible cause. Uncertainties within the modelling phase should be taken into consideration in further interpretations. By combining an up-to-date geological model and hydraulic model of the area to the temperature models presented here, a better understanding of the temperature anomalies and a clearer over all understanding of the thermal conditions of the planned disposal location will be achieved.

Based on this study a uniform classification improves the usability of data and leads into a better understanding of the possibilities and weaknesses within it. The initial bedrock temperature and the temperature gradient in Olkiluoto present thermally a relatively uniform formation. The estimates of the initial bedrock temperatures and the temperature gradient presented in this study, endorse previous estimates. Presenting the classified temperature data in 3D format generated good results in the light of thermal dimensioning of Olkiluoto by showing distinct relationships between previously created brittle fault zone (fracture zone) models.

The views and opinions presented here are those of the author, and do not necessarily reflect the views of Posiva.

Avainsanat – Nyckelord – Keywords
Olkiluoto, ONKALO, temperature, temperature gradient, PFL, Geophysical multiparameter logging, TERO, 3D layer model, brittle fault zone

Säilytyspaikka – Förvaringsställe – Where deposited
HELDA- Digital repository of the University of Helsinki

Muita tietoja – Övriga uppgifter – Additional information
61 figures and 8 tables

HELSINGIN YLIOPISTO
HELSINGFORS UNIVERSITET
UNIVERSITY OF HELSINKI

Tiedekunta/Osasto Fakultet/Sektion – Faculty	Koulutusohjelma/Utbildningsprogram– Degree programme	
Matemaattis-luonnontieteellinen tiedekunta	Geologian ja geofysiikan maisteriohjelma	
Tekijä/Författare – Author Elina Anniina Koskela		
Työn nimi / Arbetets titel – Title Olkiluodon kallion lämpötilamittaustiedon luokittelu, analysointi ja mallinnus 3D kerrosmallilla		
Opintosuunta /Studieinriktning – Study track Kiinteän maan geofysiikka		
Työn laji/Arbetets art – Level Pro gradu	Aika/Datum – Month and year 11/2019	Sivumäärä/ Sidoantal – Number of pages 102 + 5 liitettä

Tiivistelmä/Referat – Abstract

Tämä työ tarkastelee Olkiluodon kallion lämpötilamittaustietoa. Tutkimuksen tavoitteena oli luoda laatukriteeristö, jonka perusteella olemassa oleva lämpötilamittaustieto voidaan luokitella ja jaotella. Tavoitteena oli myös antaa arvio kallion häiriintymättömästä lämpötilasta tietyllä syvyydellä, arvioida alueen lämpötilagradienttia sekä mallintaa laatuluokittelun saanutta lämpötilamittaustietoa 3D formaatissa. Tällä työllä pyritään vastaamaan osaltaan haasteisiin, joita Olkiluodon termiset olosuhteet ja ominaisuudet asettavat suunnitellulle ydinjätteen loppusijoitukselle.

Posivan hallussa oleva lämpötilamittaustieto on tuotettu neljällä päämenetelmällä jakautuen geofysikaalisiin kairareikämittauksiin, Posiva-virtausmittauksiin (PFL), termisten ominaisuuksien (TERO) kairareikä-mittauksiin ja Antares-mittaukseen. Laatukriteeristölle luotiin alusta tarkastelemalla jokaista mittausmenetelmää ja kohtia, jotka ovat voineet vaikuttaa mittausten lopputulokseen ja edustavuuteen. Kaikki saatavilla oleva lämpötilamittaustieto tarkastettiin WellCad-ohjelmistolla mahdollisten häiriöiden havaitsemiseksi. Tämän perusteella jokainen yksittäinen mittaus jaettiin kuuluvaksi johonkin seuraavista kolmesta luokasta: A= paras data, joka täyttää kaikki laatukriteeristön vaatimukset ja suositellaan käytettäväksi. B= data, joka vain osittain täyttää asetetut laatukriteeristön vaatimukset ja tulisi käyttää varauksella. C= käyttökelvoton data.

Vain lämpötilamittaustietoa, joka ei osoittanut huomattavia häiriöitä lämpötila/syvyys profiilissa (A tai B luokka) käytettiin tässä tutkimuksessa. Kaikki saatavilla ollut lämpötilamittaustieto vertikaalikorjattiin, jolloin mitatut lämpötilat saatiin vastaamaan todellista syvyyttä kallioperässä. Olkiluodon kallion häiriintymättömäksi lämpötilaksi suunnitellussa sijoitussyvyydessä (412 m) saatiin geofysikaalisten kairareikämittauksien, PFL, TERO ja Antares mittausten perusteella 10.93 ± 0.09°C, 10.85 ± 0.02°C, 10.60 ± 0.08°C ja 10.75°C ja vastaavasti lämpötilagradientille 1.47°C/100m, 1.43°C/100m, 1.65°C/100m ja 1.39°C/100m.

Tässä työssä luotu 3D malli tehtiin Leapfrog Geo ohjelmistolla. Mallinnus osoitti loppusijoitussyvyyden (412 – 432 m) sijaitsevan 10.5 – 12°C lämpötila-alueella. Työssä esitetyt mallit osoittavat useita selkeitä lämpötila-anomalioita. Osan anomalioista voitiin osoittaa liittyvän Olkiluodon suurimpiin havaittuihin rakovyöhykkeisiin, mutta osaa anomalioista ei voitu selittää työssä esitettyjen havaintojen perusteella. Mallinnuksessa havaittiin tiettyjä epävarmuuksia ja nämä tulee ottaa huomioon mahdollisia lisätulkintoja tehdessä. Yhdistämällä tässä työssä esitetyt lämpötilamallit Olkiluodon geologiseen ja hydrauliseen malliin, voidaan mahdollisesti saavuttaa parempi ymmärrys suunnitellun loppusijoitustilan termisestä tilasta.

Tämän tutkimuksen perusteella yhtenäinen laatuluokittelu parantaa mittaustiedon käytettävyyttä. Työssä käytetyn lämpötilamittaustiedon perusteella Olkiluodon kallioperän lämpötila on suhteellisen homogeeninen. Työssä saavutetut tulokset kallion häiriintymättömästä lämpötilasta ja lämpötilagradientista tukevat aiempia tutkimuksia aiheesta. Työssä luotu 3D kerrosmalli osoitti selvää yhteyttä havaittujen anomalioiden ja suurimpien rakovyöhykkeiden välillä.

Tässä työssä esitetyt näkemykset ja mielipiteet ovat kirjoittajan, eivätkä välttämättä vastaa Posivan näkemystä.

Avainsanat – Nyckelord – Keywords
Olkiluoto, ONKALO, lämpötila, lämpötilagradientti, PFL, Geofysikaalinen kairareikä-mittaus, TERO, 3D kerrosmalli, rakovyöhyke

Säilytyspaikka – Förvaringställe – Where deposited
HELDA- Helsingin yliopiston digitaalinen arkisto

Muita tietoja – Övriga uppgifter – Additional information
61 kuvaa ja 8 taulukkoa

Contents

1. INTRODUCTION

The Nuclear Energy Act entered into force in 1994, states that all nuclear waste generated in Finland must be treated, stored and disposed of inside the Finnish borders (Ydinenergialaki, YEL 11.12.1987/990). The act also states that no nuclear waste from other countries shall be imported to Finland (Ydinenergialaki, YEL 11.12.1987/990). To meet the new regulations, a three-stage site selection program was performed to find a possible place for the spent nuclear fuel repository. The stages included 1) The screening study (from 1983 to 1985), covering the whole Finland, 2) The preliminary site investigations (from 1986 to 1992), and 3) detailed site investigations (from 1993 to 2000) which were carried out for four sites.

The aim of the screening study was to find a possible final disposal site for spent nuclear fuel. By eliminating several alternatives through stages two and three, in 1999 the Olkiluoto island in Eurajoki was chosen by Posiva Oy. Soon after, an application for a decision-in-principle from the government was submitted by Posiva Oy. The final disposal site was confirmed in 2000 by the Parliament, with a plan of starting the final disposal of spent nuclear fuel in the 2020's (Posiva Oy 2019a).

The disposal of spent nuclear fuel is an advanced project in the Olkiluoto site, located in Southwestern Finland and operated by Posiva Oy. The Olkiluoto site is an island, separated from the mainland only by narrow strait. The power plants and the repository for low and intermediate waste (VLJ repository) are in the western parts of the island and the underground research facility (ONKALO®) is in the central part of the island.

In order to carry out the planned disposal an extensive research projects on the area of Olkiluoto and more specifically in ONKALO must be conducted. A fundamental property of the spent nuclear fuel is the heat generation and diffusion to the surrounding rock. This leads into the need of recognizing the thermal properties and conditions of the bedrock in the planned disposal location. To model the effects of the diffusion of the heat to the release barriers, and most importantly to the last release barrier, the bedrock, it is important to understand the initial thermal stage of the bedrock. This can be achieved by observing the measurements quantifying the thermal properties and conditions of the area.

The initial temperature of the bedrock has been measured in several different occasion's throughout the research phases of the disposal site. Some of these measurements have specifically concentrated on measuring the temperature, but in most cases the measured temperatures have been a side product of the actual measurements. Now, in the last stages of the research phase, an interest has aroused in order to classify and inspect the existing temperature data that Posiva Oy has on the study location. By creating a unifying classification to all the existing temperature data, more specific values of the bedrock temperature, used in the design phase, can be achieved. Also, a 3D thermal model is needed, which combines the geological and hydrogeological models of the area, and provides new perspective to the thermal situation of the study area.

1.1 The aim of the study

The aim of this study was to carry out a survey on the existing temperature data that Posiva Oy has from the Olkiluoto and ONKALO sites. The temperature data has four main categories: 1) Posiva flow log (PFL) data, 2) temperature data from geophysical measurements 3) thermal properties (TERO) data and 4) Antares data. For all these data sets a data quality classification was carried out, ultimately eliminating unusable data, i.e. data that does not fulfil the criteria set up. All the data was plotted with WellCAD software for further inspections and to ensure easy future access and use of the data sets. This was followed by a 3D temperature model of the Olkiluoto study site, executed with Leapfrog Geo modelling software. Eventually an estimate for a reference temperature at certain depth, i.e. an undisturbed temperature field in Olkiluoto was made along with the estimate of the temperature gradient of the area. This will allow further estimations on how the temperature field in Olkiluoto will progress as a function of time, when the heating effects of the spent nuclear fuel are applied.

1.2 Significance of the thermal studies in Olkiluoto, Finland

The actual underground repository consists of limited space for the final disposal canisters. Therefore, the determination of the shortest usable, yet safe, canister spacing within the repository, is significant. To ensure efficient and economical final solution for

the spent nuclear fuel the knowledge of the thermal properties of the surrounding rock is essential.

When dealing with a high-risk material, such as spent nuclear fuel, all possible risks involved in the premeditated process must be considered. Thermally the most significant risk in the planned disposal is the heat generation from the waste and the subsequent warming of the waste canister. This warming leads to the diffusion of heat to the bentonite buffer and to the surrounding rock, creating a thermally challenging situation to model and control, especially with several canisters.

The heterogeneity of the bedrock, hydrological conditions and the variation of the ventilation air temperature in ONKALO create a variation in the repository temperature. The thermal conditions at the repository are controlled by the surrounding rock, as well as the canister and the buffer elements. It is essential to understand the combined effects that these components create. This can be achieved when all the aspects are first understood individually.

The temperature of the surrounding bedrock is not constant in the time scale of the disposal. It varies through thermal conditions and properties along with the cyclic surface temperature. To guarantee safe disposal the variations need to be studied. To do so, a model of the initial situation of the temperature field in the bedrock of Olkiluoto, before the final disposal, is needed. Currently an initial undisturbed rock temperature of 10.5°C in 420 m is assumed with +1.3 – 1.4°C temperature gradient per 100 m when increasing depth (Ikonen et al. 2018). However, this estimation is done with the current available temperature data without unifying quality classification applied to it, and therefore needs further inspection.

The thermal related issues, which the repository will undergo once in operation are significant and have a fundamental contribution to the evolution of the repository. Therefore, conducting comprehensive and precise thermal studies in Olkiluoto and ONKALO are needed (Ikonen et al. 2018).

1.3 ONKALO: the final disposal site of spent nuclear fuel

The construction of the underground repository, originally an underground research facility, known as ONKALO (Figure 1), started in September 2004 and the planned depth of 455 m was reached in 2018 (Nordbäck and Mattila 2018). ONKALO consists of

- 4986 m long access tunnel
- Vehicle connection tunnels
- Five investigation areas
- Demonstration area
- Technical facilities and,
- Four vertical shafts (a personnel shaft, a canister shaft and two ventilation shafts)

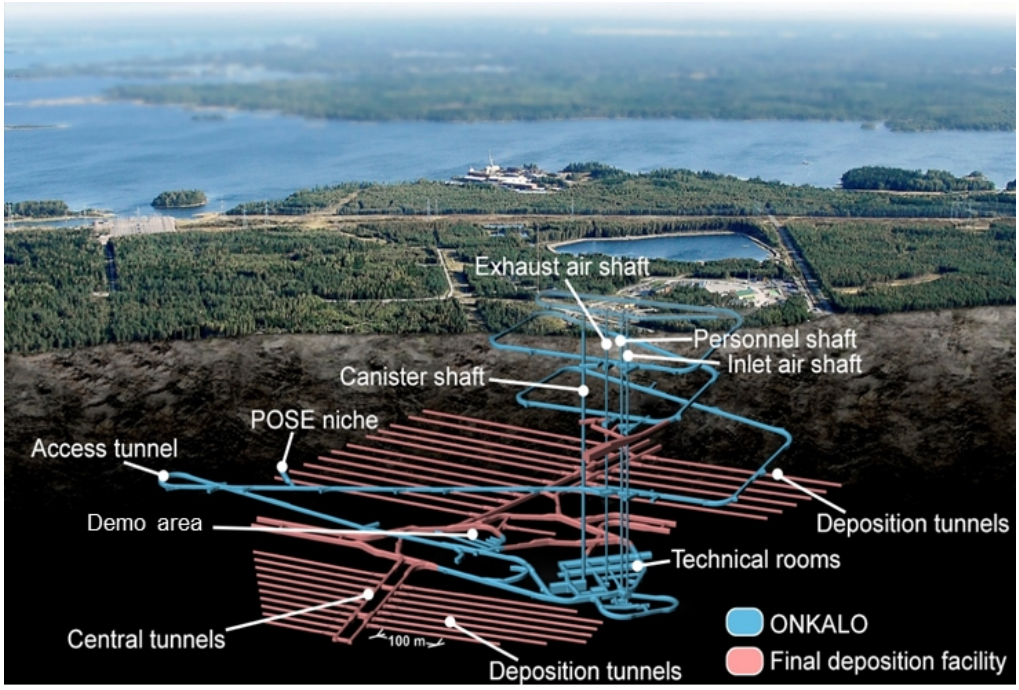

Figure 1. ONKALO research facility (Posiva 2020 figure courtesy of J.Valli)

ONKALO repository is essentially a chain of air-filled tunnels in the bedrock. The air temperature varies periodically due to ventilation and therefore has a periodical influence on the near-tunnel temperature of the bedrock. To understand the effect that the periodical variation of temperature has on the bedrock, the ventilation systems and the surface temperature needs to be understood and known along with the bedrock composition. Tunnel location and the time that the tunnel stays open, also have a direct influence on the bedrock temperature at each specific location.

1.3.1 The disposal method

The final disposal of spent nuclear fuel is based on the use of multiple release barriers which include, the physical state of the fuel, the disposal canister, the bentonite buffer, the backfilling of the tunnels and the surrounding bedrock (Figure 2). The designed disposal concept, planned to be carried out in Olkiluoto, was originally developed in Sweden by Svensk Kärnbränslehantering AB (SKB) and the concept is known as the KBS-3 (Palomäki and Ristimäki 2013).

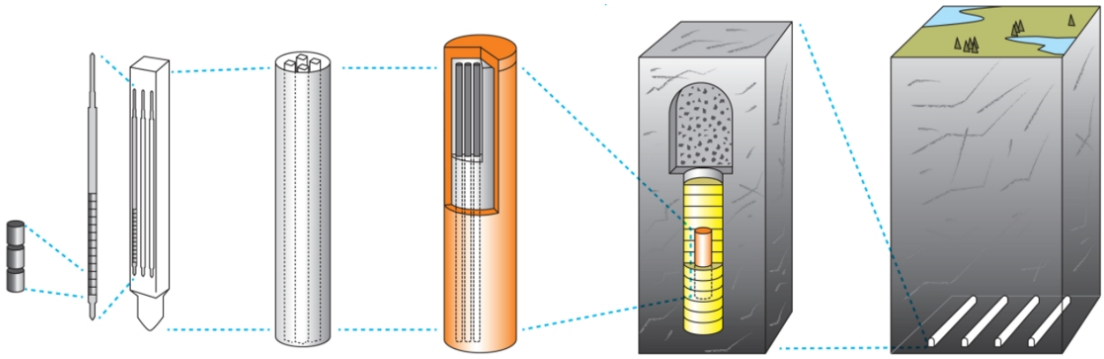

Figure 2. Designed multiple release barriers. From the left: physical state of the fuel (pellets), physical state of the fuel (the pellet rod), inner capsule, outer capsule, the bentonite buffer and the backfilling of the tunnels and the surrounding bedrock (Posiva Oy 2019b).

Out of all the barriers, bentonite is the most sensitive to the surrounding thermal conditions (Ikonen et al. 2018). Bentonite is a temperature-sensitive mixture of clay minerals, comprising mostly of montmorillonite, and this needs to be considered for it to be used as a buffer. When bentonite is heated above 100°C, illititization of the bentonite starts, resulting in the swelling properties to be compromised (Kiviranta et al. 2018). The heat production of the spent fuel can be estimated (Ikonen et al. 2018). Through this the diffusion of heat to the bentonite buffer from the disposal canister can be estimated. After the installation of the bentonite buffer hydraulically non-saturated conditions are unlikely to exist (Ikonen et al. 2018). An assumption of pre-wetting of the outer pellet gap and the prevailing of the elevated saturation is done to the base calculations considering the thermal dimensioning for Olkiluoto. When bentonite is hydraulically saturated it loses its ability to tolerate heat. Due to these properties of the bentonite, a maximum limit for temperature of the canister-buffer interface, which cannot be exceeded or withstood for

extended periods, needs to be set (Ikonen et al. 2018). Initial results for the nominal maximum temperature were obtained by Ikonen and Raiko (2012). However, due to changes in the constructional details and parameters within the disposal repository, new nominal maximum temperature was obtained by Ikonen et al. (2018). The nominal maximum temperature for canister-bentonite interface is +100°C. However, the model includes several uncertainties, including:

- variation at the thermal parameters
- geometry deviations within the design
- simplifications done in the modelling phase

These uncertainties require the nominal maximum temperature to be set to 95°C. The specifics of the 5°C safety margin can be observed from Ikonen et al. (2018) Section 1.2. The decay heat power plays the most significant role on the temperature control. Thermal conductivity of bedrock is seen to have the second greatest effect (Ikonen et al. 2018).

The bentonite barrier is surrounded by bedrock, which works as the final release barrier for the radionuclides. Initially, the surrounding bedrock has an undisturbed temperature field, which is created by the in-situ rock properties and the regional thermal conditions. As the diffusion of heat from the waste to the surrounding elements, including the bedrock, cannot be prevented this undisturbed temperature field is subject to change as well. Ultimately, in very long term the heat is also conducted to the surrounding atmosphere (Ikonen et al. 2018). The properties and conditions of the bedrock cannot be modified. Therefore, a comprehensive understanding of the initial conditions of the last release barrier, the bedrock, is needed.

1.4 Geological setting of Olkiluoto, Finland

The bedrock of Finland is part of the Precambrian Fennoscandian shield, which covers land areas from Sweden, Norway and Russia among Finland (Luukas et al. 2017). The oldest parts of the Finnish bedrock are found in the North-eastern Finland and are dated to be 3.1 – 2.5 Ga old (Figure 3). This area is known as the Archean basement complex and it consists mainly of gneiss and migmatites. The youngest rocks of the Finnish bedrock are found in the in the North-western shores of the Gulf of Bothnia and in the Satakunta region. These formations are Jotnian sandstones and are dated to be 1.4 – 1.3

Ga old (Figure 3) and are cut by even younger 1.27 – 1.25 Ga (Figure 3) old Postjotnian olivine diabase dykes and sills. Also, few younger dykes (1.1 – 1.0 Ga (Figure 3)) are found in Northern Finland. However, the Finnish bedrock mainly consists of igneous rocks and Paleoproterozoic metamorphic rocks, which belong to the Svecofennian Domain, continuing from central Lapland to Southwest parts of Finland (Luukas et al. 2017).

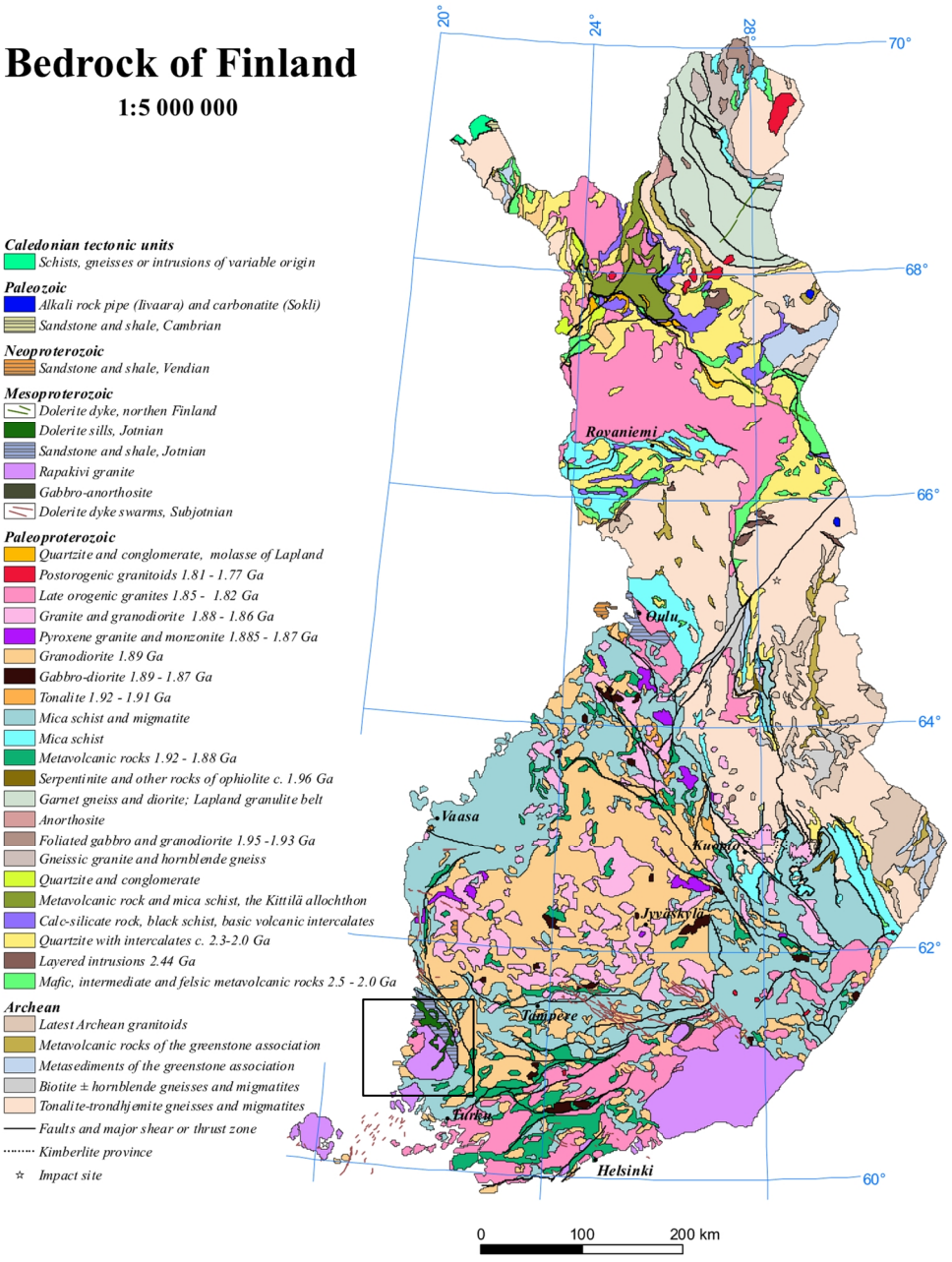

Figure 3. Generalized bedrock map of Finland. Black box shows the approximate location of Satakunta region (GTK 2019).

The study area of Olkiluoto is located in Southwest Finland in the region of Satakunta (Figure 3). The region is bordered by the Bothnian sea in the west and includes parts of the costal archipelago. However, most of the region's areal coverage is mainland. The study area of Olkiluoto island is located in the middle of Satakunta, in the municipality of Eurajoki between the cities of Rauma and Pori. The structural and geological evolution of Satakunta is documented by the Finnish geological survey (GTK) and the information is combined into working reports and POSIVA reports (e.g. Paulamäki et al. 2002 and Aaltonen et al. 2010). The rocks in Satakunta are divided into pelitic migmatite (mica gneisses with quartz-feldspar-rich and biotite-rich layers) belt, psammitic migmatite (mainly migmatized gneisses) belt, rapakivi granites, diabase dykes and sills (Sub- and Postjotnian) and Satakunta sandstones (Paulamäki et al. 2002).

Geology of Olkiluoto was summarized by Aaltonen et al. (2016). Olkiluoto's rock types can be divided into two main categories: 1) migmatic gneisses, and 2) granitic pegmatoids and diabase dykes, the first group being the dominant one (Figure 4). The migmatitic gneisses of the area can be divided into three subgroups: 1) veined gneisses, 2) stromatic (Tonalite-granodioritic-granitic) gneisses and 3) diatexitic gneisses based on the variations in the migmatitic structure (Aaltonen et al. 2010). The acquired geological information of the area heavily lies on the observations done from the deep drillholes (Figure 5), the "B" drillholes and the drillholes located in ONKALO. The so-called B drillholes are considerably shorter, when compared to the deep drillholes, only reaching in average approximately 30 m depth. They are located next to the deep drillholes and are labelled accordingly. The main purpose for the B drillholes is to provided information of the A drillhole which is covered by a casing of approximately 30 m.

Bedrock of Olkiluoto has been subject to brittle deformation and hydrothermal alteration which has occurred in several different phases (Nordbäck and Mattila 2018). These transformations are modelled as several individual brittle fault zones (BFZ). Brittle fault zones or fracture zones, are defined as " a zone of incohesive or low-cohesive fault gouge, fault breccia and/or crushed rock, accompanied by slickensided fractures, "damage zones", wall-rock alteration, and evidence of displacement, indicating lateral movement of the country rock on one side relative to the other side of the zone" (Nordbäck and Mattila 2018). Location of these BFZ zones have been identified for example with

geological mapping of the study area and geophysical drillhole loggings. Several hydraulic zones (HZ) have been identified at the study area. These zones indicate the connections between the major water flows and leakages. Some correlation between the brittle fault zones and the hydraulic zones can be identified. However, it is important to understand that BF zones and hydraulic zones still present two completely individual models of the area.

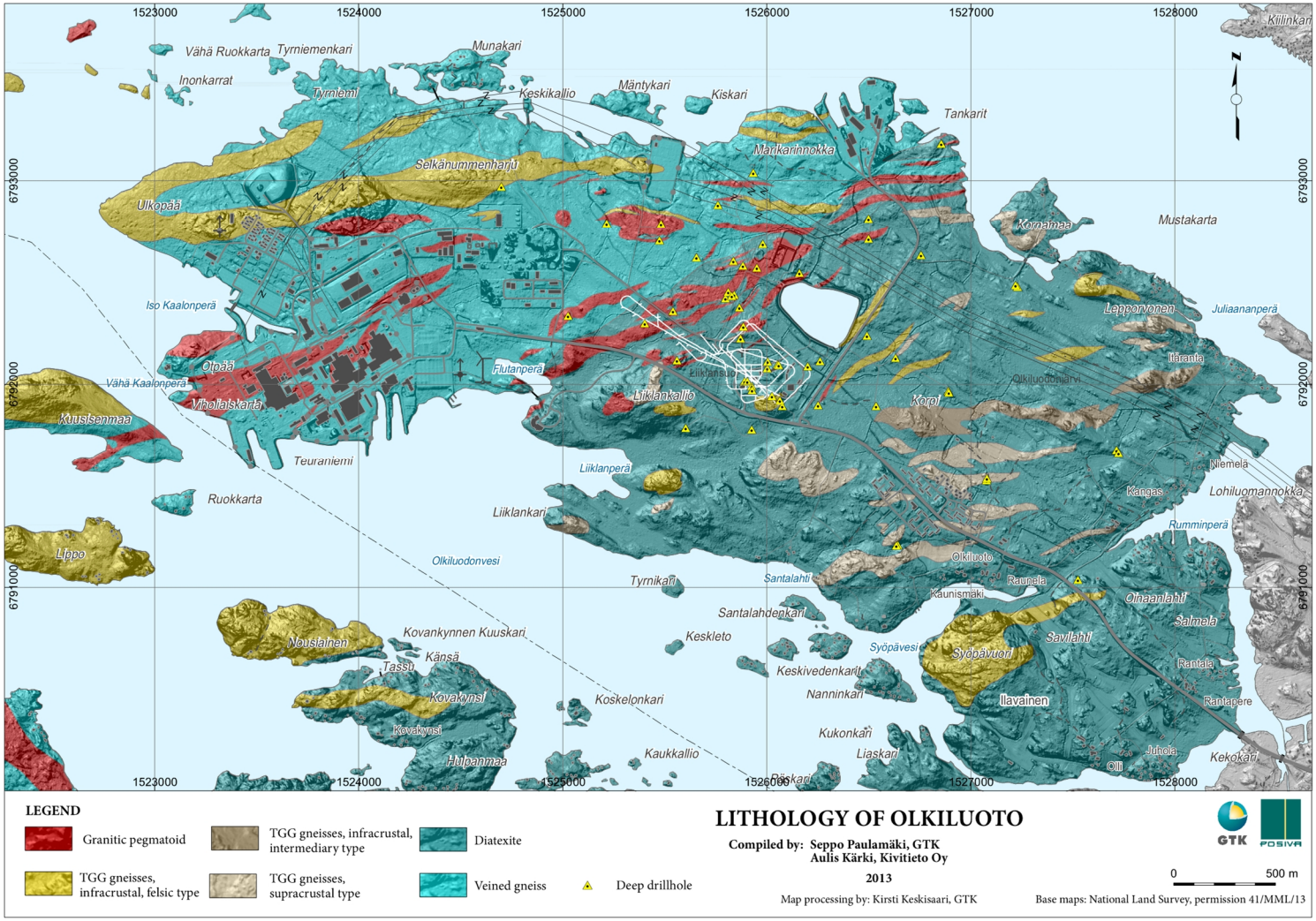

Figure 4. Lithology of Olkiluoto (Aaltonen et al. 2016).

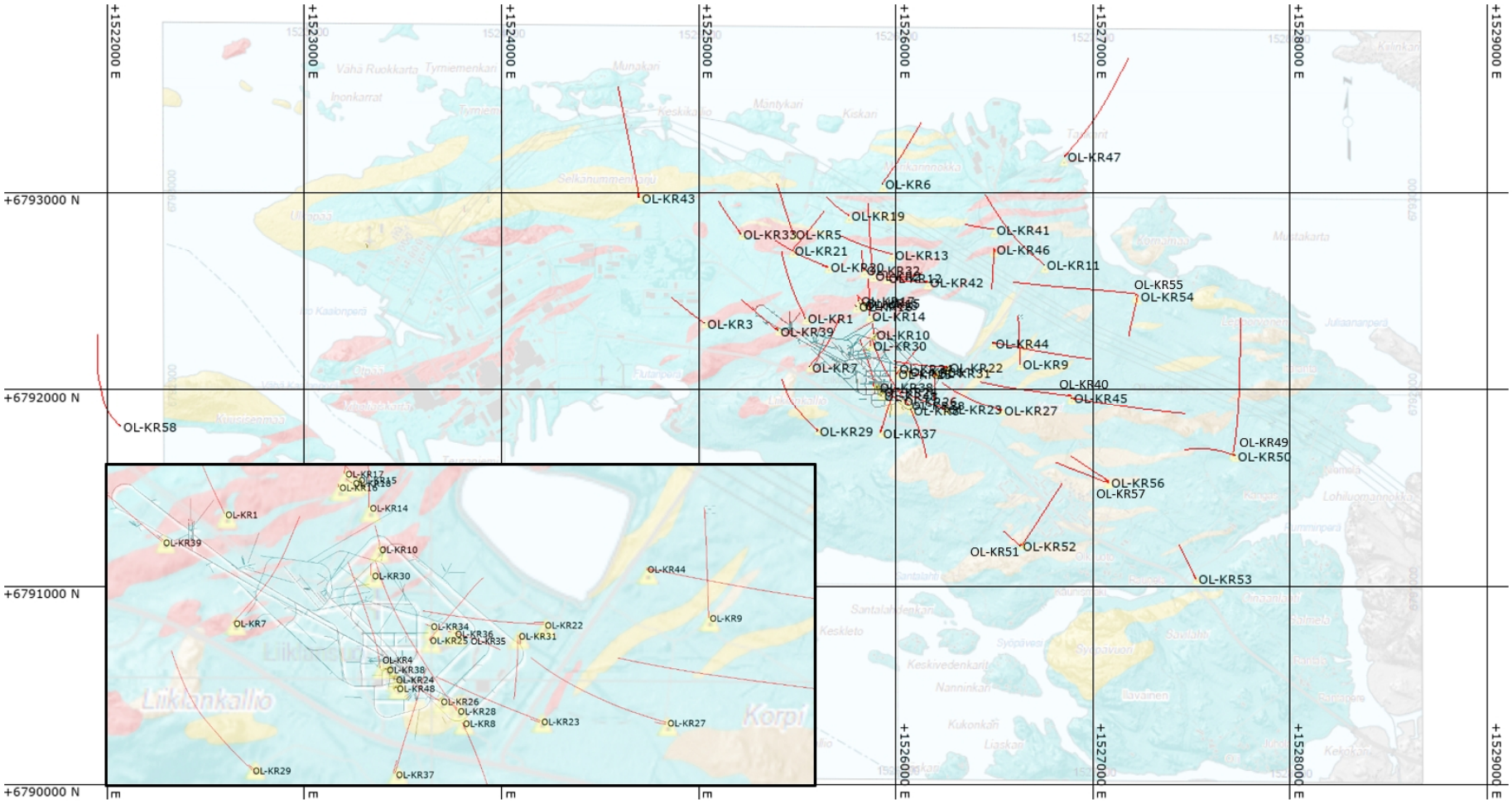

Figure 5. Adjacent deep drillholes and their projected directions in Olkiluoto. B drillholes are always located right next to the same numbered deep drillhole. Base map by Aaltonen et al. (2016).

1.5 Thermal properties of Olkiluoto rock types

A study conducted by Kukkonen et al. (2014) found that the migmatic gneisses of Olkiluoto can thermally be divided into conductive neosome and less conductive paleosome parts. The neosome part is granitic material and is mostly comprised of light minerals such as quartz and feldspar whereas the paleosome part typify an older material and is mostly composed of more mafic minerals such as biotite and hornblende (Kukkonen et al. 2014). The elements which are met within the paleosome part are seen to be older whereas the material composing the neosome part were emplaced in the rock relatively late while being partially in molten state.

Granitic pegmatoids have distinctly different petrophysical properties when compared to migmatite gneisses (Aaltonen et al. 2009). Ultimately this is due to the rock's mineral composition. The thermal properties of Olkiluoto rock types have been studied and summarized by Kukkonen et al. (2000), Kukkonen et al. (2011) and most recently in Kukkonen (2015) and are listed in Table 1. The list of the drillholes used for sampling can been seen in Kukkonen (2015). Variations within in the thermal properties due to the varying rock composition create a challenge to determine the in-situ thermal properties of the bedrock in Olkiluoto.

Table 1. Table after Kukkonen (2015) summary of thermal properties of rocks in Olkiluoto in 25 °C. Std = standard deviation; N = number of samples; Rock types: VGN, veined gneiss; TGG, tonalitic-granodioritic-granitic gneiss; DGN, diatexitic gneiss; MGN, mica gneiss; PGR, granitic pegmatoid; KFP, potassium-feldspar porphyry; QGN, quartzitic gneiss. For data corrected for 60°C and 100°C, see Kukkonen (2015).

Rock type abbreviation	Density, ρ [kgm^{-3}]	Std	N	Thermal conductivity, λ [W m^{-1} K^{-1}]	Std	N	Diffusivity, κ *10^{6} [m^{2}s^{-1}]	Std	N	Specific heat capacity, c [Jkg^{-1}K^{-1}]	Std	N
VGN	2740	40	301	2.74	0.52	300	1.31	0.25	231	732	30	233
TGG	2708	38	65	2.70	0.42	67	1.28	0.17	32	709	26	33
DGN	2728	51	89	2.73	0.61	89	1.35	0.32	86	740	25	86
MGN	2781	71	35	2.39	0.43	35	1.17	0.22	35	739	26	35
PGR	2635	42	158	3.0	0.48	158	1.57	0.27	130	714	29	130
KFP	2729	n.a.	1	2.78	n.a.	1	1.48	n.a.	1	687	n.a.	1
QGN	2766	n.a.	2	2.49	n.a.	2	1.01	n.a.	1	714	n.a.	1
All samples	2712	64	651	2.77	0.53	652	1.37	0.29	516	728	30	519

However, when thermal dimensioning the Olkiluoto site it might be beneficial to use average weighted values for the thermal properties. In this way the actual rock quantities of the study area are taken into account (Ikonen et al. 2018). However, this leads to an assumption that all rock types are located everywhere in the same proportions in Olkiluoto, which is not the case. For example, the average weighted thermal conductivity, which takes into account the latest geological model by Aaltonen et al. (2016) is 2.57 W/ mK at 60°C (Ikonen et al. 2018) and the average of laboratory samples is 2.71 W/ mK at 60°C (Kukkonen 2015).

Lithosphere thickness and the local heat flow are both important factors within geothermal studies. Studies done for lithospheric thickness in the Fennoscandian shield have implied that the Fennoscandian shield lithosphere appears relatively thick, except in areas of Southern Norway and Danish and German basins where the lithosphere appears relatively thin (Balling 2013). On continental crust the highest heat flow values are obtained in regions with recent or active tectonic activity, whereas the lowest heat flow values are measured in regions of old and thick crust, such as the region of the Precambrian shield where the study area of Olkiluoto is located (Fowler 2005). A study conducted by Pollack et al. (1993) presented a large global dataset and yielded values of 65 ± 1.6 mWm^{-2}, 101 ± 2.2 mWm^{-2} and 87 ± 2.0 mWm^{-2} for continental, oceanic and global heat flow, respectively.

A study conducted by Kukkonen et al. (2015) calculated heat flow values by using temperature data obtained with Antares measurement configuration on drillhole OL-KR56. The study showed heat flow values of 32.6 – 42.7 mWm^{-2} calculated from the data in 100 m intervals at depths greater than 100 m. Thermal conductivity was measured with 5 m intervals from drill core specimens. Variation in the heat flow was greater than the determined errors and was seen partly to be due to the small depth intervals and variations in the thermal conductivity. These result show values for only one drillhole in the Olkiluoto study site. However, as the study area is located on the thick and stable shield area, the results can be taken as indicative when trying to comprehend the order of magnitude that the heat flow has in Olkiluoto.

2. HEAT TRANSFER IN EARTH'S CRUST

Earth's interior is significantly hotter than the surface. As direct observations are limited approximately to the top 12 km of the crust, the global models on internal thermal structure are based on the data from seismic methods and density models supporting them (Beardsmore and Cull 2001). To gain direct information of composition and physical properties of a small region, mantle xenoliths are used, where available. With these direct and indirect methods, an increasing temperature profile with increasing depth for Earth is obtained. Heat generation, heat transfer, the measuring techniques of individual physical quantity describing the heat transfer and the possible mathematical applications to model the heat transfer in Earth's crust are all discussed in the following subsections.

2.1 Heat generation

The Earth's internal heat results from primordial sources and unevenly distributed secondary processes. The primordial sources are associated with the formation of the Earth itself while the secondary processes are the processes generating heat internally (Beardsmore and Cull 2001). Radioactive isotopic decay, exothermic metamorphic and diagenetic processes and friction due to intraplate strain and plate motion are considered to be the main crustal heat sources (Beardsmore and Cull 2001). The magnitude of each source is relative and dependent on the geographic location (Beardsmore and Cull 2001). However, even when this is taken into consideration the radiogenic heat sources are seen to be the most dominant of the crustal heat sources (Jaupart and Mareschal 2011). The major heat sources in rocks are the decay series of uranium (^{238}U and ^{235}U), thorium (^{232}Th) and potassium (^{40}K). Other heat producing elements, such as ^{87}Rb and ^{147}Sm, are less abundant in rocks and are considered insignificant in crustal geothermal studies (Jaupart and Mareschal 2011).

2.2 Heat transfer mechanisms

Heat is transported by radiation, conduction, convection and advection (Figure 6). In radiation, heat moves by electromagnetic radiation, either in the form of waves or particles. In conduction, the heat moves by atomic or molecular interaction within the material. In convection the particles themselves move, transporting heat. Advection is a form of a convection and in geological sense it is considered to be associated with uplift of hot regions or isostatic rebound, i.e. heat that is lifted up with the rocks (Fowler 2005). Out of these, conduction represents the most dominant in the means of heat transport in oceanic and continental lithosphere and in the inner core (Fowler 2005).

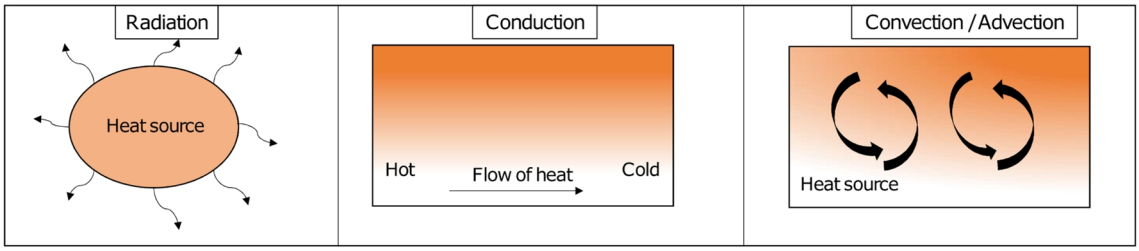

Figure 6. Heat transfer mechanisms after Fowler (2005).

2.3 Fourier's laws of heat conduction

Heat flows from hot regions to cold regions through conduction. The phenomenon is described by Fourier's 1st law of heat conduction (Equation 1).

$$Q_0 = Q_d + \int A(z)\partial z = \lambda_d \left[\frac{\partial T}{\partial z}\right]_d + \int A(z)\partial z \qquad 1$$

where Q_0= surface heat flow [Wm^{-2}], Q_d = heat flow [Wm^{-2}], $\int A(z)\partial z$ = volumetric heat generation from the surface to d, λ_d= thermal conductivity [W/mK] at certain depth and $\left[\frac{\partial T}{\partial z}\right]$ = temperature gradient [°C/m] at certain depth. For Q_d Equation 1 can be written as

$$Q_d = \lambda_d \left[\frac{\partial T}{\partial z}\right]_d \quad (2)$$

When a limit of $\partial z \rightarrow 0$ is set with an assumption of that the temperature increases downwards (positive z direction) and that the heat flows from hot regions to cold regions i.e. upwards (negative z direction), Equation 2 is expressed as

$$Q_d(z) = -\lambda_d \left[\frac{\partial T}{\partial z}\right]_d \quad (3)$$

Where *d* refers to the directions. Surface heat generation, A_0 [Wm^{-3}], and surface heat flow, Q_o[Wm^{-2}], have a linear relationship (Lachenbruch 1968 and Birch et al. 1968) (Equation 4) and can be expressed as

$$A_0 = \frac{Q_o - Q_d}{D} \quad (4)$$

Where Q_o= surface heat flow, Q_d= constant heat flow from the mantle and *D* = thickness of the heat producing layer [m]. Fourier's 2nd law of heat conduction (Equation 5) describes how the temperature varies as a function of time and depth. In one dimension it is expressed as

$$\frac{\partial T}{\partial t} = \frac{\lambda}{\rho c}\frac{\partial^2 T}{\partial z^2} + \frac{A}{\rho c} \quad (5)$$

Where *A* is heat generation, λ is thermal conductivity, ρ is density, c is specific heat capacity, *T* is temperature and *t* is time. Thermal conductivity, specific heat capacity and thermal diffusivity are the three fundamental thermal properties in geothermal studies. The term $\frac{\lambda}{\rho c}$ describes the measured in situ parameters and is known as the thermal diffusivity, κ. If the temperature is a function of *x*, *y* and *z* directions, Equation 5 can be modified into three-dimensions (Equation 6) using any coordinate system (here Cartesian).

$$\frac{\partial T}{\partial t} = \frac{\lambda}{\rho c}\left(\frac{\partial^2 T}{\partial x^2} + \frac{\partial^2 T}{\partial y^2} + \frac{\partial^2 T}{\partial z^2}\right) + \frac{A}{\rho c} \quad (6)$$

$$\rightarrow$$

$$\frac{\partial T}{\partial t} = \frac{\lambda}{\rho c} \nabla^2 T + \frac{A}{\rho c}$$

Where the geometric component $(\frac{\partial^2 T}{\partial x^2} + \frac{\partial^2 T}{\partial y^2} + \frac{\partial^2 T}{\partial z^2})$ can be described with the definition of del.

2.4 Thermal properties of rocks and their measurement applications

2.4.1 Thermal conductivity

Thermal conductivity, λ, characterizes the heat flow Q_d as a result of temperature gradient (Equation 3) (Schön 2015b). I.e. it represents the ability of a substance to transfer heat through it by conduction and is the function of the geometric relationships and conductivities of present minerals and fluids (Beardsmore and Cull 2001). Thus, inspecting rock formations on individual crystal level does not give information on the mean conductivity of in-situ rock formations. Therefore, three main mixing models describing the geometry of such rock formation need to be considered (Beardsmore and Cull 2001). Arithmetic mean describes a situation where the conductors are parallel (Equation 7 and Figure 7), harmonic mean describes a situation where conductors are perpendicular (Equation 8 and Figure 7) and geometric mean describes a situation where conductors are randomly oriented (Equation 9 and Figure 7).

$$\lambda_{ar} = \sum n_i \lambda_i \quad (7)$$

$$\lambda_{har} = 1 / \sum n_i / \lambda_i \quad (8)$$

$$\lambda_{geo} = \prod \lambda_i^{n_i} \quad (9)$$

Where n_i refers to the volume proportion of the i^{th} mineral component and λ_i is the thermal conductivity of the component i.

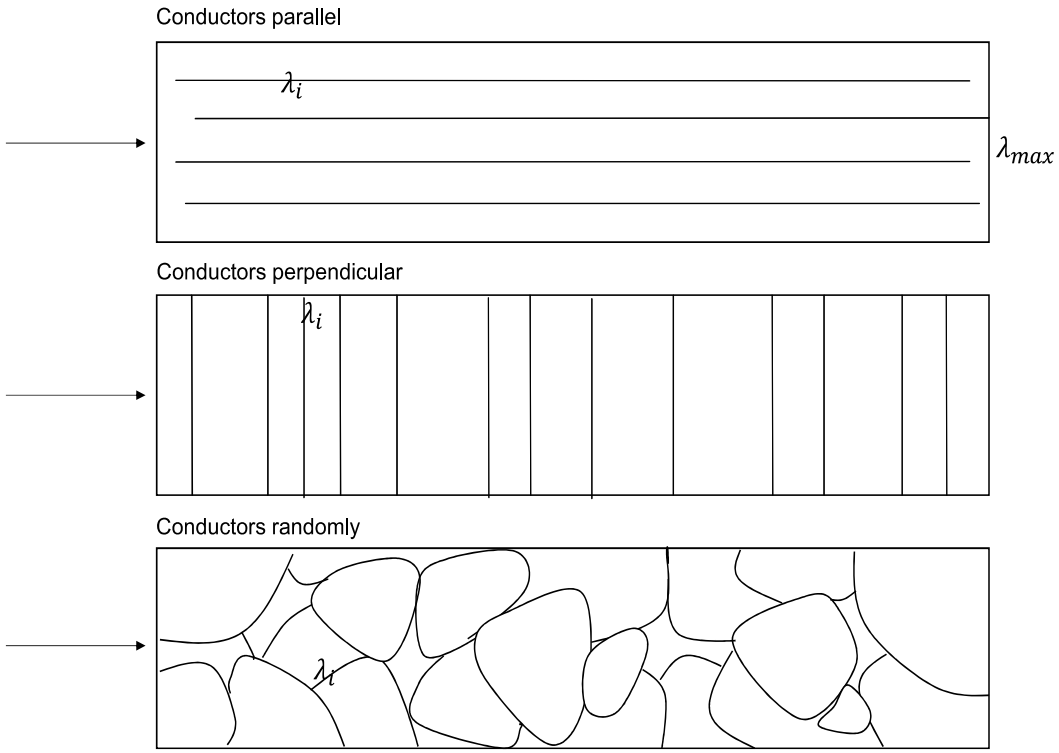

Figure 7. Conductor texture models after Beardsmore and Cull (2001).

As thermal conductivity depends on the geometric relationships occurring in the study region, the importance of modelling and sampling of each lithology section within the study region is emphasized. If the conductivity of a granular matrix is defined along with porosity, a bulk conductivity can be determined (Beardsmore and Cull 2001).

Thermal conductivity depends on the temperature and therefore is not constant (Carslaw and Jaeger 1990). However, if the range of temperature is limited, the change in λ can be neglected (Carslaw and Jaeger 1990). Main methods to measure rock conductivity are the steady-state method and the transient method. The steady-state method usually uses a divided-bar apparatus whereas the most commonly used transient tool is a line-source needle probe (Figure 8) (Beardsmore and Cull 2001).

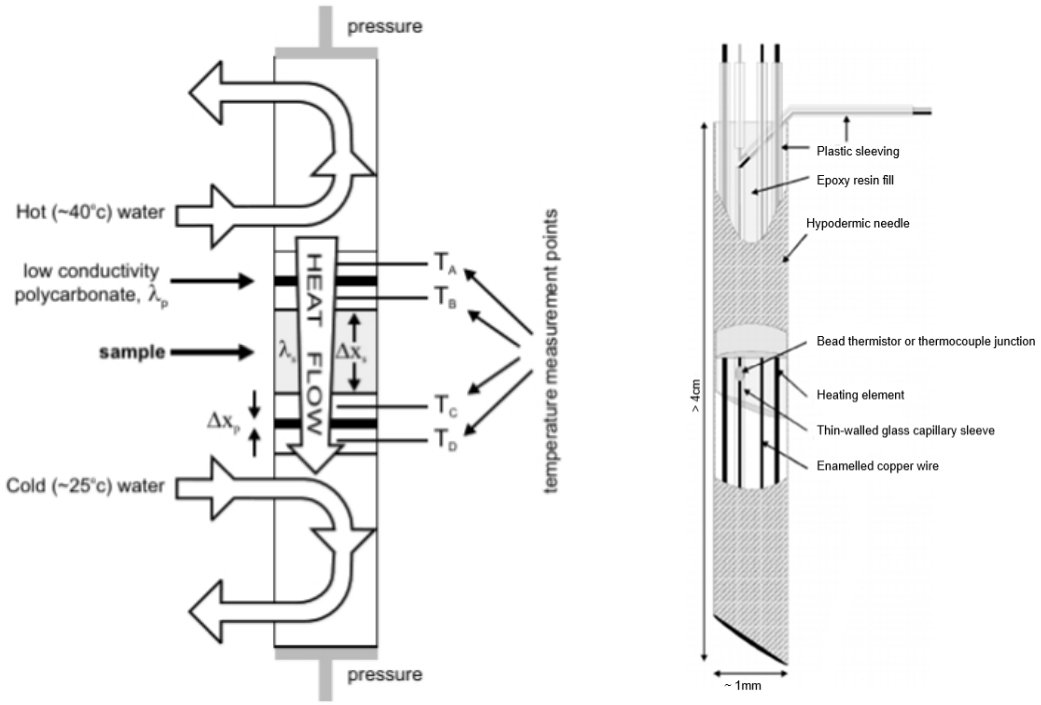

Figure 8. Left: Divided-bar apparatus. Right: line-source needle probe. After Beardsmore and Cull (2001).

2.4.2 Specific heat capacity

Specific heat capacity or unit mass heat capacity, c, is the amount of energy required to raise the temperature of one unit mass of the substance by one degree, i.e. the capability of a material to store heat. Specific heat capacity (Equation 10) can be defined through heat capacity, C [JK^{-1}], density, ρ [kgm^{-3}], and the volume of the body, V [m^3]. The unit of the specific heat capacity is $Jkg^{-1}K^{-1} = m^2s^{-2}K^{-1}$.

$$c = \frac{C}{\rho V} = \frac{E}{m\Delta T} \qquad 10$$

Where m is mass, ΔT is the change in temperature and E is energy. Specific heat capacity is used in several geothermal applications, such as temperature predictions for tunnels, heat extraction and storage in the bedrock and thermal effects of spent nuclear fuel (Schön 2015b). The measurements of specific heat capacity have traditionally required expensive and time-consuming measurement procedures (Schärli and Rybach 2001). Commonly used measurement technique for borehole cuttings is known as the ‘drop method’ or the calorimetric method. The principle of the method is to mix two substances with different

measurable temperatures. To carry out the measurements, the weight of both substances and specific heat capacity of one of the substances is required (Schärli and Rybach 2001).

2.4.3 Density

Density [kgm^{-3}], also known as the volumetric mass density is the quotient of mass, m and volume, V (Equation 11). The constituent elements of a mineral along with the internal structure and boundary variations control the density of a mineral (Schön 2015a).

$$\rho = \frac{m}{V} \qquad 11$$

The density of a rock varies through its components, and therefore yields different definitions within the density. Bulk density (ρ) is the mean density of a rock (e.g. density of a gneiss) including pore space. Density of individual (ρ_i) is the individual density of a rock component (e.g. feldspar). Density of a matrix (ρ_{ma}) or grain density is the density of the mixture of minerals, not including the pore space. Finally, the density of fluid (ρ_f) is the density of a pore or fracture fluid such as water. (Schön 2015a). Bulk density of a rock sample can be defined when the weight of the sample in air and in water are known, along with the density of the water in certain temperature (Archimedean principle). In order to get plausible results, the calculations are compared to known densities of standard laboratory samples.

2.4.4 Thermal expansion

Thermal expansion occurs when temperature changes, resulting in a change in the material's length (linear expansion), area (areal expansion) and volume (volumetric expansion). The phenomenon occurs due to a change in the matters kinetic energy, resulting in larger average separation between molecules (Tro 2013). For solids the change in shape is described through a linear coefficient of thermal expansion, α, varying with material (Huotari and Kukkonen 2004). Linear expansion is shown in Equation 12, whereas for areal expansion the change in area is twice the linear expansion and volumetric expansion the change in volume is thrice the linear expansion.

$$\Delta l = l_0 \alpha \Delta T \quad (12)$$

Where l_0 is the original length, α is the linear coefficient of thermal expansion depending on the material and ΔT is the change in temperature.

Texture, constituent minerals, relative proportions of different minerals, mineral orientations, pore space, pressure and temperature are all properties which influence the thermal expansion of a rock (Huotari and Kukkonen 2004). As thermal expansion is a sum of several rock properties, the scale of the influence on region or formation vary. Huotari and Kukkonen (2004) summarize the most commonly used measuring methods of linear expansion. The most suitable methods were found to be dilatometers (measures the length change during the temperature change) and strain gauge (measures the strain in certain direction and point with varying strain measurement sensors) systems.

2.4.5 Thermal diffusivity

Thermal diffusivity, κ [m^2s^{-1}], is a parameter that expresses the ability of a material to lose heat by conduction, i.e. it is the parameter which controls the time-dependent distribution of the temperature (Schön 2015b). Thermal diffusivity (Equation 13) is expressed through thermal conductivity λ [m^2s^{-1}], specific heat capacity c [J $kg^{-1}K^{-1}$] (Equation 10) and density ρ [kgm^{-3}] (Equation 11), the three fundamental geothermal properties described above.

$$\kappa = \frac{\lambda}{\rho c} \quad (13)$$

2.4.6 Thermal property measurements in Olkiluoto

Measurements for the thermal properties seen in Table 1 by Kukkonen (2015) for Olkiluoto rocks were conducted between 1994 and 2015 in the petrophysical laboratory of the Geological survey of Finland (GTK). The measurement for the thermal conductivity were carried out with the divided bar method (Figure 8). The apparatus was

built at GTK and differed from the apparatus seen in Figure 8 by using quartz disks as standards instead of polycarbonate disks (Kukkonen 2015). The average thermal conductivity in Olkiluoto at 25°C is 2.77 W/mK (Table 1). The specific heat capacity measurements were carried out with the calorimetric method resulting in average specific heat capacity of 728 $Jkg^{-1}K^{-1}$ (Table 1). The bulk density measurements were carried out with method using the Archimedean principle resulting in average bulk density of 2712 kg m^{-3}(Table 1). The thermal diffusivity was calculated by using the obtained measured values of the thermal conductivity, specific heat capacity and the bulk density, resulting in average thermal diffusivity of $1.37 \cdot 10^{-6}$ m^2s^{-1} (Table 1). For the thermal expansion, Huotari and Kukkonen (2004) found the thermal expansion coefficient (α) to be 7^{-10} 10^{-6}/°C for Olkiluoto veined and tonalitic-granodioritic-granitic gneiss (previously referred as mica gneiss in Posiva working reports) when the temperatures are between 20°C – 60°C.

2.5 Quantitative heat transfer

Temperature of a bedrock is affected by internal and external thermal conditions and properties. Internal thermal regime of the Earth can be defined and modelled through the concepts of temperature gradient, heat flow and heat budget. In Olkiluoto the internal temperature conditions have been previously studied through temperature gradient and heat flow calculations (Kukkonen et al. 2015).

2.5.1 Temperature gradient

Temperature gradient (Equation 14) is a vector quantity which depends on the distribution of temperature, ultimately in three dimensions and can be expressed as

$$\Delta T = \frac{\partial T}{\partial x}\,\boldsymbol{i} + \frac{\partial T}{\partial y}\boldsymbol{j} + \frac{\partial T}{\partial z}\,\boldsymbol{k} \qquad 14$$

Where T is the temperature, and **i, j** and **k** are the unit vectors along the *x*, *y* and *z* axes. However, the temperature gradient can be reduced into one dimension (Equation 15) by assuming vertical maximum gradient within the upper crust (Beardsmore and Cull 2001).

$$\Delta T = \frac{\partial T}{\partial z}\,\boldsymbol{k} \qquad 15$$

Temperature gradient can be defined through direct measurement methods and indirect temperature indicators. Direct measuring techniques involve a measuring device which is lowered down to desired measurement location in e.g. drillhole or mineshaft. When such measurements are conducted, it is important to consider, what does the device actually measure, for example the temperature of the surrounding rock, the temperature of the drillhole fluid or the temperature of the measuring apparatus. The main indirect temperature indicators used are mantle xenoliths, curie depth and upper mantle resistivity logs (Beardsmore and Cull 2001). These are used specifically to constrain deep temperature gradients in or below the crust, at depths inaccessible by direct methods.

2.5.2 Heat flow

Present day heat flow (Equation 16) is defined through heat generation, temperature gradient and thermal conductivity and it follows Fourier's law of conduction (Equation 1). Geotherms are used to calculate temperature-depth profiles within Earth. When T=0 at z=0 the temperature within a column is given by

$$T = \frac{Q_0}{\lambda}\, z - \frac{A}{2\lambda} z^2 + T_n \qquad 16$$

Where Q_0= surface heat flow [Wm^{-2}], λ= conductivity [Wm^{-1}], A = heat generation (heat production rate) [Wm^{-3}], T_n = Temperature [°C] at the upper boundary of each possible layer and z =thickness of each possible layer [m]. The geotherm can be applied to have several layers, with varying constants. Erosion and sedimentation have rapid influence on geotherm, and therefore need to be taken in consideration when geotherms are modelled (Beardsmore and Cull 2001).

2.5.3 Heat budget

Heat budget refers to the heat loss and heat gain that Earth experiences on a daily basis. Models of "cooling Earth" focus on understanding the balance between cooling

mechanisms and the heat sources. However, it is important to understand that heat budget and heat transfer mechanisms are two individual concepts (Jaupart and Mareschal 2011). Regardless of being completely independent issues, both heat gain and loss, can have same heat transfer mechanisms. Plate tectonics are seen as the main consequence of the cooling Earth (Fowler 2005) and mantle convection as the main heat transfer mechanism in the Earth (Jaupart and Mareschal 2011). For global heat loss Pollack et al. (1993) obtained a value of $44.2 \pm 1 \cdot 10^{12}$ W, out of which 71 % occurs through the oceanic lithosphere.

3. OLKILUOTO TEMPERATURE DATA

The temperature data that Posiva Oy has from Olkiluoto and ONKALO sites from in-situ measurements in drillholes can be divided into four main categories: 1) The Posiva flow log (PFL) data, 2) temperature data from geophysical measurements, 3) TERO data and 4) Antares data. The four main data categories are explained further in the following three subsections, including:

- The available data packages
- The measuring apparatus and configurations
- The measured property and the usability of the data

There are several aspects that affect the measured temperature and these variations need to be taken in consideration when the temperature data is evaluated in terms of this study. The variations within measured temperatures can be considered through

- The measured property e.g. drillhole fluid or direct bedrock temperature
- The measurement configuration
    a. The location of the heat producing elements and the temperature sensor within the probe
- A calibration history of a measuring device
- The drillhole environment
    a. Hydrological condition within a drillhole (regional water flow, water flow from fractures and drillhole tilt).

b. Adjacent drillholes (Figure 5) and their characteristics
c. Simultaneous work conducted at the drillhole while measuring the temperature.
d. Work conducted at adjacent drillholes during the measuring period.

- The measuring conditions
    a. Diurnal, annual and long-term temperature variations in the surface temperature.

3.1 Posiva Flow Log (PFL)

PFL is a tool used for hydrogeological investigations developed for the needs of Posiva Oy by PRG-Tec Oy, a company bought by Pöyry Oy in 2012. Posiva Oy owns all the rights to the device. The development of the equipment started already 30 years ago, and the first measurements were conducted in the early 1990's (Komulainen 2017). The equipment is suitable for hydrogeological studies where precise accuracy is needed and therefore the designed final disposal repositories in Finland and Sweden have been the main targets for investigations. PFL is specifically used to determine the hydraulic conductivity and the hydraulic head of an isolated section of a drillhole where fracture zones are located. The measurement kit measures water flow, electrical conductivity (EC), pressure and temperature of the drillhole water along with single point resistance of the drillhole wall (Komulainen at al. 2018).

For this study the interest lies within the temperature measurements of the drillhole water. The temperature measurements of the drillhole water are merely a co-product for the flow measurements. Therefore, the PFL temperature data set needs to be considered through the theory and the evolution of the measurements itself. The first PFL measurements were conducted at Olkiluoto site at 1996 (Öhberg and Rouhiainen 2000). The interest for the temperature data only rose later and systematic reporting and documentation begun in 2000 (Pöllänen and Rouhiainen 2001). In order to use the side product data, it is important to understand the execution of the data acquisition, to understand how the temperatures are measured, i.e. what temperature does the tool actually measure. The theory and the execution of the data acquisition with PFL is explained and reported in detail by

Komulainen and Hurmerinta (2018), Komulainen (2017) and Komulainen at al. (2018). The following two sections summarize this information.

3.1.1 Theoretical background

The basic idea of the PFL tool is to confine the desired measurement section in the drillhole with rubber disks at both ends of the section. These flexible rubber disks are used to create an isolated section for the flow measurements. The isolation even holds when the tool is moved from a measurement location to other. The method of the flow measurement is through thermal pulse and thermal dilution, i.e. the flow rate is obtained from the decay of a heat pulse. “The faster the temperature drops after the heat pulse the larger the flow rate” (Komulainen 2017). In order to define the flow rate in different fracture zones, several measurement section lengths are used. Shorter section lengths allow determination of separate anomalies even if they are close to each other. Longer section length allows to generalization of the flow anomalies and gives a sense of the overall flow conditions within the drillhole. Varying section length also works as a confirmation tool for the flow determination, it is important to make sure that the tool is measuring flow from the fractures rather than some abnormalities such as leakages caused by the insulation disks. Before the heat pulse, the PFL tool also measures and records the initial temperature of the drillhole water. This is done with and without pumping of excess water.

3.1.2 Data acquisition

For the PFL measurements Posiva Oy owns and operates 5 individual measurement units. These units are better known as the trailers, as the configurations are assembled into trailers which can be either towed or transported into the measurement sites. The measurement configuration includes a winch, a pump and a logging computer (Figure 9). The probe includes: flexible rubber disks, flow sensor, pressure sensor (connected to the drillhole water through a tube and located at a watertight electronic assembly) and digital distance counter (located between the uppermost rubber sealing disk) (Figure 9). The digital distance counter is used to measure single point resistance and depth. Inside the flow sensor are:

- Three thermistors, the middle one has a heating function and other two measure the temperature
- At the top of the flow sensor, the electrode, which is used to measure the electrical conductivity of the drillhole water.

This means that the parts that measure the temperature are located above the parts measuring the depth (Figure 9). Thus, creating a bias into the true measurement depth of the temperature. However, this approximately 20 cm difference within the parts can be considered to be insignificant when the whole scale of the measurement is taken into account.

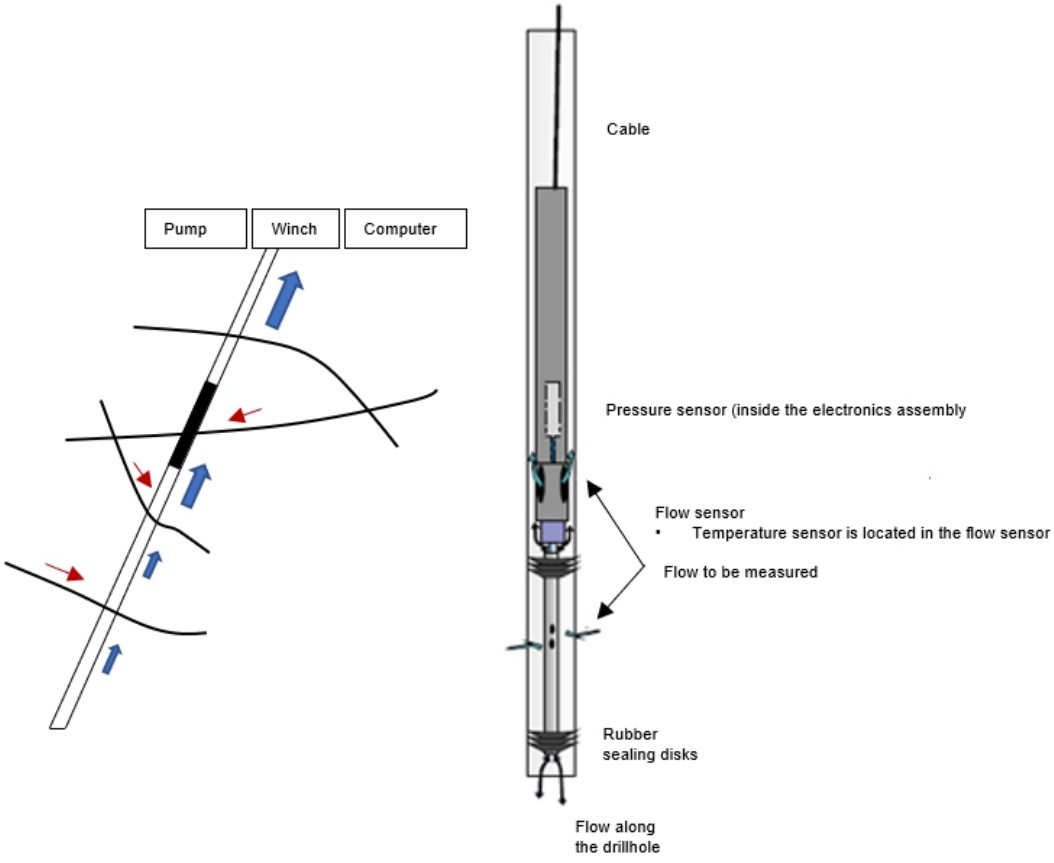

Figure 9. PFL tool specifics (right) and the measurement phase (left), where the arrows indicate the flow of water in fractures (red) and in the drillhole (blue) after Komulainen and Hurmerinta (2018).

Drillhole desired to be measured with the PFL tool can be up to 1500 m deep with a diameter of 56 mm to 120 mm. Ideally the drillhole should be smooth to ensure proper isolation of the measurement section by the rubber disks. The desired measurement

section can be from 0.5 m to 10 m and the station interval is usually 1/5 of the measurement section. Each measurement takes 45 seconds. A speed of 5 cm/s can be obtained. The basic execution of the actual measurement can be seen in the Figure 10. Calibration of the device follows each time a similar procedure and is reported in separate calibration diaries.

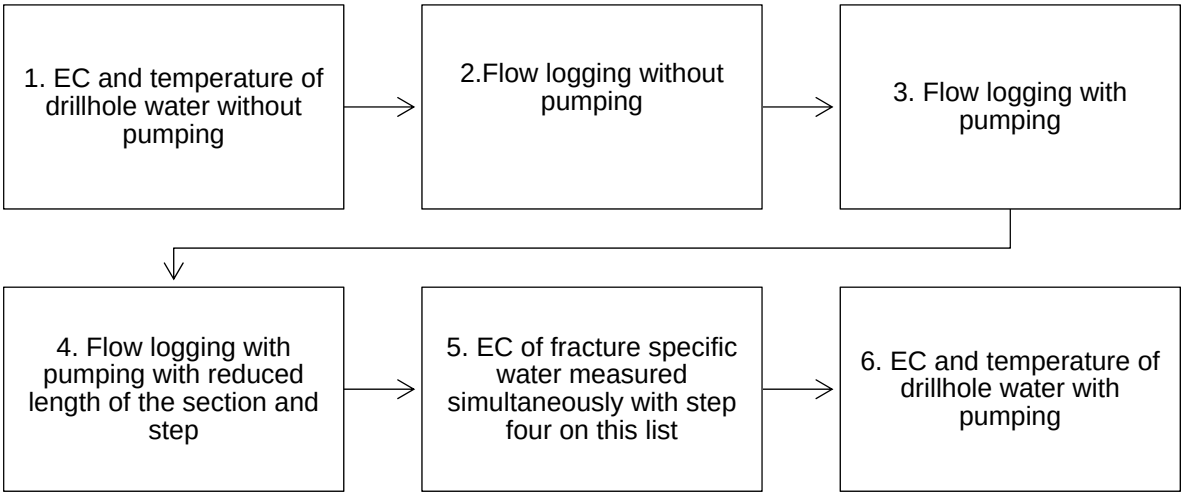

Figure 10. Basic execution of PFL measurements. Step one relevant for this study.

PFL temperature data that Posiva Oy has from the drillholes has been reported since 2000's and the measurements are still ongoing (as of January 2019). The data package includes measurements done with all five trailer units. Temperature data acquired with PFL measurements includes the up and down temperatures with and without pumping. In this study the interest lies within the undisturbed temperature of the bedrock. The temperatures which are measured with pumping thus do not reflect the undisturbed temperature due the mixing of water (Haapalehto et al. 2017).

As the probe is modified for measurements done without pumping, a bias in the measurement depth occurs. The error occurs because the tool is lowered down or pulled up with constant velocity resulting in that the tool has already moved along from the reported depth when it actually measures the temperature. It is important to understand that the measured depth is not the absolute depth in these cases.

When comparing the downward and upward temperature measurements without pumping the difference is small, almost insignificant (e.g. Pöllänen and Rouhiainen 2001). However, as the interest in this study lies within the undisturbed temperatures of the bedrock it is not ideal to use the upward temperature measurements, as when they are measured, disturbance have occurred to the drillhole. In the light of this study, the least disturbed temperature is achieved with measurement done to down direction and without pumping of excess water and with the rubber sealing disks open, as this ensures the free flow of water (Haapalehto et al. 2017). Only these temperature measurements are considered further in this study. The temperature measured is in all cases the temperature of the drillhole fluid, not the direct temperature of the bedrock. However, in the least disturbed conditions as described previously, the fluid temperature does present the initial temperature of the surrounding bedrock and therefore can be made into use in the light of this study.

3.2 Geophysical measurements (fluid temperature)

Geophysical multiparameter drillhole logging is done to gain information on the bedrock of the study area through physical properties of rocks. The multiparameter survey allows utilization of several methods simultaneously, or within the same measurement occasion. The following methods are generally always carried out in every Posiva drillhole logged with geophysical methods, regardless of equipment configuration (e.g. Lahti and Heikkinen 2005, Julkunen et al. 2004, Lahti et al. 2003, Julkunen et al. 2000 and Julkunen et al. 1996)

- Fluid resistivity and fluid temperature
- Long normal- and short normal resistivities
- Single point resistance
- Magnetic susceptibility
- Gamma-gamma density
- Natural gamma radiation
- Acoustic caliper
- Full waveform sonic logging
- Induced polarization (IP)

- Dual laterolog (DLL)

Geophysical investigations started already in the preliminary site investigation phase for the suitable location of the spent nuclear fuel. The first geophysical measurements in Olkiluoto study site were conducted in the summer of 1989, starting from the first deep drillhole OL-KR1. Geophysical drillhole investigations are still conducted as part of the production phase in Olkiluoto and in the ONKALO site. In this study the interest lies within the fluid temperature measurements (the ground water temperature), and therefore the other methods and results yielded from them are not elaborated further.

The fluid temperature measurements have been carried out during the past 30 years, resulting in changes in the measurement configuration and equipment. More advanced units have taken over the inferior models. There are three main categories within the geophysics measurements for temperature data acquisition. 1. Temperature measurements with varying temperature-fluid resistivity probes which are designed for temperature measurements, 2. Induced polarization (IP) measurements where drillhole temperature is measured as a side product and 3. Dual laterolog (DLL) measurements where the drillhole temperatures could be measured as a side product.

Appendix 4 shows the date of the measurements, the measuring device, the contractor and the possible calibration of the tool for the fluid temperature measurements in each drillhole. All applied measuring devices are discussed in detail in the following subsections.

3.2.1 SGAB and VTT/GEO manufactured temperature-fluid resistivity probes

The first geophysical drillhole loggings at Olkiluoto were carried out in the summer of 1989 (Niva 1989). The measurements were part of the preliminary site investigation phase and included measurements conducted in OL-KR1, OL-KR2 and OL-KR3. The measurements in OL-KR1 were carried out by ABEM åb, a subcontractor of SwedPower/SKB, while the measurements in OL-KR2 and OL-KR3 were carried out by Suomen Malmi Oy (Okko et al. 1990). In the summer of 1990 measurements in OL-KR4 and OL-KR5 were conducted by Suomen Malmi Oy (Julkunen 1990).

The geophysical borehole logging conducted in 1989 in OL-KR1 was carried out with SGAB manufactured logging probe. The same probe was used to measure temperature and resistivity simultaneously. The surface equipment consists of Compaq II computer, measuring wheel along digital counter, winch with a cable and generator (Niva 1989). Calibration of the thermistor was carried out in laboratory with quartz thermometer (Niva 1989).

For OL-KR2, OL-KR3, OL-KR4 and OL-KR5 the measurement configuration was similar to the one used in OL-KR1. Temperature measurements were carried out with VTT/GEO Manufactured (Abem Terrameter) PT-100 temperature-fluid resistivity probe. The surface unit consists of IBM-PC computer, winch with a cable, measuring wheel along with digital counter and power supply (Julkunen 1990). The actual temperature measurements were carried out with a PT-100 thermistor within the probe. No separate calibration was carried out to the probe. Operability of the machine was checked approximately a couple times a year, before these measurements in December 1989 (Julkunen 1989).

With both configurations the temperatures measured were drillhole fluid temperatures. In OL-KR2, OL-KR3, OL-KR4 and OL-KR5 the measurements were carried out with so called fluid logging technique, where the water is changed in the drillhole and the measurements are carried out five times. This means that temperature of the drillhole water is not stabilized. The main function for these temperature measurements was to observe fractures where inflow of water occurs by using the temperature differences within these 5 measurements sets (Heikkinen 2019). From OL-KR1 also 5 measurement sets are available, and they show the same disturbed trend as the measurements conducted at OL-KR2 – OL-KR5.

In this study the interest lies within the undisturbed temperature of the bedrock. Temperatures acquired from OL-KR1 – OL-KR5 between 1989 – 1990 do not represent this and are therefore not usable in the sense of modelling the undisturbed temperature of the bedrock.

3.2.2 Malå GeoScience's Wellmac/Li

In 1995 Malå GeoScience’s Wellmac/Li was introduced for the geophysical multiparameter drillhole loggings. Essentially two models of the Malå GeoScience's Wellmac/Li have been used, model 1994 – 1999 and model 1994 – 2001. The main difference being the changes in the data collection (from inner controller to computer software) and updates in the measuring thermistor (Julkunen at al. 1995, Julkunen et al. 1996, Lahti et al. 2001 and Lahti et al. 2003).

The temperature measurements have been conducted with fluid resistivity and temperature sensor package available for the Wellmac logging system either with PT-100 or PT-1000 measuring thermistor, meaning that the used configurations are:

- Malå GeoScience's Wellmac/Li model 1994-99 with PT100
- Malå GeoScience's Wellmac/Li model 1994-99 with PT1000
- Malå GeoScience's Wellmac/Li model 1994-2001 with PT100
- Malå GeoScience's Wellmac/Li model 1994-2001 with PT1000

There is no difference in the temperature function between the PT100 or PT1000 measuring thermistor. The sensors merely define the resistance value at certain temperature, PT1000 values being factor 10 higher (depending on material) resulting in larger slope. This higher Ω per ºC results in smaller measuring error (higher resolution) in the acquired temperature range and is the reason why the latter measuring configurations have used PT1000 sensor instead of the PT100 sensor (Julkunen at al. 1995, Julkunen et al. 1996, Lahti et al. 2001 and Lahti et al. 2003).

The drillholes, where Malå GeoScience's Wellmac/Li measurement configuration has been used, can be seen in Appendix 4. The measurement unit configuration for Malå GeoScience's Wellmac/Li can be seen in Figure 11.

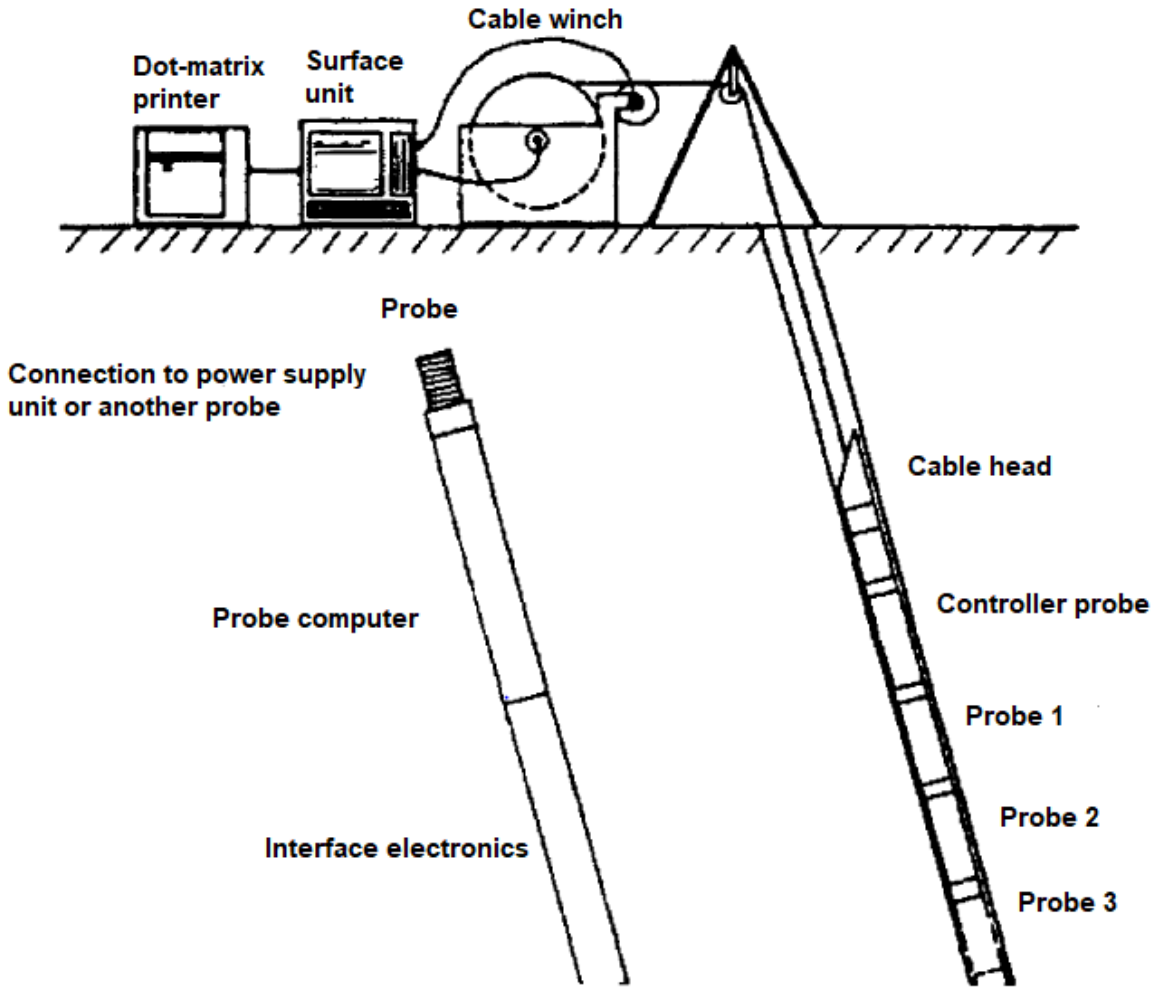

Figure 11. Wellmac-Li logging system after Julkunen et al. (2000)

The measurement configuration includes the surface unit (a computer, Wellmac/Li interface unit, power supply and data communication unit), cable winch, cable and controller probe including the probe computer and interface electronics. Below the controller probe other probes can be installed if necessary, allowing up to eight methods to be measured simultaneously. However, not all assemblies can be conducted due to the restrictions that some of the probes have for location within the assembly, for example the need of being connected as the lowest probe (Julkunen et al. 2000). The computer and the Wellmac/Li interface unit are connected through serial connection link and the interface unit is connected to the cable winch and ultimately through it to the controller probe (Julkunen et al. 2000).

The calibration of the fluid resistivity and temperature sensor has taken place in several different ways listed in Appendix 4. The probe sketch can be seen in Figure 12. The tool specifics for each model can be seen in Table 2.

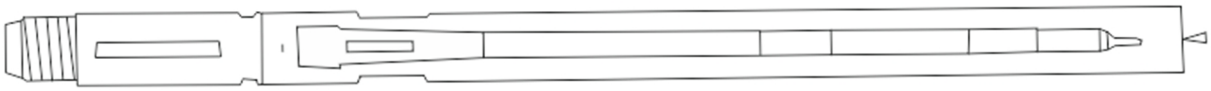

Figure 12. Wellmac-Li fluid resistivity and temperature sensor after Lahti et al. (2003) Appendix 65.1.6. Water inlet located on the right end of the probe. Location of the temperature sensor is not specified.

Table 2. Model 1994 – 1999 (Julkunen at al. 1995 Appendix 14 and Julkunen et al. 1996 Appendix 4) and model 1994 – 2001 (Lahti et al. 2001 Appendix 28.1.5 and Lahti et al. 2003 Appendix 65.1.6) fluid resistivity/temperature sensor package specifics.

Model 1994-1999			**Model 1994-2001**		
General parameters					
Pressure rating (bar)	150		Pressure rating (bar)	150	
Heat tolerance(°C)	70		Heat tolerance(°C)	70	
Length (m)	0.6		Length (m)	0.79	
Diameter (mm)	42		Diameter (mm)	42.4	
mass (kg)	1.8		mass (kg)	1.9	
Temperature measurements					
Resolution (°C)	0.01		Resolution (°C)	0.01	
Measurement range (°C)	From	to	Measurement range (°C)	From	to
	0	70		0	70
Restrictions The drillhole must be full of water. The res/temp sensor must be the lowest probe in the probe suit					

3.2.3 ELGI KTRMQ-3-120-43Y probe

ELGI measurement configuration has only been used once in geophysical drillhole logging survey (Laurila and Tammenmaa 1996). The fluid (ground water) temperature measurements took place in 1996 in OL-KR10. The measurements were conducted with temperature element placed in KTRMQ-3-120-43Y probe. The measurements were conducted by Suomen Malmi Oy (SMOY). The calibration of the probe was carried out in the range from 0°C – 20°C with 0.1°C accuracy by using a laboratory thermometer.

The location of the heat producing elements and the location of the temperature sensor in the KTRMQ-3-120-43Y probe can be seen in Figure 13. The tool specifics can be seen in Table 3. The probe is manufactured by Hungarian company ELGI and the configuration is initially designed to measure the salinity (TDS) of the ground water. The salinity can be calculated from the fluid resistivity and the temperature of the fluid (Hassinen 1998). In 1997 a survey was carried out in drillholes OL-KR1 – OL-KR4 and OL-KR9 for TDS determination. Only the temperature data from the 1996 survey is available.

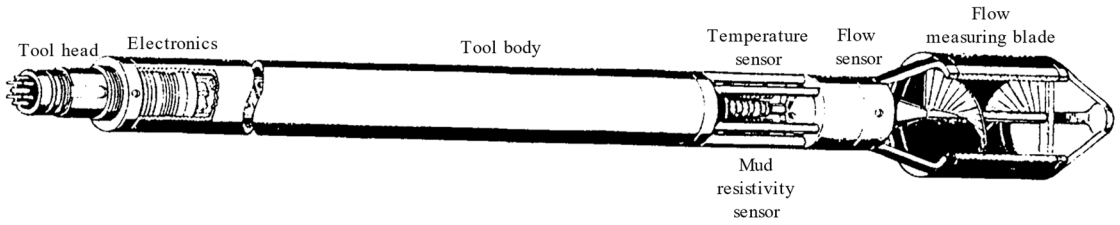

Figure 13. ELGI KTRMQ-3-120-43Y probe modified from Hassinen (1998) Appendix 2.

Table 3. ELGI KTRMQ-3-120-43Y probe specifics (Laurila and Tammenmaa 1996 Appendix 9).

General parameters		
	Pressure rating (bar)	260
	Heat tolerance(°C)	120
	Length (mm)	1500
	Diameter (mm)	63, 65 or 110 mm depending on the flow sensor
	mass (kg)	7
	Cable head	36 mm diameter connector with 7 guilt contact
	Applicable cable	single-core armoured cable
Temperature measurements		
	Measurement range (°C)	0 – 25
	Absolute accuracy (°C)	± 3
	Resolution (°C)	<0.01
	Time constant (s)	2

3.2.4 Mount Sopris temperature-fluid resistivity probe

After 2003 the geophysical drillhole loggings in Olkiluoto and ONKALO have been carried out with sensors manufactured by Advanced Logic Technology (ALT). The system allows different tools, sondes and probes to be connected to the surface unit if

they are compatible with the ALT Matrix system (Tarvainen 2007). The drillholes, where Mount Sopris temperature-fluid resistivity probe has been used, can be seen in Appendix 4.

The surface unit includes computer interface, a winch and a cable. The Mount Sopris temperature-fluid resistivity sonde is compatible with the ALT Matrix acquisition system. The model of the used probe is 2PFA-1000 (Tarvainen 2007) (Figure 14), which can have several configurations (Mount Sopris 2013).

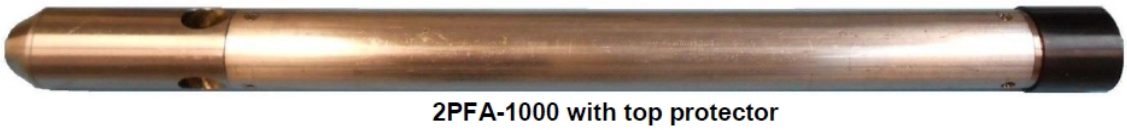

Figure 14. Mount Sopris temperature-fluid resistivity 2PFA-1000 probe (Mount Sopris 2013). The temperature sensor located at the bottom (left) of the probe next to the drillhole fluid exit ports.

Regardless of configurations, the tool includes seven electrodes mirrored Wenner array, which is used to measure the drillhole fluid resistivity. Temperature sensor is located at the bottom of the probe (Mount Sopris 2013). Table 4 shows the Mount Sopris temperature-fluid resistivity 2PFA-1000 probe specifics. Calibration of the probe, along factory calibration, is conducted with comparing the functionality with PT1000 sensor. This procedure leaves the accuracy of the calibration to be uncertain in the terms of the temperature, especially when compared to other probes and measuring techniques, which are calibrated in required procedures.

Table 4. Mount Sopris temperature-fluid resistivity 2PFA-1000 probe specifics (Mount Sopris 2013).

General parameters		
Pressure rating (Pa)	13.8	
Heat tolerance(°C)	70	
Length (mm)	Depends on the configuration	
Diameter (mm)	38	
mass (kg)	Depends on the configuration	
Temperature measurements		
Absolute accuracy (%)	better than 1	
Resolution (°C)	0.1	
Measurement range (°C)	From	to
	-20	80

3.2.5 Induced polarization (IP) measurements

Temperature measurements conducted with IP measurement apparatus are a by-product of the actual IP measurements. When the data is plodded along data acquired from the PFL and fluid temperature-resistivity measurements, it is evident that the IP measured temperatures are the temperature of the machine itself, not the undisturbed temperature of the surrounding bedrock or the temperature of a drillhole fluid (Figure 29). Therefore, temperature data acquired with IP measurements is unusable for this study and is not considered further.

3.2.6 Dual laterolog (DLL) measurements

DLL (resistivity laterolog) apparatus has the possibility to measure temperature as a side product for the main measurements. However, for some reason the temperatures have not been measured or at least recorded within the measurements carried out in ONKALO and Olkiluoto drillholes. Thus, as there is no temperature data from the DLL measurements, the method is not considered further in this study.

3.3 TERO

To carry out in-situ rock thermal property measurements in 56 mm and 76 mm diameter drillholes a device called ‘TERO’ was developed by Posiva Oy (Kukkonen et al. 2005). The word ‘TERO’ is an abbreviation for Finnish words ”Termiset Ominaisuudet”, eng. ”Thermal Properties” and is designed to measure the thermal conductivity and diffusivity in drillholes.

3.3.1 Theoretical background

The TERO surface unit configuration includes a winch installed on a trailer and related software (Figure 15). The actual TERO device is a downhole probe with heating cylinder and temperature sensors. There are three TERO-devices: 1.) TERO56 (Figure 16), 2.) TERO76 v1 (Figure 17), and 3.) TERO76 v2 (Figure 17), where the 56 or 76 stands for the drillhole diameter in mm. TERO76 v2 is in essentially just a more advanced version of the TER076 v1. The main new features include possibilities to do rapid interpretation while on the field, where as the actual measuring features remain the same (Korpisalo et al. 2013). Thus, the measurement unit featured in Figure 17 is applicable also for TERO76 v2. Just like with PFL the TERO measurements are carried out by isolating the measurement section in the drillhole with rubber disks at both ends of the section.

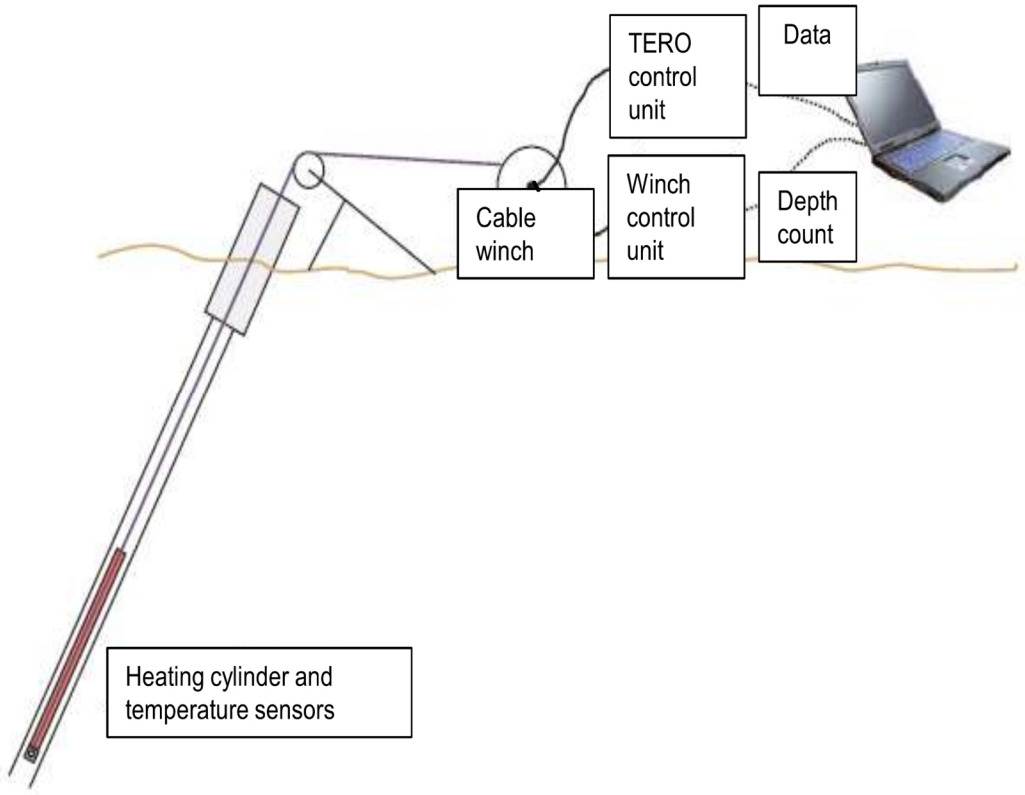

Figure 15. TERO logging device configuration modified from Kukkonen et al. (2005).

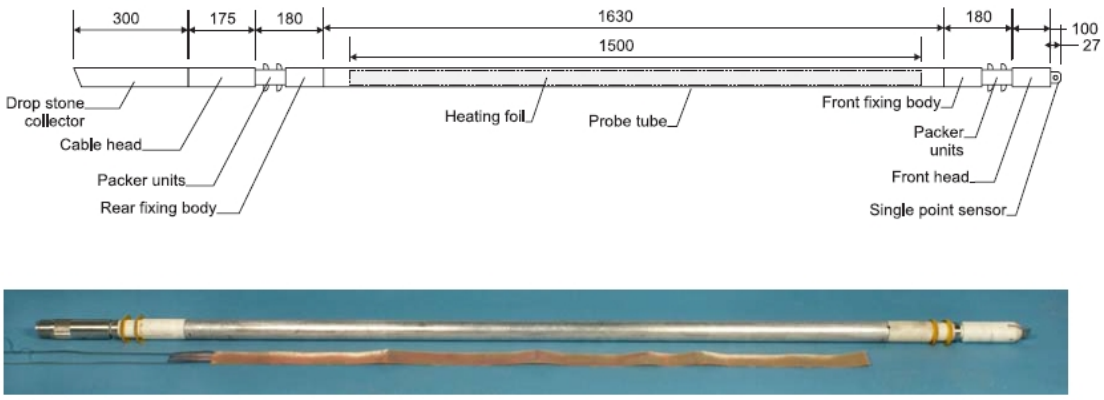

Figure 16. The main parts and dimension of the TERO56 device (above) and the constructed probe and the heating and thermistor foil (1.5m) (bottom) (Kukkonen et al. 2005).

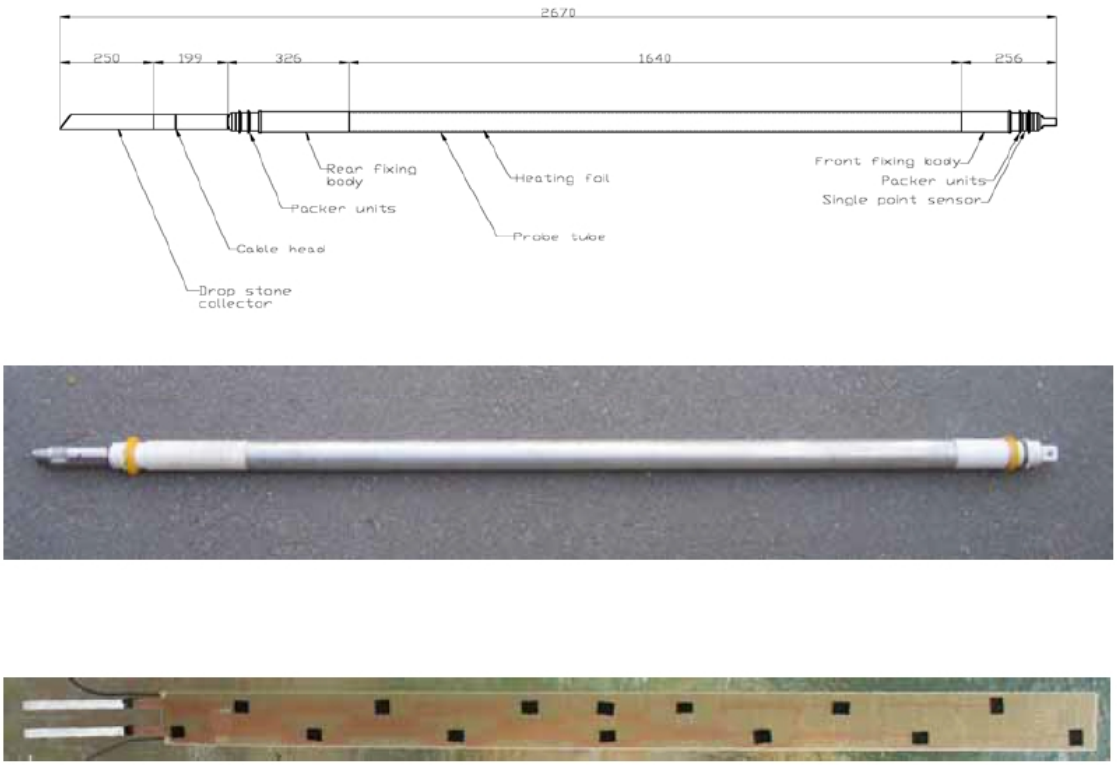

Figure 17. The main parts and dimension of the TERO76 v1 and TERO76 v2 device (above), the constructed probe (middle) and the heating and thermistor foil (bottom) (Kukkonen et al. 2007).

All the devices use the same principles for the measurements (Korpisalo et al. 2013). These principles include (Kukkonen et al. 2005):

- a cylindrical heater in a drillhole
- the temperatures of the heater are measured with time
- the heating cooling-response of the probe depends on

  a) heating power

  b) thermal properties of the probe, drillhole fluid and surrounding rock mass

3.3.2 Data acquisition

TERO measurements have taken place between 2004 and 2015 in Olkiluoto and in ONKALO (Appendix 5). TERO measurement procedure can be seen in Figure 18. The temperatures are registered while lowering the probe down to the drillhole, during the equilibrating phase and during the heating cooling phase. Out of these only the

temperature change between the heating and cooling is interpreted previously (Kukkonen et al. 2005).

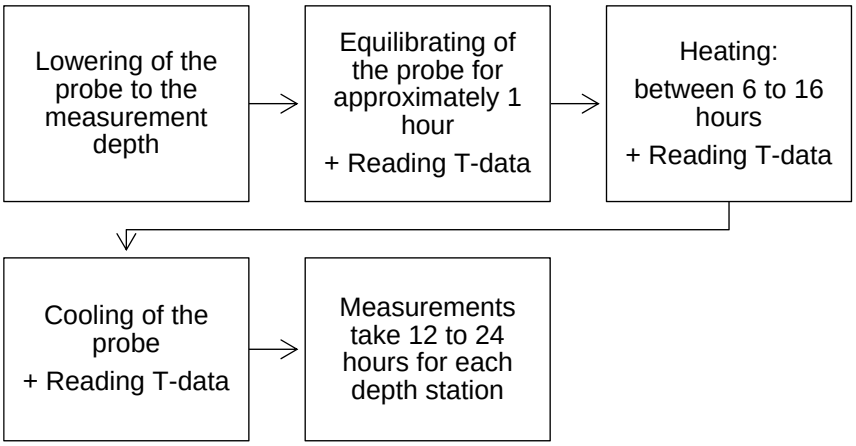

Figure 18. The TERO measurement procedure. Step two relevant for this study.

However, in this study the interest lies within the least undisturbed temperature measurements that present the undisturbed temperature of bedrock. For TERO measurements this temperature data is the one conducted at the equilibrium phase of the probe, when no heating of the probe is applied.

3.4 Antares temperature probe

In April 2014 temperature measurements were carried out in OL-KR56. Purpose of the study was to conduct a paleoclimatic inversion of ground surface temperature history. The measurements were carried out with surface configuration designed for TERO measurements. For the actual measurements, a memory logger probe manufactured by Antares GmbH was used (Kukkonen et al. 2015). The probe parameters can be seen in Table 5. The measurements were conducted with 2.5 m measuring interval and with downward logging direction, each measurement lasting for 1 min. The temperature readings were saved in 1 s intervals (Kukkonen et al. 2015). Drillhole OL-KR56 is 1248 m deep but only 1191.6 m depth was reached. The Antares measurements include only one measurement occasion in one drillhole. However, as the measurements are specifically designed to measure temperature in depth the study cannot be overlooked. In

the light of this study, data acquired presents the undisturbed temperature of the bedrock and can be taken in advantage.

Table 5. Antares probe parameters.

Instrument parameters	
Absolute accuracy (mK)	0.1
Resolution at 20°C (mK)	1.2
Resolution at 1°C (mK)	0.75
time constant (s)	2

4. DATA QUALITY CLASSIFICATION

In this section principles for the data classification are created. The main purpose of this study is to carry out a data quality classification for the available temperature data acquired from ONKALO and Olkiluoto sites, in order to improve the estimation of the initial undisturbed temperature field of Olkiluoto bedrock. These data sets are described in the previous parts. Data that will be going under the data quality classification, under the four main categories, are as follows

PFL:

1. Suitable for this study: down without pumping of excess water and disks open
2. Unsuitable for this study: up without pumping of excess water and any other measurements with pumping of excess water

Geophysical measurements (fluid temperature):

1. Suitable for this study: Fluid temperature (fluid in equilibrium/stabilized = no water pumping or changing)
2. Unsuitable for this study: fluid temperature (fluid not in equilibrium/stabilized stage = water pumping or changing present)

Geophysical measurements (IP and DLL):

1. Unsuitable for this study: Induced polarization and resistivity (measured simultaneously) measurements. Temperature is measured as a byproduct but

presents the temperature of the machine rather than the undisturbed temperature of the bedrock.

2. Unsuitable for this study: DLL no temperature data available

TERO:

1. Suitable for this study: Equilibrium phase temperature measurements with TERO
2. Unsuitable for this study: Temperature measurements from heating-cooling response

Antares:

1. Suitable for this study: Measurements done in OL-KR56 with TERO surface set and Antares probe. Only one dataset is available.

For temperature data acquired with PFL the qualification is done only for data suitable for this study by the drillhole number. For the geophysical data set the qualification is done for all of the measurements done with any of the previously listed configurations, listed according to the drillhole number. For TERO measurements the qualification is done for all the TERO measurements done with previously listed configuration, according to the drillhole number. All the listed temperature data is plotted with WellCAD software for further inspection and comparison. These plots are used to identify possible groundwater flows, fractures or other disturbances within the drillhole. Groundwater flow often causes a pouch like disturbance within the temperature gradient, whereas fractures cause more spike like disturbance. To ensure and demonstrate that temperature data from IP measurements is not suitable for this study, they were plotted and compared to the other data sets.

In order to justify the division, each data set, and each measurement needs to be considered individually. However, the sets need to be put under the same classification framework to achieve a uniform division. The data is divided into three groups:

- A = The best data, recommended for further use. Fulfils all quality criteria.
- B = Data that should be used with reservations. Only partly fulfils quality criteria.
- C = Unusable data

4.1 Data division

Figure 19 shows the criteria, that the temperature data previously described, goes through to get a classification. Only if the data does not represent the undisturbed bedrock temperature or the measurement configuration has not been calibrated in anyway, the qualification results as class C. These two aspects are seen to have the biggest effect on the quality and reliability of the data. In order to maintain unity within the classification, the principles are strict, and the class is lowered down even if just one requirement of certain class is not met. Principles of data classification are further elaborated and specified in Figure 20.

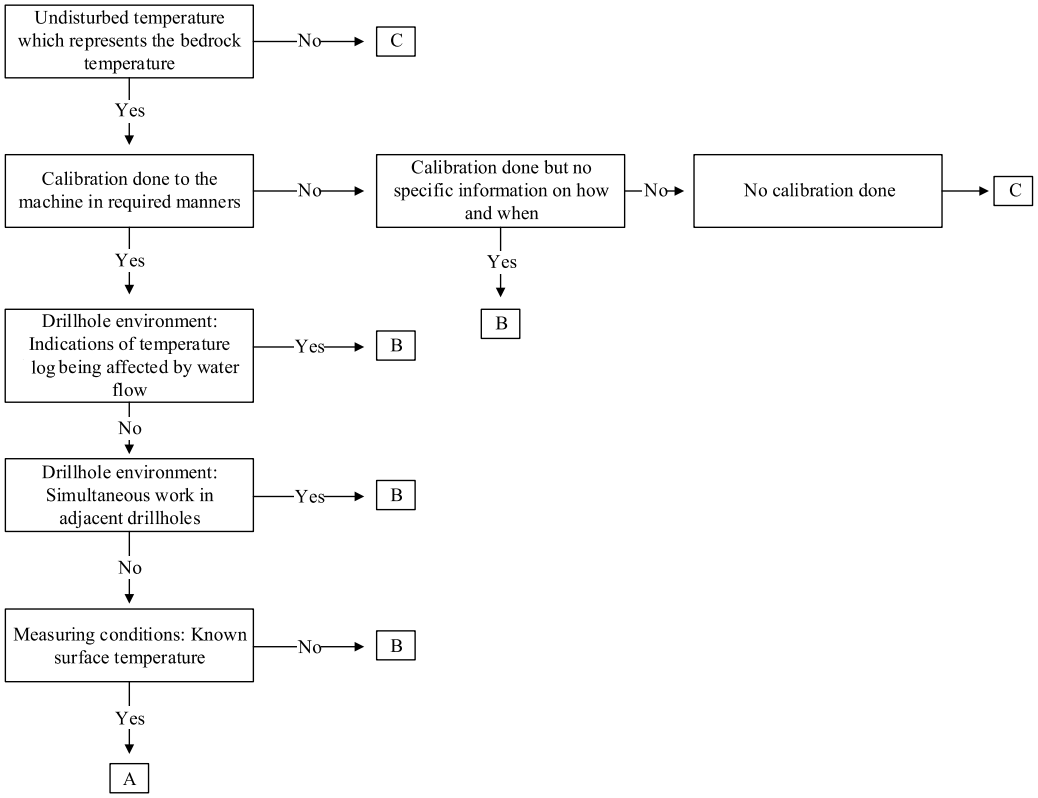

Figure 19. Principles of data qualification

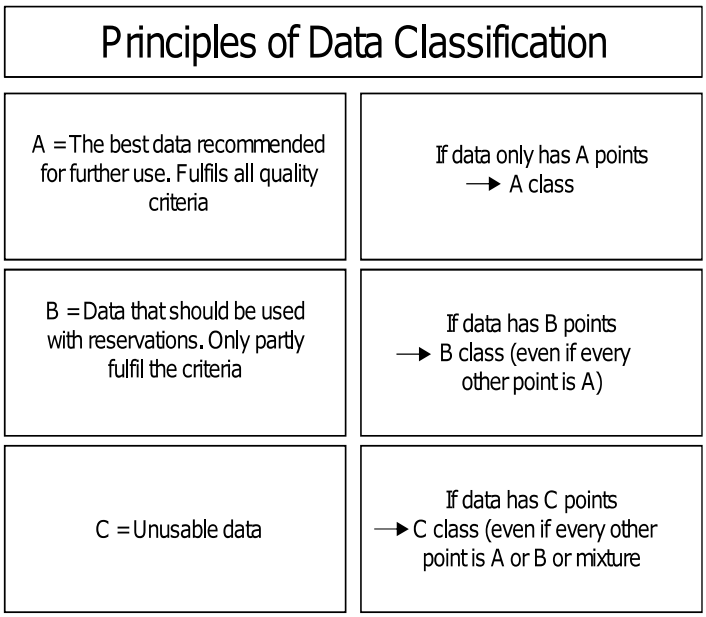

Figure 20. Principles of data classification.

The specifics i.e. reasons for certain class, can be observed in detail for each data set and individual measurement (Appendix 3, Appendix 4 and Appendix 5). It is important to realize that data can be classified as B-class data for several different reasons. However, the reasons are treated with same severity. From Appendix 3, Appendix 4 and Appendix 5 a certain trend, on why does data result in a certain class within a data set, can be observed. This is due to the individual and unique features that each data set obtains. The analogy and influence between these features are further discussed in the latter parts of this study. The classification is created in such way that it is easy for one to track back the reasons for certain class. The usability of the data sets considered in this study are not limited just to this study. Therefore, it is important to make the decision straightforward on the usability of certain individual data in possible further studies.

The data qualification takes in consideration the measured property e.g. drillhole fluid or bedrock temperature, the measurement configuration, a calibration history of a measuring device and the drillhole environment. However, it does not consider the measuring conditions i.e. diurnal, annual and long-term temperature variations in the surface temperature. The effects that the measuring conditions have on the measured temperature data are considered in the following sections.

5. THE UNDISTURBED TEMPERATURE FIELD AT OLKILUOTO

Previous study conducted by Sedighi et al. (2014) carried out analysis for temperature data obtained from the Olkiluoto site. The datasets included: 1) PFL data with and without pumping (from 2001 to 2012) 2) geophysical loggings in drillholes OL-KR1, 2, 4, 12, 13, 19, 25, 37-54 and, 3) surface temperature measurements. The initial undisturbed temperature field of Olkiluoto bedrock, according to the PFL measurements (without pumping), was found to be 10°C – 11°C in the deposition depth of ~ 400 m with temperature gradient of +1.4°C for every decreasing 100 meters (Sedighi et al. 2014). The geophysical loggings used in the study indicated similar initial temperature profile in the deposition depth of ~ 400 m as the PFL measurements. However, the temperature gradient was found to be approximately 1.2°C for every decreasing 100 meters (Sedighi et al. 2014).

5.1 Diurnal, annual and glacial temperature variations of a bedrock

Surface temperature varies cyclically. The varying temperature penetrates into the bedrock and therefore has an effect on the undisturbed temperature field of the bedrock. The penetration depth however depends on the duration of the cycle. Study conducted by Sedighi et al. (2014) found no significant variation within the temperature at depths below 50 m at the Olkiluoto study site. This indicates, that the effect that the cyclical variation has on the bedrock temperature is limited to depths not relevant to this study. However, to demonstrate this, the penetration is considered through diurnal, annual and glacial (long term) temperature variation in the following sections.

5.1.1 Theoretical background

Heat penetrates into the bedrock through surface by conduction. The surface temperature varies in cycles. The penetration is considered in diurnal, annual and in glacial (long term) cycles, when the temperature variation is assumed to be a periodic wave. With boundary conditions (Equation 17) stating that 1.) at depth 0 the periodic contribution to the surface

temperatures is $T_0 e^{it\omega}$ and 2.) temperatures at great depth are not affected by the surface temperature variation, can T (z, t) be defined as seen in Equation 19 (Fowler 2005).

$$(1) T(0,t) = T_0 e^{it\omega} \quad (2)\ T(z,t) \to 0\ as\ z \to \infty \tag{17}$$

Where T_0 is the max variation of the surface temperature, t is time, i is $\sqrt{-1}$ and ω is

$$\omega = 2\pi f = 2\pi\left(\frac{1}{t}\right) \tag{18}$$

$$T(z,t) = T_0 exp\left(-z\sqrt{\frac{\omega\rho c}{2\lambda}}\right) exp\left[i\left(\omega t - z\sqrt{\frac{\omega\rho c}{2\lambda}}\right)\right] \tag{19}$$

Where ρ is density, c is specific heat capacity and λ is thermal conductivity. Skin depth (Equation 20), is defined as the depth L where the periodic disturbance has an amplitude of 1/e of the amplitude at the surface (Fowler 2005).

$$L = \sqrt{\frac{2\lambda}{\omega\rho c}} \tag{20}$$

The depth L therefore shows the penetration depth of the periodic wave, within different cycles (Fowler 2005). For the mica gneiss bedrock of Olkiluoto, average values of thermal conductivity (at 25°C), Specific heat capacity (at 25°C) and for bulk density (at 25°C) by Kukkonen (2015) can be applied. Table 6 shows the skin depth values for diurnal, annual and for glacial cycles. The glacial cycle is considered here as 100 000 years.

Table 6. Periodic variation of the surface temperature and the skin depth.

Rock type	Thermal conductivity, λ, [W m- K^{-1}]	Density, ρ, [kgm^{-3}]	Specific heat capacity, c, [$Jkg^{-1}K^{-1}$]	The cycle	ω [s]	Skin depth, L [m]
Mica gneiss	2.77	2712	728	Diurnal	7.27^{-05}	0.12
				Annual	1.99^{-07}	3.75
				glacial	1.99^{-12}	1186.75

The longer the cycle is, the deeper the penetration propagates (Table 6). In general, and much like in Olkiluoto, rocks have low thermal conductivity, and therefore their ability to respond to surface temperature variations takes a long time. This results in short-term changes, i.e. diurnal cycle, only to penetrate approximately 20 cm of the bedrock in Olkiluoto, and therefore to be insignificant (Table 6). The annual cycle has a penetration depth of 3.8 m and the glacial cycle (100 000 years) has a penetration larger than 1 km (Table 6). Therefore, the effects caused by the cycles over one year, and most importantly the glacial cycle, cannot be ignored and must be reviewed further.

For long-term variation, a step-like change in temperature can be approximated to model the disturbance (Equation 21) (Jaupart and Mareschal 2011).

$$\Delta T(z,t) = \sum_{n=1}^{N} \Delta T_n erfc \frac{z}{\sqrt{4t\kappa}} \qquad 21$$

Where ΔT_n is the magnitude of the temperature step, t is time in seconds, z is depth and κ is diffusivity. The effect of a cycle is calculated by summing together the effects of the step-changes. To demonstrate the disturbance of a long term cycle (i.e. a glacial cycle) in Olkiluoto, a glaciation (100 ka) and deglaciation (11 ka) with surface temperature of -1°C during glaciation and + 4°C before and after, is assumed. The correction is calculated for vertically corrected temperature data, which is measured with Mount Sopris configuration in OL-KR56. OL-KR56 has data reaching the depth of 1159 m and therefore present a representative data set. Thermal diffusivity, κ (Equation 12) is calculated with values presented in Table 6 resulting in value of $1.40 \cdot 10^{-6}$ m^2s^{-1}. For the glacial cycle a trend of increasing disturbance with increasing depth is observed (Figure 21). In the deposition depth of ~ 400 m the effect is approximately 1°C degree to the measured temperature. When modelling the undisturbed temperature field of Olkiluoto this should be taken into consideration.

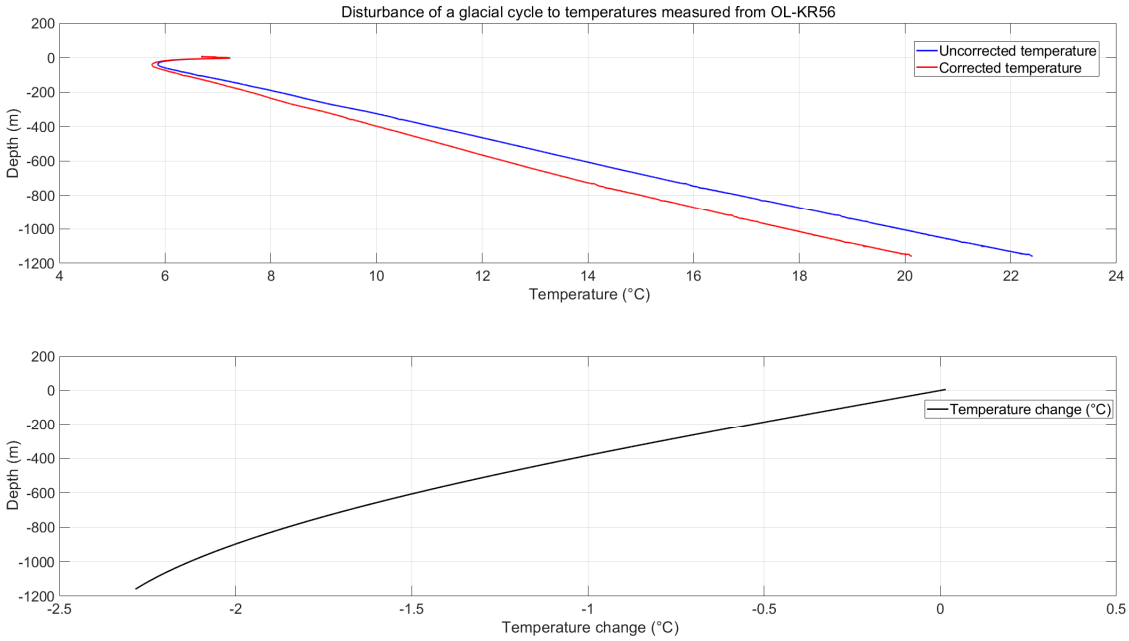

Figure 21. Effect of a glaciation for measured borehole temperatures in OL-KR56. Assuming a ground surface temperature of -1°C during 100 ka – 11ka and +4°C thereafter.

Calculations presented here only consider one step of variation in the climate history. Therefore, the results should only be considered indicative. For more accurate estimations the entire climate history should be taken into consideration when modelling the effect of a long-term cycle (Jaupart and Mareschal 2011). Kukkonen (1987) presented paleoclimatic disturbances to temperature gradient and to temperature by using accurate climate history data. The study recognized paleoclimatic effects and ground water circulation in the bedrock to be the two main factors to affect the vertical heat flow measurements. This should be taken in consideration when the undisturbed temperature field in Olkiluoto is modelled further.

5.2 Initial bedrock temperature in Olkiluoto

Temperature data obtained from the drillholes initially presents the temperature against the measured depth (MD) of the drillhole. In order to examine the temperature variation within the depth, all the temperature data is vertically corrected to the true vertical depth (TVD), so that the temperature data is interpolated to the actual depth of the data point according to the surface by using the drillhole collar information. Figure 22 shows all the PFL data acquired between 2000 – 2018 without pumping. Several erroneous

measurements can be observed. The errors can be caused by several different occasions, but in general the four most fundamental ones are recognized to be

- flow of water in large scale (e.g hydraulic zone)
- flow of water in small scale (e.g through fractures)
- mistakes in the measuring protocol

Depending on the scale of the hydraulic disturbance a spike like or wider pouch like disturbance can be observed in the temperature-depth profile. Figure 23 presents the undisturbed temperature profiles acquired with PFL (without pumping) between 2000 – 2018. Only these undisturbed measurements are further used in this study. The exact specifics of the filtered data can be observed from Appendix 2 and Appendix 3. For the geophysical temperature data obtained between 1989 – 2012, the temperature profiles are presented according to the measuring configuration (Figure 24). All the configurations are seen to contain several erroneous measurements. Figure 25 present all the geophysical temperature data divided into erroneous and un-erroneous measurements. Figure 26 presents only the undisturbed measurements acquired with the geophysical multiparameter loggings. Only these undisturbed measurements are further used in this study. The exact specifics of the filtered data can be observed from Appendix 2 and Appendix 4. Figure 27 presents the temperature profiles acquired with TERO and Antares configurations. No noticeable disturbance can be observed.

All of the deep drillhole temperatures acquired with any of the previous configurations are plotted together for easier comparison (Figure 28). Disturbances caused by all the above-mentioned reasons can be observed within the temperature profiles. For more detailed observations each drillhole data can be inspected from WellCAD temperature-MD (Appendix 1) plots or from WellCAD temperature- TVD plots (Appendix 2) created for each drillhole. The final data set, where all the data with major disturbances is excluded, can be seen in Figure 29. Only this data is further used in this study. For the PFL and geophysical datasets there are temperature data also from the adjacent B drillholes (Figure 30 and Figure 31). These datasets only have data down to 30 m of depth. The annual variation of the surface temperature can clearly be seen in the short B drillholes, but also in the deep drillholes. A relatively linear trend can be observed approximately at 50 m depth when examining the deep drillholes. The data acquired from

the B drillholes is not used further in the computation for neither the average bedrock temperature or the temperature gradient.

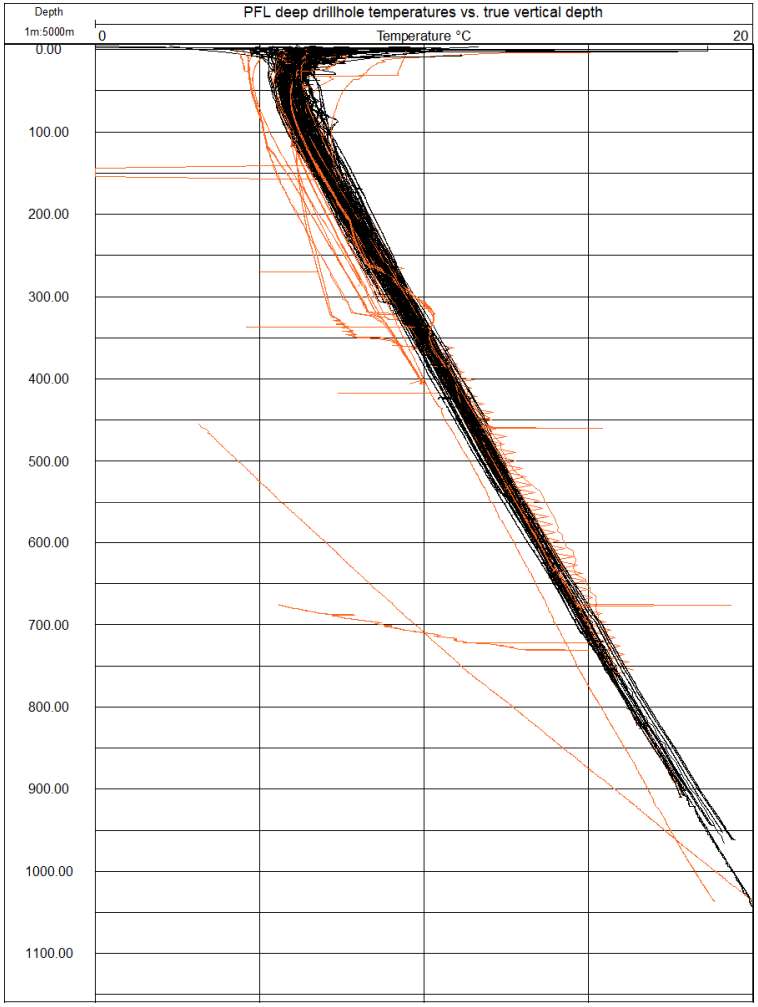

Figure 22. Category A, B and C deep drillhole temperature data acquired with PFL (without pumping) between 2000-2018. Measurements affected with e.g. water flow or are otherwise erroneous (orange) and measurements with no major visible errors (black). For drillhole specifics see Appendix 2.

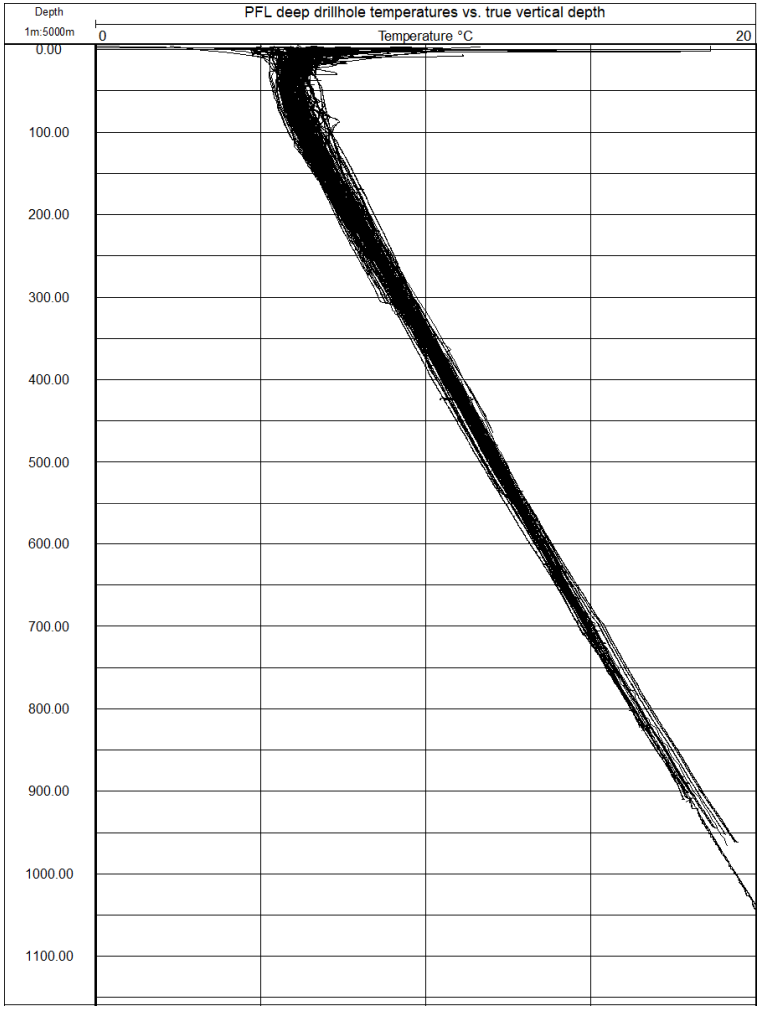

Figure 23. Category A and B deep drillhole temperature data with PFL (without pumping) between 2000-2018. For drillhole specifics see Appendix 2.

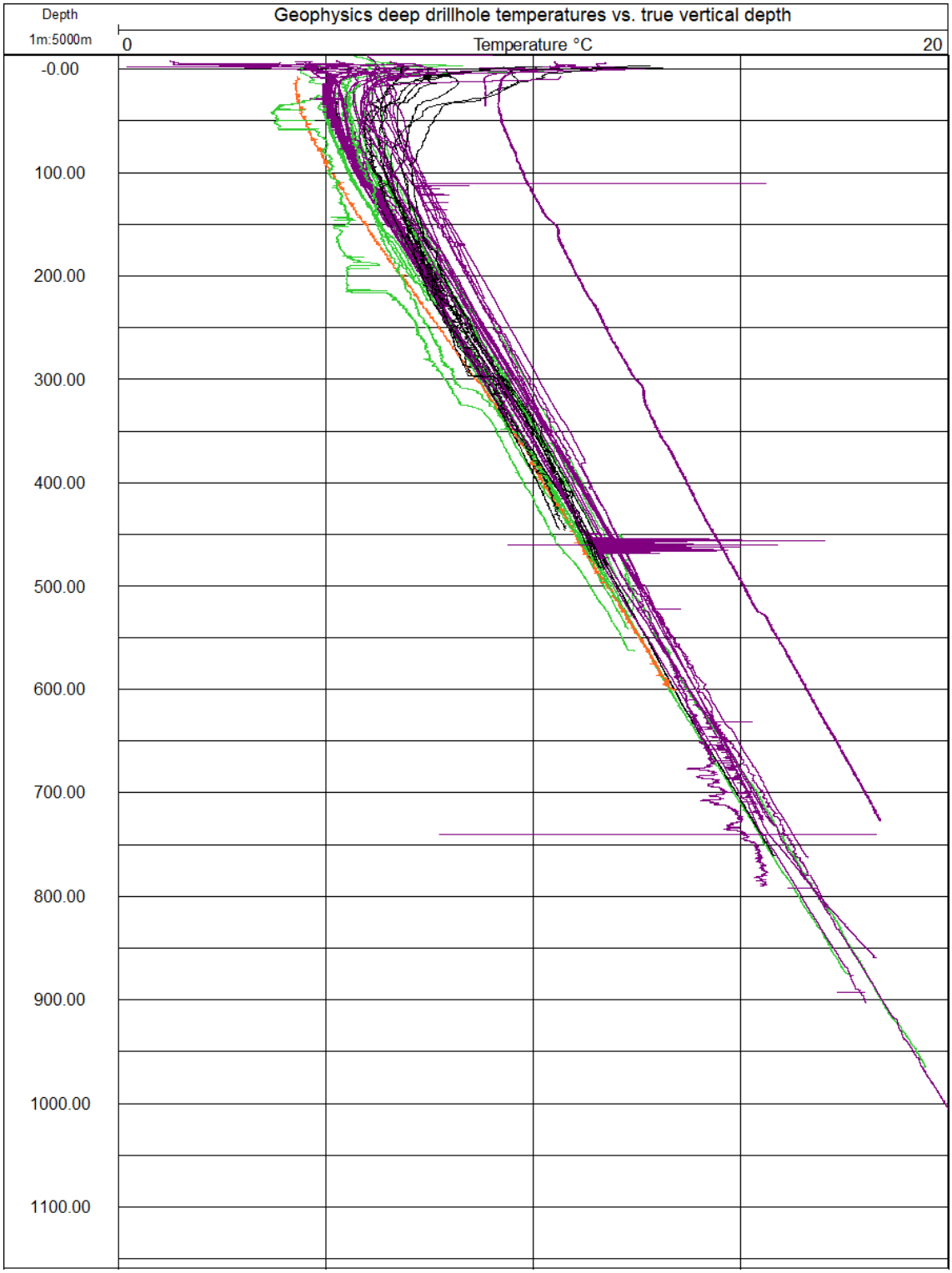

Figure 24. Category A, B and C deep drillhole temperature data acquired with Geophysical multiparameter drillhole loggings between 1989 – 2012. SGAB and VTT configurations in black, ELGI in orange, all Malå Wellmac/Li models in lime and Mount Sopris in violet. For drillhole specifics see Appendix 2.

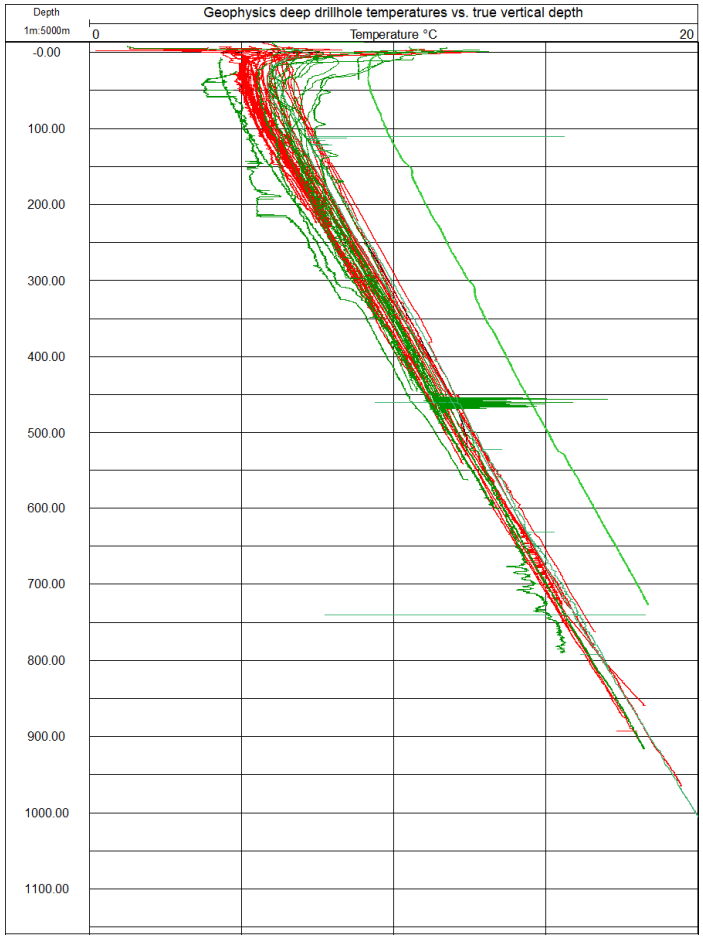

Figure 25. Category A, B and C deep drillhole temperature data acquired with geophysical multiparameter drillhole loggings between 1989 – 2012. Measurements affected with e.g. water flow or are otherwise erroneous (green) and measurements with no major visible errors (red). For drillhole specifics see Appendix 2.

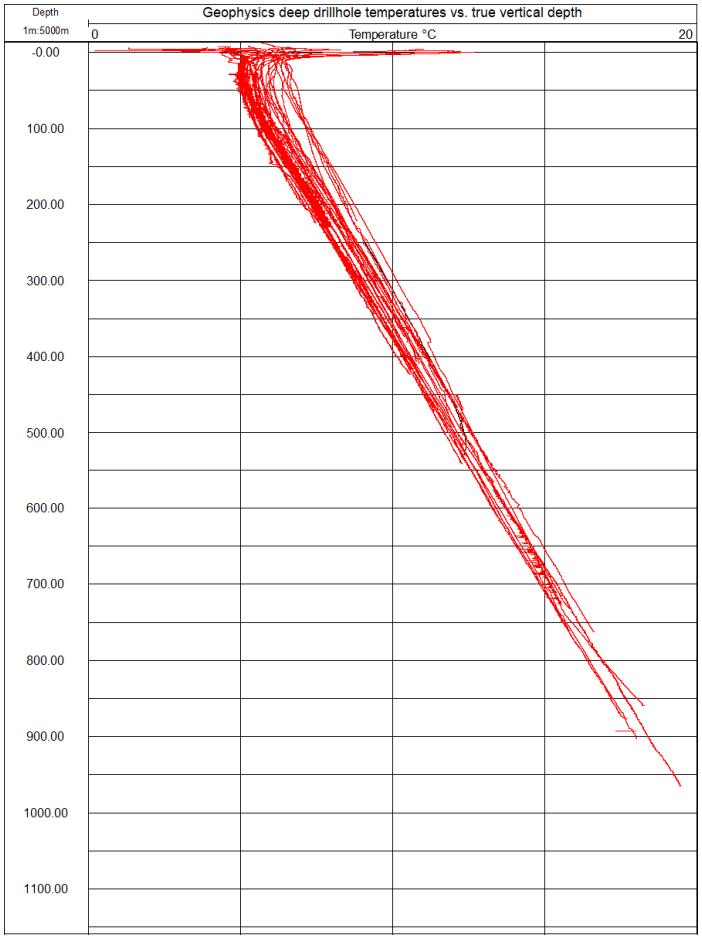

Figure 26. Category A and B deep drillhole temperature data acquired with geophysical multiparameter drillhole loggings between 1989 – 2012. For drillhole specifics see Appendix 2.

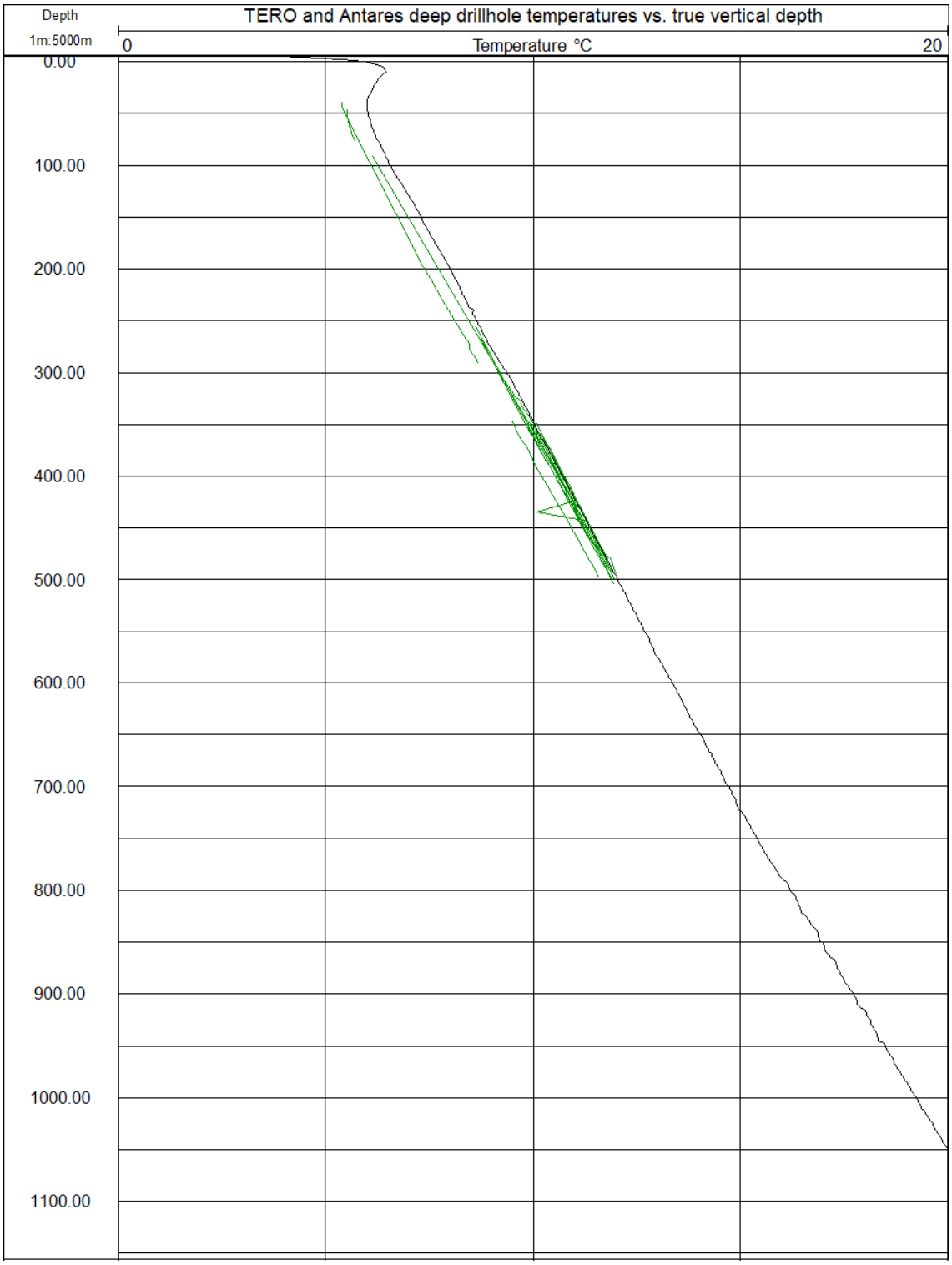

Figure 27. Category A, B and C deep drillhole temperature data acquired with TERO (green) and Antares (black) configurations between 2004 – 2015. For drillhole specifics see Appendix 2.

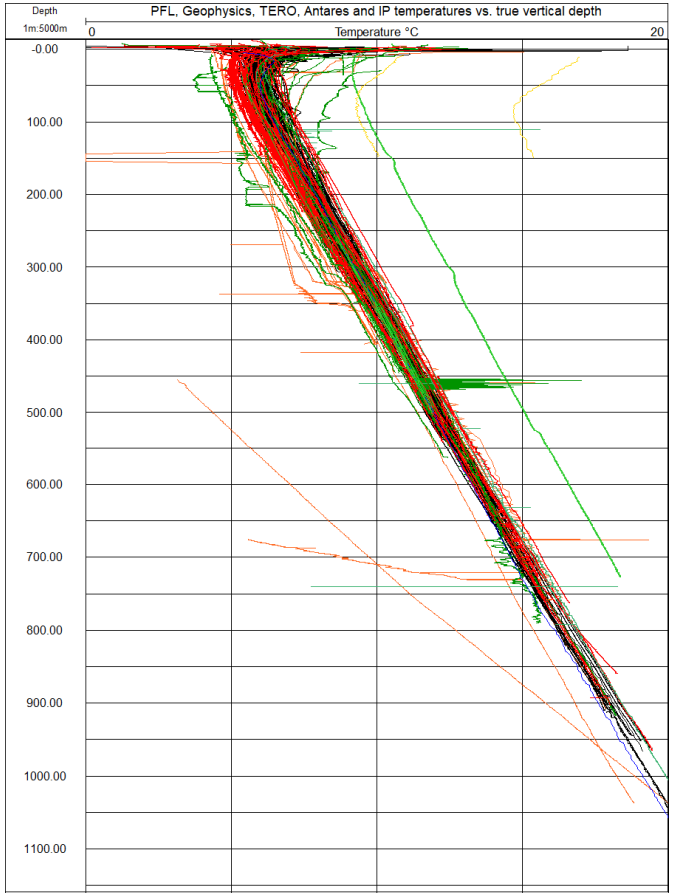

Figure 28. Category A, B and C deep drillhole temperature data acquired with PFL (black), geophysical multiparameter logging (red), TERO (lime) and Antares (blue). Measurements affected with e.g. water flow or are otherwise erroneous PFL (orange), geophysics (green) and IP (yellow). For drillhole specifics see Appendix 2.

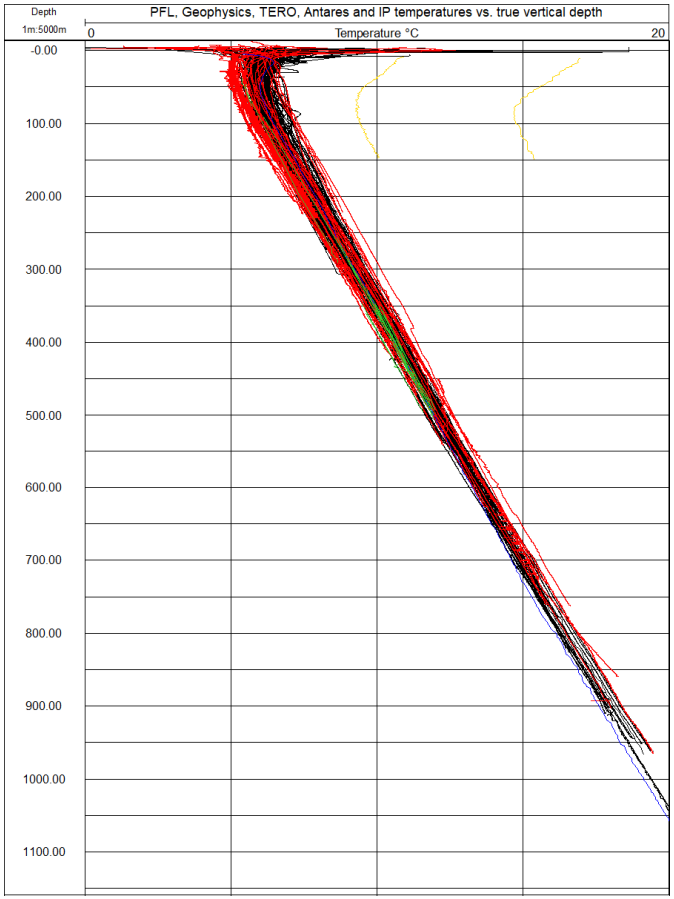

Figure 29. Category A and B deep drillhole temperature data acquired with PFL (black), geophysical multiparameter logging (red), TERO (lime) and Antares (blue). The IP (yellow) measurements are not used in this study. For drillhole specifics see Appendix 2.

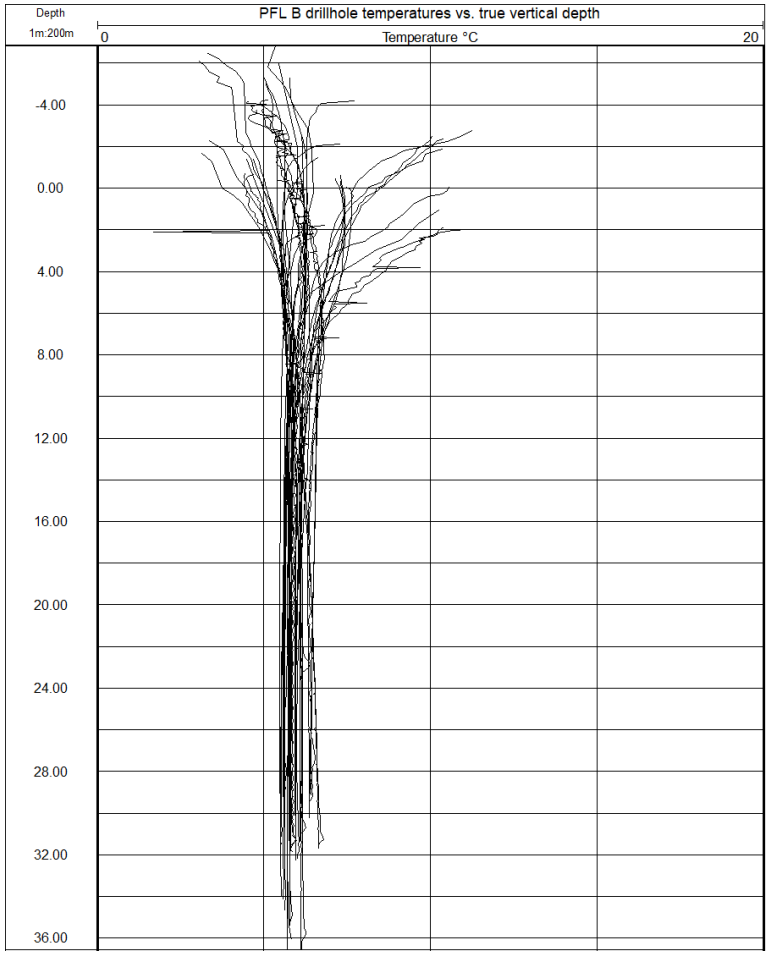

Figure 30. B drillhole temperatures acquired with PFL (without pumping) between 2000 – 2018. For drillhole specifics see Appendix 2

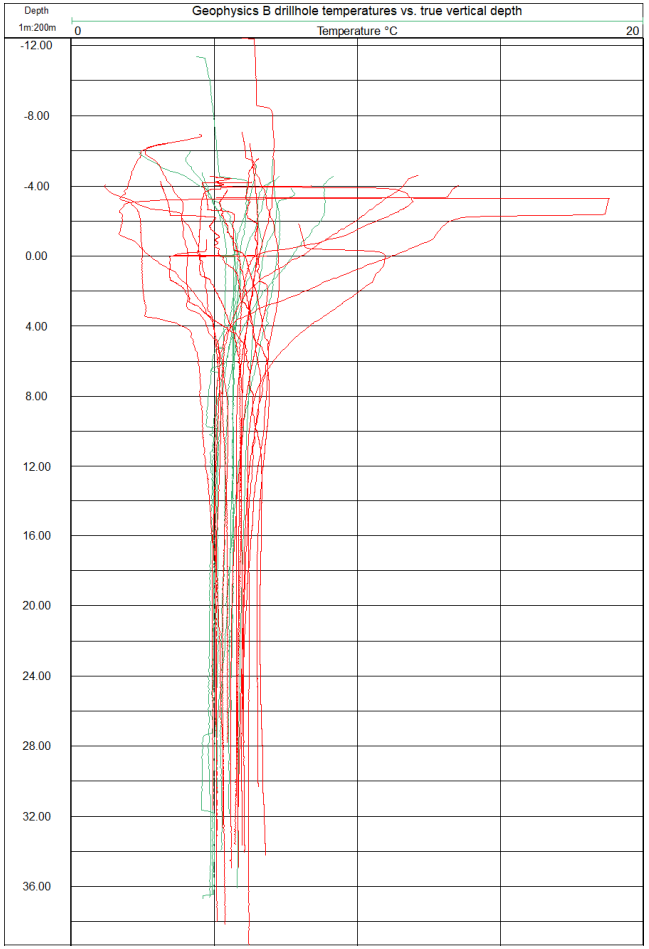

Figure 31. B drillhole temperatures acquired with geophysical multiparameter drillhole loggings between 2001 – 2015. Malå geoscience configuration in green and Mount Sopris configuration in red. For drillhole specifics see Appendix 2.

5.2.1 Effects of tunneling in ONKALO

Disturbances met in the temperature data acquired from ONKALO cannot only be described and explained through the previously described phenomena. ONKALO being essentially a tunneling network, the effects of the tunneling must be taken in consideration when the disturbances are described. The air temperature of the tunneling network is not stable, it varies due to ventilation periodically in a one-year cycle and is observed from the ONKALO drillholes. However, what makes the situation unique when compared to the normal surface temperature variation, is that the ventilation system is man controlled in ONKALO. Each tunneling location has been open for different period of time and each specific tunneling location is located sporadically according to the ventilation systems. This creates a challenging system to interpret the temperature profiles. To address the issue a continuous monitoring of the bedrock temperatures in ONKALO took place between March 11, 2009 to December 2012 in holes ONK-PP165 – ONK-PP167 (with varying time for each drillhole). The study conducted by Suppala et al. (2013) modelled the measured temperatures as function of depth and the time on the surface of the opening. The results indicated clear variation in the measured temperatures in depth during a diurnal cycle and in the heat propagation in to the bedrock with time.

There are noticeable disturbances within the ONKALO drillhole temperature data acquired with PFL (without pumping) during the first ~10 m (Figure 32 and Figure 33). This disturbance can be interpreted to be caused by the air temperature variation within the tunnels, much like the varying surface temperature creates a disturbance to the deep drillholes. Disturbances caused by water flow are also evident. Measurements conducted with TERO in ONKALO show no similar disturbance as the measurements conducted with PFL (Figure 34 and Figure 35). However, it can neither be excluded, as the length of the drillholes only reach maximum of approximately 5.5 m and the first measurement points are at 2 m in depth. All the TERO measurements in ONKALO cover only the depths where whole of the measurement length is affected by the periodical cycle. It should also be recognized that the shape of the temperature profile is affected by the time of the year when measuring. Within the ONK-PP379, ONK-PP380, ONK-PP381 and ONK-PP382 drillholes a step like temperature change can be observed with temperatures decreasing with increasing depth (Figure 35). The location of the drillholes can be seen in Figure 36. The measurements conducted in the above listed drillholes were carried out

in four consecutive days. The drillholes are located so that the distance between the drillholes ONK-PP379-ONK-PP380 and ONK-PP381-ONK-PP382 is 9 m and between ONK-PP380-ONK-PP381 11.5 m. Due to this the possibility of the step like change being caused by the heating carried out in the adjacent drillhole, can be excluded.

In general, the measurements conducted with PFL and TERO in ONKALO present a relatively small and disturbed datasets. Neither of the measurement packages acquired in ONKALO are used in the evaluation of the temperature gradient or the average bedrock temperature in Olkiluoto in this study. The data is excluded due to the errors that cannot be specified and connected to a certain cause.

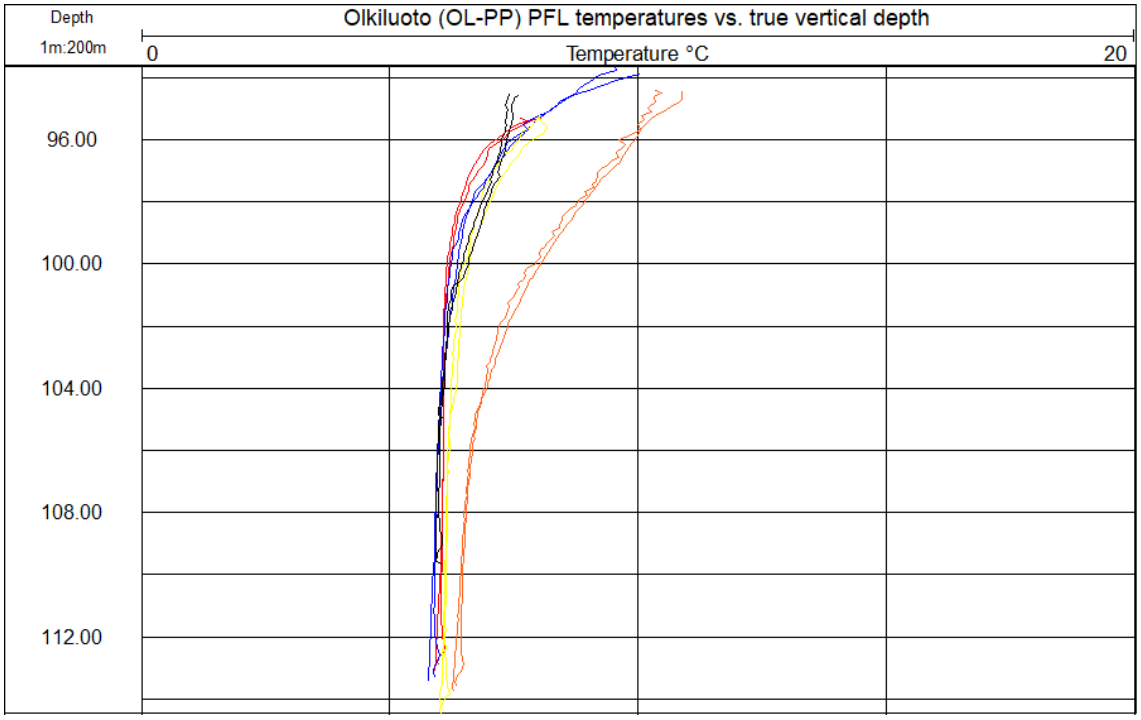

Figure 32. Olkiluoto (OL-PP66 (red), OL-PP67 (blue), OL-PP68 (yellow), OL-PP69 (orange) and OL-PP70 (black)) drillhole temperatures acquired with PFL.

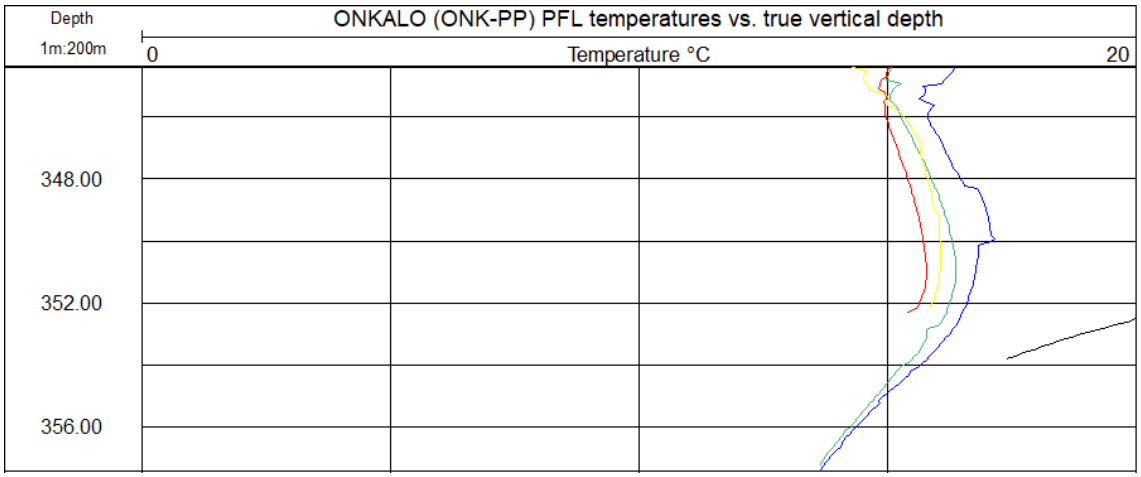

Figure 33. ONKALO (ONK-PP398 (red), ONK-PP400 (green), ONK-PP402 (blue), ONK-PP404 (yellow) and ONK-PP413 (black)) drillhole temperatures acquired with PFL.

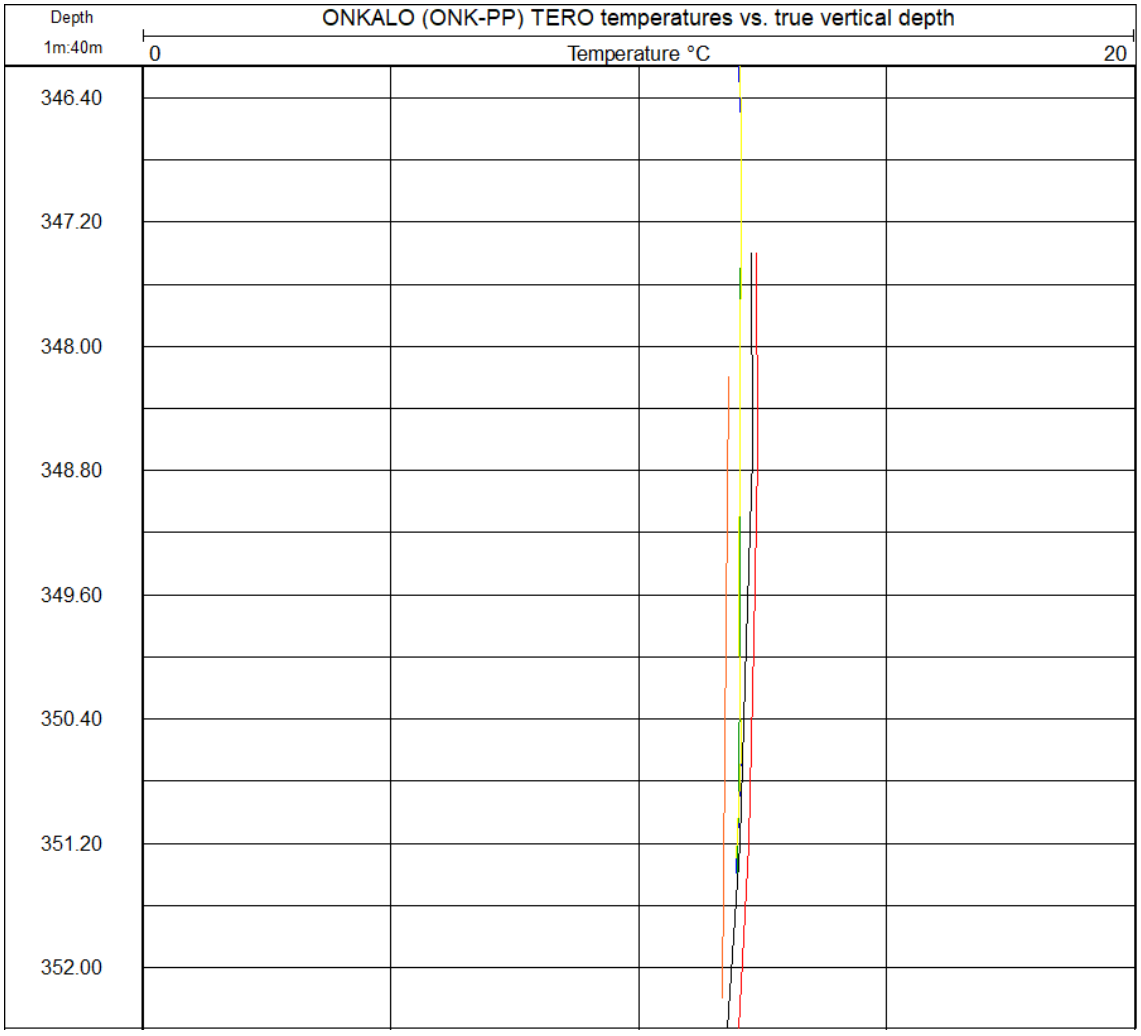

Figure 34. ONKALO (ONK-PP340 (black), ONK-PP346 (red), ONK-PP398 (blue), ONK-PP399 (green), ONK-PP405 (yellow) and ONK-PP411 (orange)) drillhole temperatures acquired with TERO configuration.

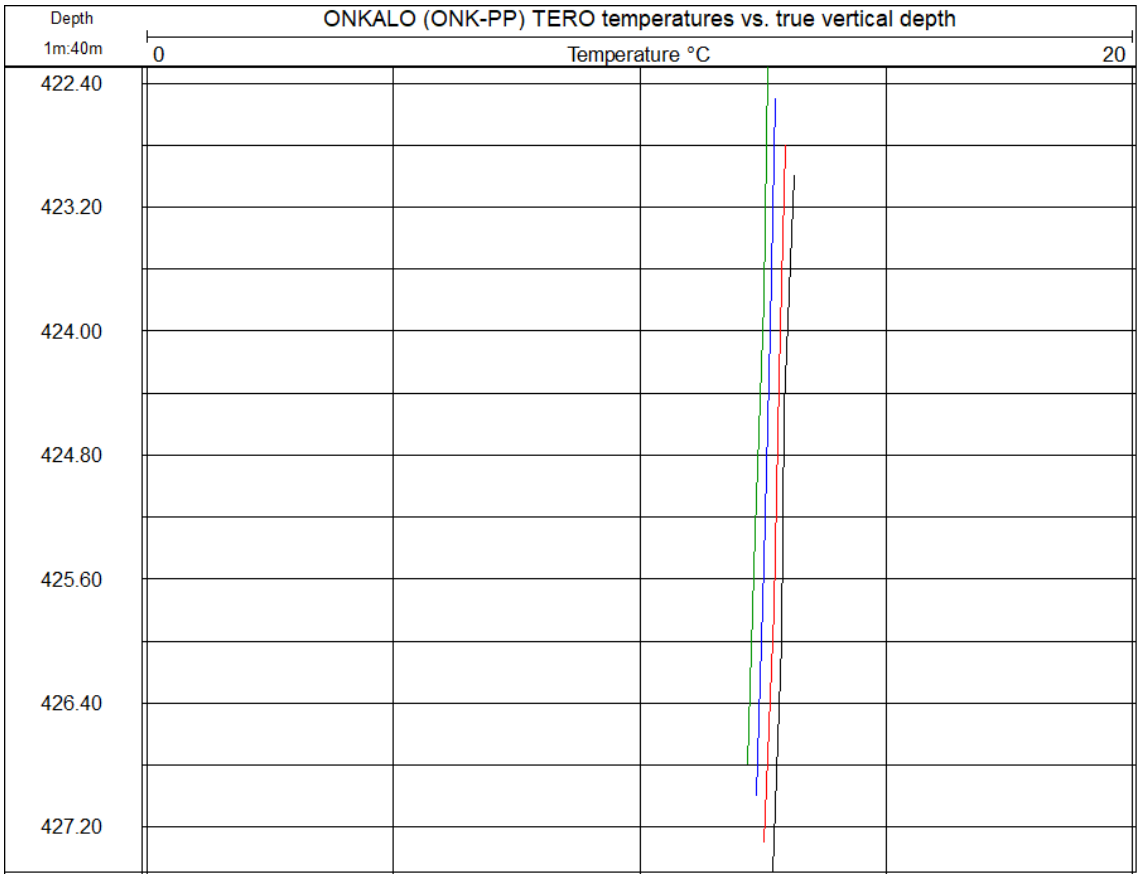

Figure 35. ONKALO (ONK-PP379 (black), ONK-PP380 (red), ONK-PP381 (blue) and ONK-PP382 (green)) drillhole temperatures acquired with TERO configuration.

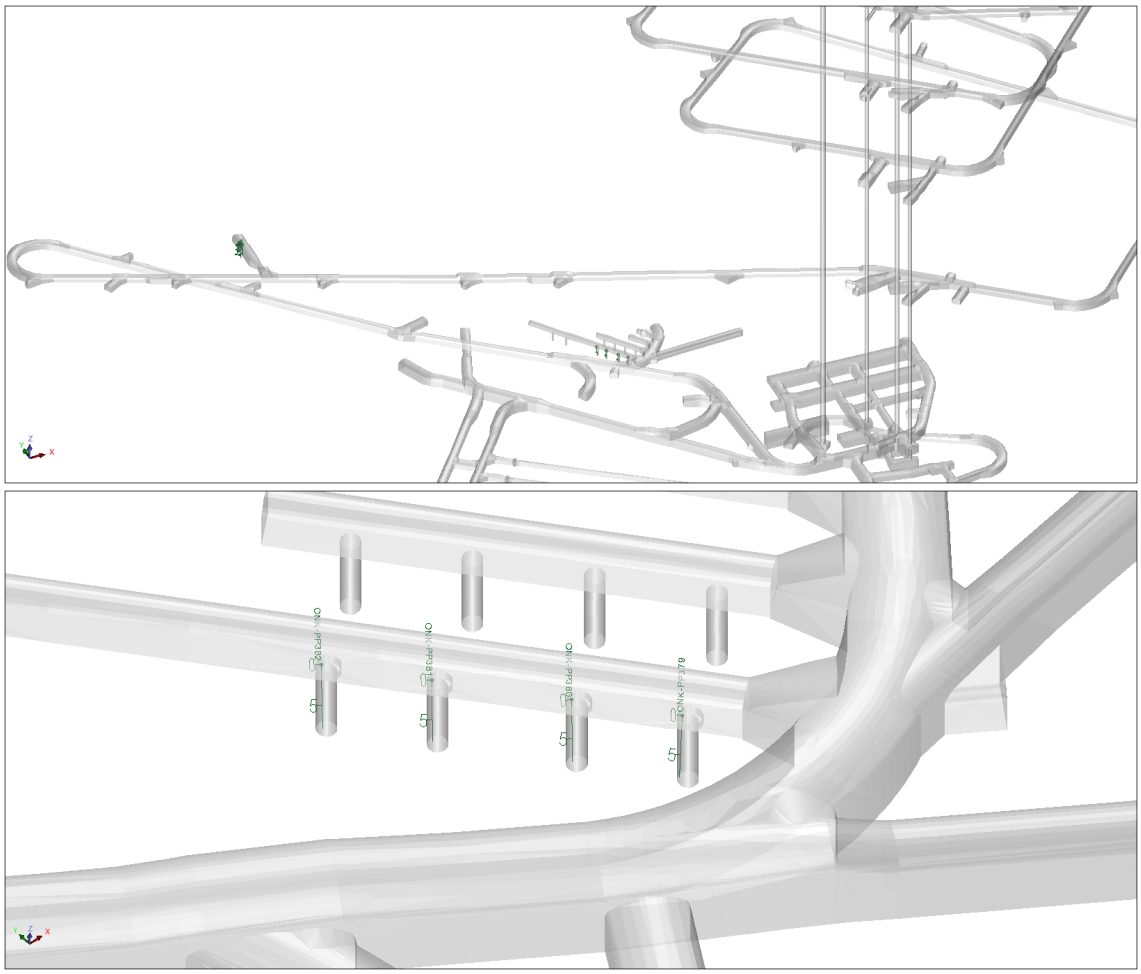

Figure 36. Top: ONKALO chain system and the location of the temperature measurements conducted in ONKALO (in green) bottom: location of ONK-PP379 (right), ONK-PP380, ONK-PP381 and ONK-PP382 drillholes in ONKALO. (Figure courtesy of Haapalehto 2019).

5.3 Temperature gradient and the average temperature of Olkiluoto bedrock

The initial undisturbed average temperature of Olkiluoto bedrock, according to the geophysical measurements, PFL measurements (without pumping), TERO measurements and Antares measurements were found to be 10.93 ± 0.09°C, 10.85 ± 0.02°C, 10.60 ± 0.08°C and 10.75°C respectively, at the deposition depth of 412 m (Table 7 and Figure 37). The calculations included the category A and B data from each method in certain depth (Table 7). Standard errors for the values were obtained from the standard deviation (s) and from the number of measurement points at certain depth (N) (Equation 22)

$$Stderror = \frac{s}{\sqrt{N}} \quad (22)$$

Table 7. Average temperatures according to the A and B category data for each measurement unit at the deposition depth of 412 – 432 m with 5 m intervals. N= the number of measurement points at certain depth.

Measurement unit	Depth (m)	N	Average (°C)	STDEV	Standard error (±°C)
TERO	412	12	10.598	0.264	0.076
	417	12	10.675	0.284	0.082
	422	12	10.781	0.214	0.062
	427	11	10.904	0.119	0.036
	432	11	10.950	0.136	0.041
PFL	412	130	10.848	0.190	0.017
	417	130	10.915	0.196	0.017
	422	130	10.982	0.198	0.017
	427	120	11.056	0.216	0.020
	432	116	11.122	0.220	0.020
Geophysical multiparameter drillhole logging	412	18	10.933	0.365	0.086
	417	18	11.004	0.356	0.084
	422	18	11.073	0.356	0.084
	427	17	11.178	0.338	0.082
	432	16	11.263	0.344	0.086
Antares	412	1	10.750		
	417	1	10.820		
	422	1	10.890		
	427	1	10.950		
	432	1	11.020		

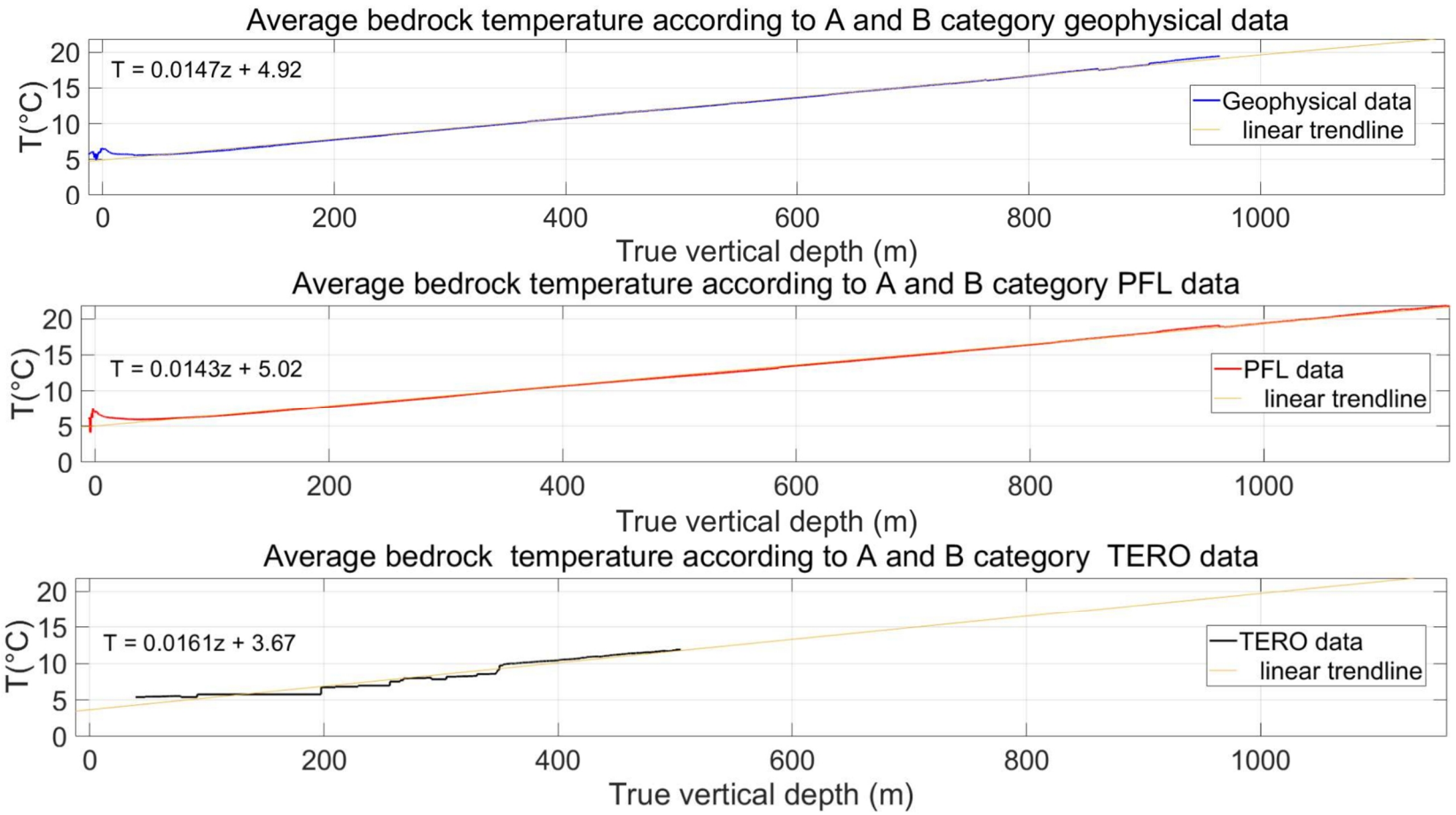

Figure 37. Average undisturbed bedrock temperatures according to geophysical, PFL, and TERO temperature data with fitted linear trendline. For geophysical data T=0.0147z+4.92, for PFL data T =0.0143z+5.02 and for TERO T=0.0147z+4.42. Exact drillholes used for computing can be observed from Appendix 2.

The average bedrock temperatures can also be estimated from Figure 29 by simply defining the min and max values of the temperature for each method. With the geophysical and TERO measurements the average temperature values for Olkiluoto bedrock obtained with min/max resulted to be practically the same as the average values obtained from the trendline (Table 8). The largest differences between the average bedrock temperatures obtained from the trendline and with the min/max method are within the PFL data. For all the datasets the standard error is noticeably larger with the min/max method and therefore the average values calculated from the trendline can be considered more representative.

Table 8. Average temperatures at the deposition depth of 412 – 432 m with 5 m intervals calculated from the min and max values at certain depth. Antares unit is not included as there is only 1 measurement occasion with it.

Measurement unit	Depth (m)	Min (°C)	Max (°C)	Average (°C)	STDEV	Standard error (±°C)
TERO	412	10.050	10.840	10.445	0.264	0.187
	417	10.050	10.940	10.495	0.284	0.201
	422	10.253	11.010	10.631	0.214	0.152
	427	10.590	11.028	10.809	0.119	0.084
	432	10.640	11.120	10.880	0.136	0.096
PFL	412	10.060	11.374	10.717	0.190	0.135
	417	10.060	11.415	10.737	0.196	0.138
	422	10.060	11.417	10.739	0.198	0.140
	427	10.060	11.550	10.805	0.216	0.153
	432	10.060	11.585	10.822	0.220	0.156
Geophysical multiparameter drillhole logging	412	10.344	11.502	10.923	0.365	0.258
	417	10.467	11.569	11.018	0.356	0.252
	422	10.528	11.649	11.088	0.356	0.252
	427	10.711	11.735	11.223	0.338	0.239
	432	10.774	11.790	11.282	0.344	0.243

The average temperature values for the Olkiluoto bedrock obtained in this study replicate the results obtained by Sedighi et al. (2014), in respect of the Geophysical and PFL measurements. No previous studies had overlooked the TERO and Antares data, but the results presented here, show that they also fall into the 10 – 11°C temperature range presented by Sedighi et al. (2014).

The temperature gradient is obtained by fitting a linear trend to the data sets and is given as follows for the geophysical data (Equation 23a), PFL data (Equation 23b), TERO data (Equation 23c) and for Antares measurement (Equation 23d).

$$T = 0.0147z + 4.92 \quad (23a)$$

$$T = 0.0143z + 5.02 \quad (23b)$$

$$T = 0.0161z + 3.67 \quad (23c)$$

$$T = 0.0139z + 5.98 \quad (23d)$$

Where T is temperature (°C) and z is the depth (m). The temperature gradient according to the geophysical measurements, the PFL measurements (without pumping) and the TERO measurements were found to be 1.47°C/100m, 1.43°C/100m, 1.65°C/100m, respectively (Figure 37). For the Antares measurement the temperature gradient was found to be and 1.39°C/100m. These increasements in the temperature in every 100 m support the previous results by Sedighi et al. (2014) when considering the PFL measurements. Also, the results for the temperature gradient conducted with geophysical methods, TERO and Antares configurations in this study reinforce the previous results, by replicating the results acquired with PFL measurements. The reliability of the results is further discussed in the following sections.

6. 3D LAYER MODEL OF OLKILUOTO

For comprehensible understanding of the research question it is ideal to examine the situation in 3D. In order to do so, a layered temperature model of the Olkiluoto area is created by using Leapfrog Geo software. The model presented here is not a geothermal heat transfer model, as it does not solve the conduction equations or take into account the thermal properties. Leapfrog software only provides an interpolation of the measured data between drillholes. The aim of the model conducted in this study is to present the datasets

classified and study them in 3D format and provide baseline information for future thermal dimensioning and modelling of the study area.

The modelling project includes all available drillhole data from Olkiluoto and ONKALO including lithology and topography of the area, ONKALO tunnel layout, the planned disposal tunnel network and the vertically corrected temperature data from the three data sets and Antares measurement, discussed above.

6.1 Model specifics

One of the aims of the thermal model is to create a baseline information for future thermal dimensioning of the repository. To do so, all the vertically corrected temperature data is brought into the modelling project. In Leapfrog Geo each individual file needs to be uploaded individually and thus remains time consuming. Therefore, it is ideal to have one platform where all the data is brought and can be accessed and updated easily. Not all the temperature data is applied on the model. Data that is used to create the model is seen in Figure 29. Only the measurements which do not show major disturbance within the Temperature/Depth profile are used (categories A and B see Appendix 3, Appendix 4 and Appendix 5). B drillholes, ONK-PP or OL-PP measurements are not used. OL-KR58 located at Kuusisenmaa, a small island next to Olkiluoto, is also excluded from the model even though there is no indication of temperature disturbance. This is done to maximize the accuracy of the model at the deposition location and due to the sensitivity of the Leapfrog interpolation for data points located far away from the main data set.

Geostatistics, and especially the Kriging method provides good baseline information in order to understand the interpolation logic behind the built-in Leapfrog Geo interpolation features. Kriging method solves for several geostatistical techniques, such as how to interpolate values between known location of data to nearby locations with no data. The 3D temperature model is generated by using numeric model module, a built-in feature in Leapfrog Geo (Leapfro Geo User Manual 2019). As the temperature data is measured from drillholes it creates very steep vertical trend to it. In order to create horizontal layered model, the data needs to be interpolated between the known and unknown data points. This is done with linear interpolant and linear drift. The linear interpolant assumes that data that is closer to the computed point is more important than data farther away,

meaning that the interpolant value of an unknown point strongly reflects the close by data points and their average. Linear drift allows negative values for points located long way from data, making the interpolant behave linearly. However, if there is no close by points, the linear interpolation will use the closest available data point. Therefore, excluding isolated data such as OL-KR58 located at Kuusisenmaa, is justified in the light of this model. An alternative for linear interpolant is spherical interpolant. A method where a range (the distance) between the interpolated data point and input data can be defined. Spherical interpolant considers the close by data points up to the range to be more important than the further away data points, but after the set range it considers all the data to be as important i.e. not decreasing the importance further. Therefore, if there is no close by data point within the range, the interpolated output value will reflect approximate average of all the data beyond the range. Leapfrog Geo is designed for geological modelling, and when using these functions for temperature interpolation it should be done with reservations. Both interpolations methods were tested during the modelling phase, resulting in relatively small differences, which is probably due to the good data coverage of the area. The models, 1. covering the whole island of Olkiluoto and 2. restricted to the deposit depth, presented in this study are both generated with linear interpolation function. The decision on using the linear interpolant rather than spherical interpolant was based on the previously described features. As the model presented here works as a base for possible subsequent models it was ideal to retain the methodological choices as straightforward as possible.

Total sill (5) and base range (2000) define the slope of the interpolant. At base range distance the value of the interpolant is the total sill. Nugget value i.e. the noise reduction can be used to reduce the effect caused by erroneous data points. By increasing the nugget value more emphasis is given to the average values of data points surrounding the inaccurate point. Here the nugget value is set to 0. The data set used in the modelling includes only data with no major errors or disturbances. However, as the data is not inspected point by point, there is a possibility of an error within. By not reducing the noise level, all the possible anomalies can be observed allowing further examination of the point. This results in easier way of identifying possible false anomalies directly rather than evening out the error into all the surrounding data.

To create horizontal trend in the data the trend function can be altered. Here a global trend is used, and ellipsoid ratios, which determine the relative shape and strength, are

altered to maximum = 3, intermediate = 3 and minimum = 1. The directions are kept at dip = 0, dip azimuth = 0 and pitch = 90.

Essentially, two models are created with the same base settings but different areal extends. The first model covers the whole island of Olkiluoto as the boundary of the model is set to topography extend and the elevation to -1300 m in depth. This model is used to identify large scale anomalies within the temperature/depth profile, to examine the effects that the surroundings e.g. sea floor or surface air has on the model, to observe possible correlation between the temperature anomalies and major brittle fault zones and to observe the progress of the temperature/depth profile in time, if possible. The second model is restricted to the planned deposition depth of 412 – 432 m. The model is generated to create a better understanding of the critical area of the model. The model allows closer inspection of present temperature anomalies with relation to the tunneling network and the major brittle fault zones.

6.2 Resultant model

For all the drillholes a geological drillhole log is available. Bedrock of the study area is heterogenous with varying rock types (Figure 38). For comprehensible understanding of the geological setting a thorough geological model is needed. Such a model is under construction by Posiva and could later be combined to the temperature models presented in this study. However, as base of this study also lies within the thermal properties of a bedrock it is ideal to combine the available drillcore information into the models presented here. Three major rock types can be observed from the drillcore loggings, diatexitic gneiss (DGN), veined gneiss (VGN) and granitic pegmatoid (PGR), where PGR appears as vein liked formations. For almost all the drillholes at the Olkiluoto island there are temperature data (Figure 39). However, not all this data is applied to the models presented here. The ONKALO chain system and the planned disposal tunnels are also well covered with the temperature data sets presented in this study (Figure 39). Fracture structure models OL-BFZ020a, OL-BFZ020b, OL-BFZ099 and OL-BFZ300 indicate the major brittle fault zones and are plotted along the temperature data (Figure 40). The fracture zones are modelled by Posiva Oy and are included in the model as such. The base

of these structure models lies within the drillcore fracture loggings and geological mapping conduced at the study site.

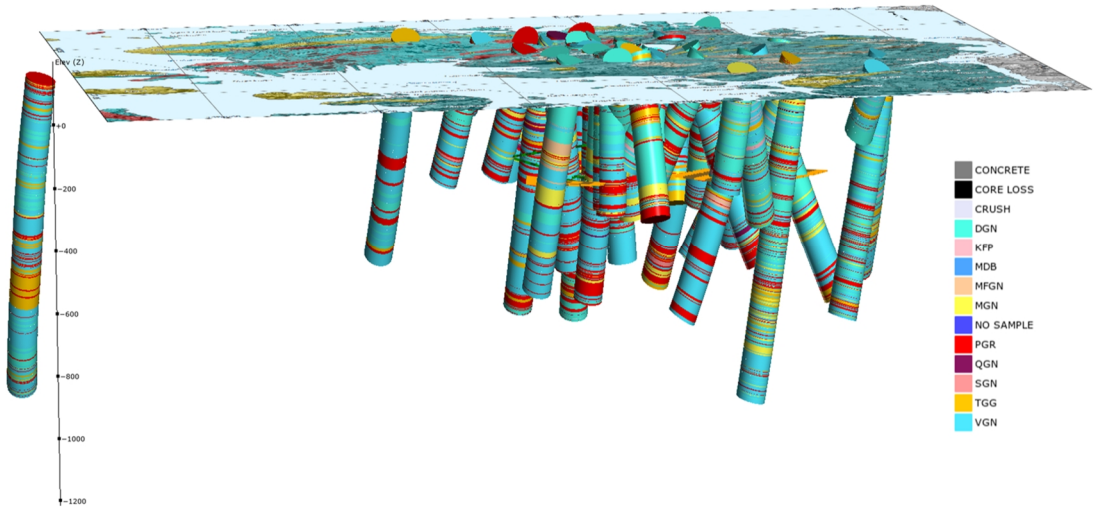

Figure 38. Olkiluoto island rock type information. Rock types: VGN, veined gneiss; TGG, tonalitic-granodioritic-granitic gneiss; DGN, diatexitic gneiss; MGN, mica gneiss; PGR, granitic pegmatoid; KFP, potassium-feldspar porphyry; QGN, quartzitic gneiss.

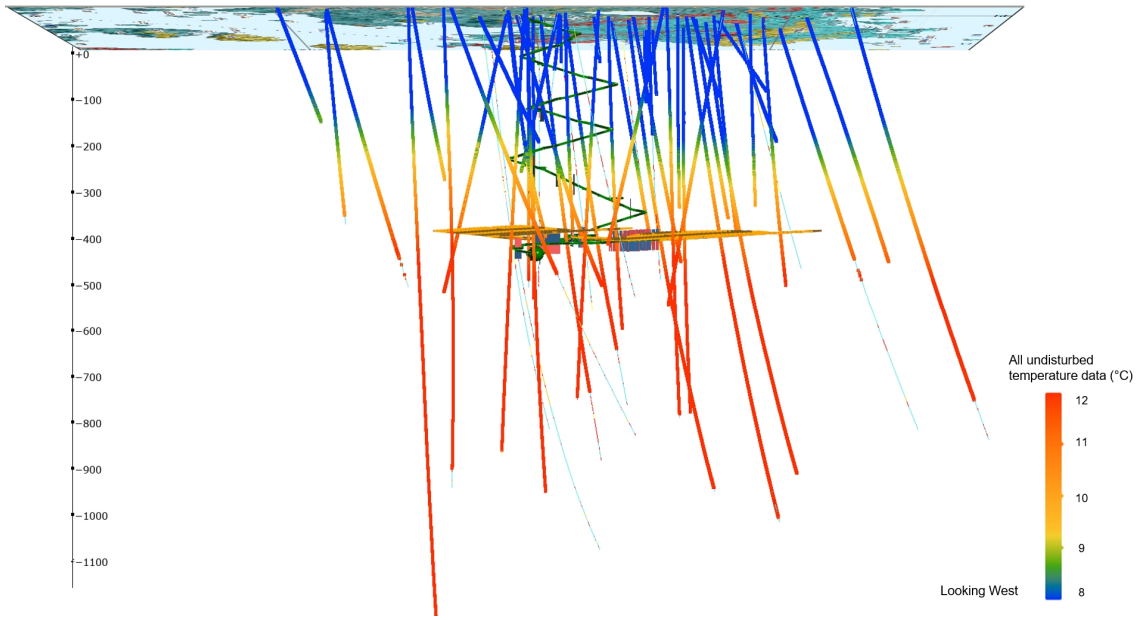

Figure 39. Temperature data that is applied to the final 3D model on top of the drillcore rock type information. ONKALO chain system and the planned location for the disposal tunnels.

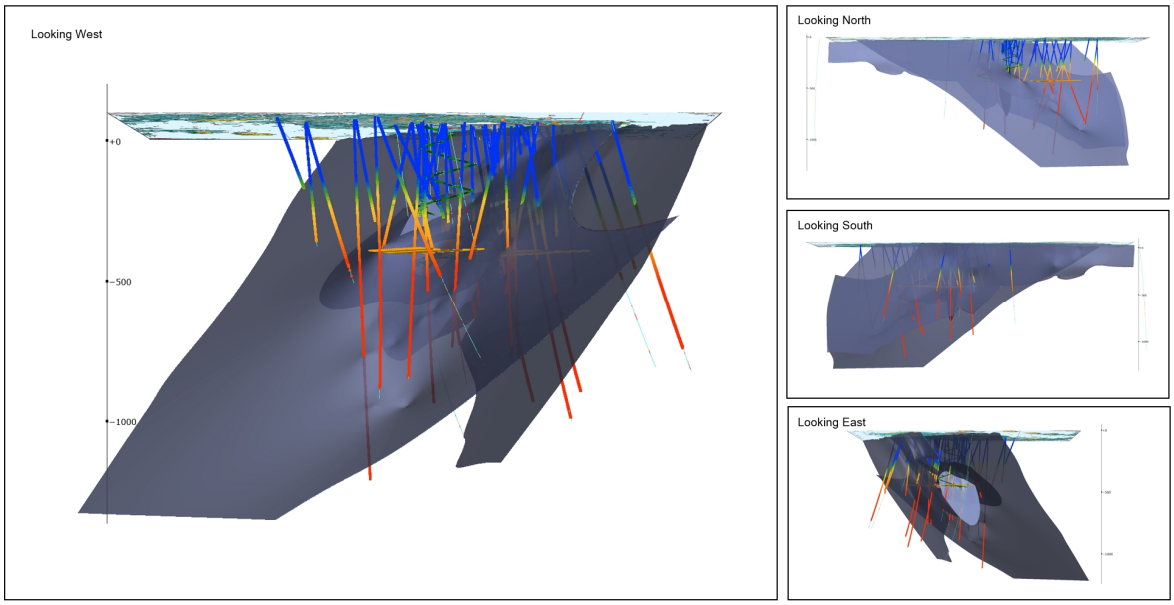

Figure 40. Temperature data that is applied to the final 3D model on top of the drillcore rock type information. ONKALO chain system and the planned location for the disposal tunnels. Fracture structure models OL-BFZ020A, OL-BFZ020B, OL-BFZ099 and OL-BFZ300 indicate the major brittle fault zones.

The resultant 3D layer model created for the whole island of Olkiluoto can be seen in Figure 41. The model presents the available drillcore information, the layer model created with the numeric module by using linear interpolation and the four major brittle fault zones. An increasing temperature profile with increasing depth can be observed). One major anomaly between the coordinates of E1526000 – E1527000 can be detected when looking south. The anomaly presents a local temperature low creating approximately 1°C – 2°C difference to the surrounding model. The model is sliced from E1526000, E1526500 and E1527000 (marked as A, B, C, respectively) when looking south and the slices are turned to look west (Figure 42, Figure 43 and Figure 44). At the surface, above the distinguished anomaly is located the area of Marikarinnokka including the small lake of Olkiluoto island (Figure 4). Figure 43 presents the bottom of the anomaly whereas Figure 42 and Figure 44 present the sides. The anomaly can be seen to continue approximately half way through the model in north to south direction, beyond the planned disposal tunnelling network and the ONKALO chain system (Figure 44). When the major brittle fault zones are shown in the model it appears that OL-BFZ099 is located right at the detected temperature anomaly.

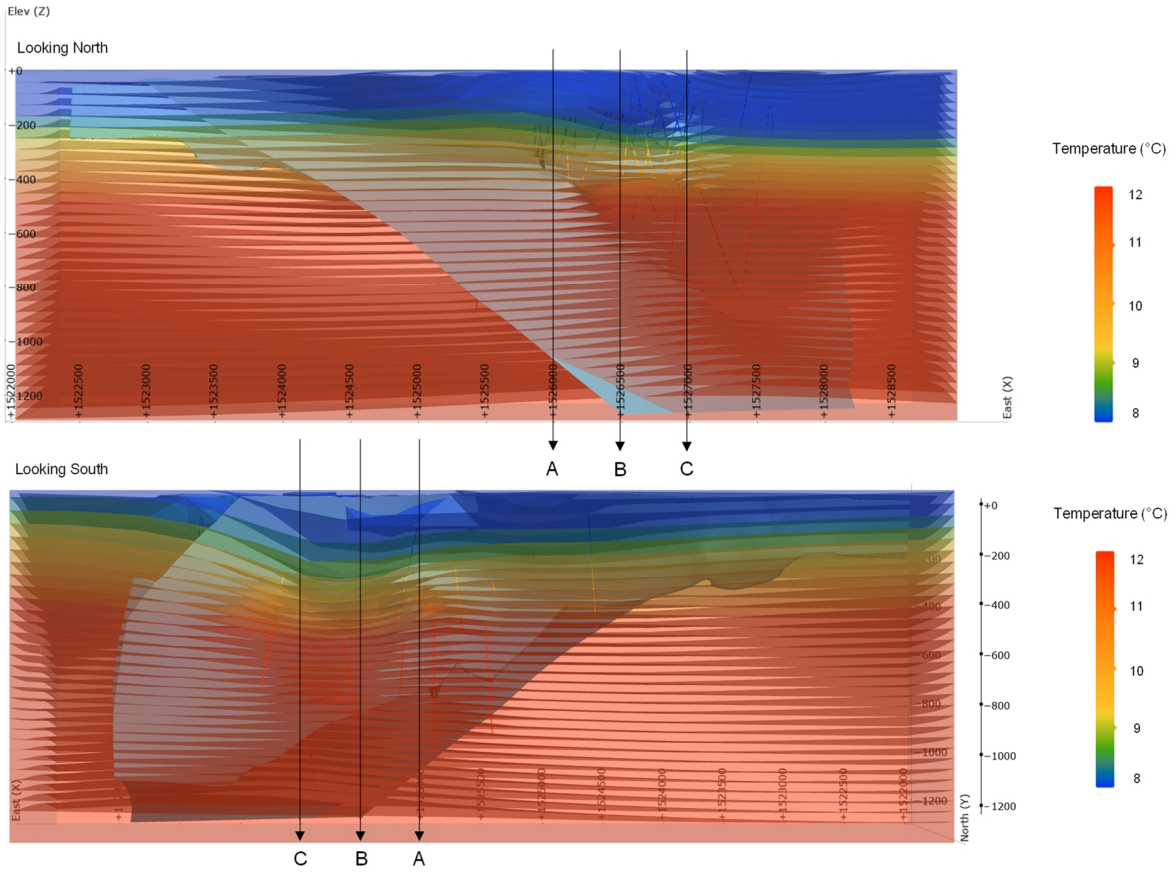

Figure 41. Resultant 3D layer model looking north (top) and south (bottom) for the whole island of Olkiluoto. The arrows indicate the location of the same temperature anomaly on both sides of the model at E1526000, E1526500 and E1527000 marked as A, B, C, respectively. Inside the model are plotted the drillholes and the applied data as well as the four major brittle fault zones (OL-BFZ020a, OL-BFZ020b, OL-BFZ099 and OL-BFZ300).

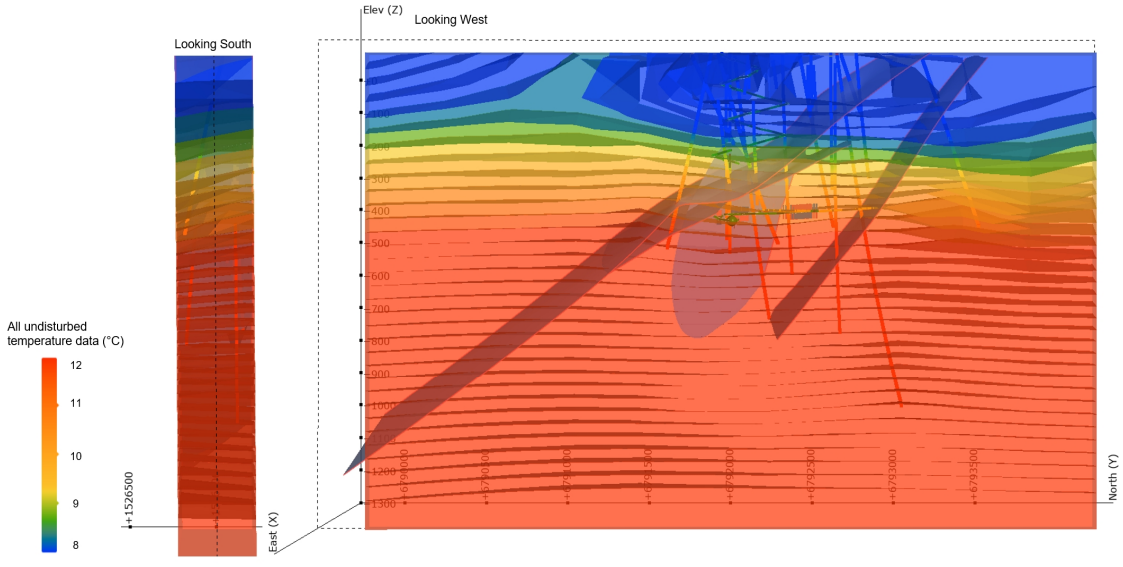

Figure 42. Resultant 3D layer model sliced at E1526000 (A) at the side of the observed anomaly. Inside the model are plotted the drillholes and the applied data, ONKALO chain system and the planned location for the disposal tunnels as well as the four major brittle fault zones (OL-BFZ020a, OL-BFZ020b, OL-BFZ099 and OL-BFZ300). Major temperature disturbance can be observed in the centre part of the sliced model as well as on the north end of the model approximately reaching 400m in depth. In horizontal direction the disturbance is restricted to the most northern brittle fault zone (OL-BFZ099).

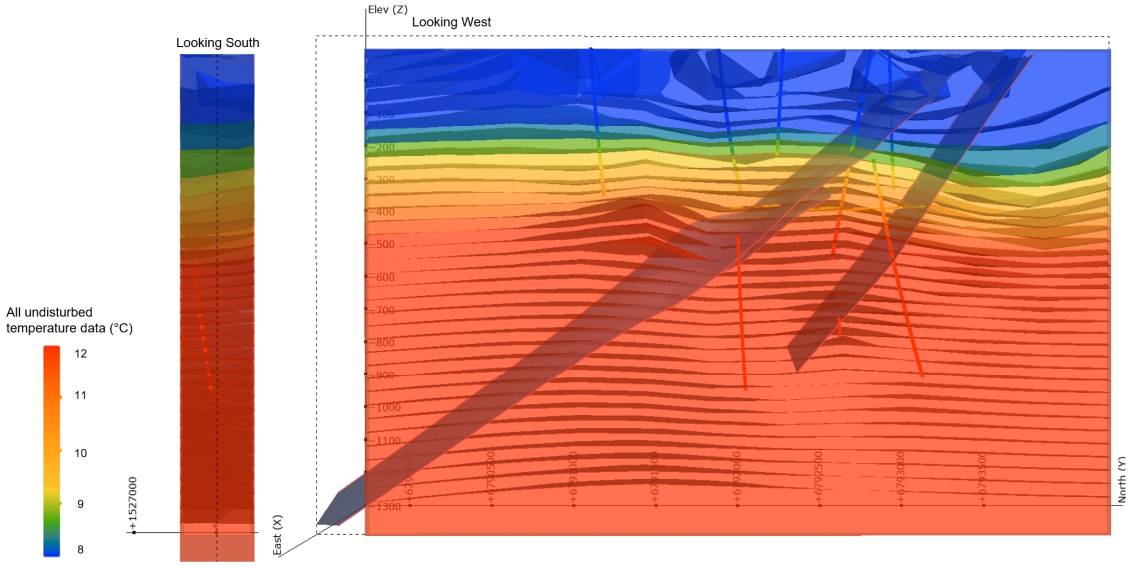

Figure 43. Resultant 3D layer model sliced at E1526500 (B) at the bottom of the observed anomaly. Inside the model are plotted the drillholes and the applied data, ONKALO chain system and the planned location for the disposal tunnels as well as the four major brittle fault zones (OL-BFZ020a, OL-BFZ020b, OL-BFZ099 and OL-BFZ300). Major temperature disturbance can be observed in the north end of the model approximately reaching 500 m in depth. A secondary anomaly, not observed in Figure 41, can be seen between 400 – 500 m in depth in the middle of the model on top of the OL-BFZ020a BFZ.

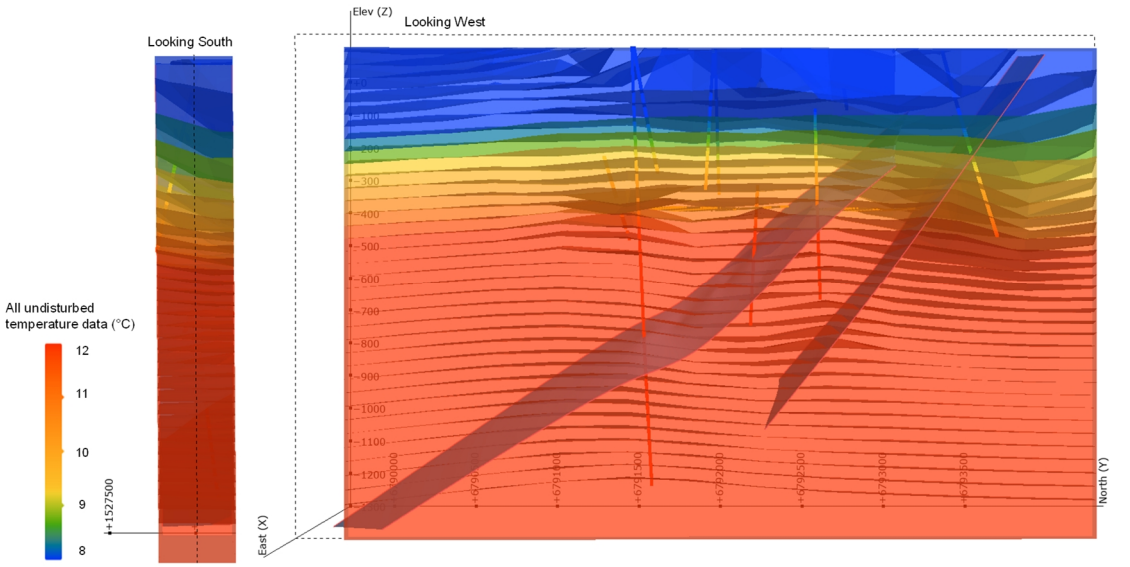

Figure 44. Resultant 3D layer model sliced at E1527000 (C) at the side of the observed anomaly. Inside the model are plotted the drillholes and the applied data, ONKALO chain system and the planned location for the disposal tunnels as well as the four major brittle fault zones (OL-BFZ020a, OL-BFZ020b, OL-BFZ099 and OL-BFZ300). Major temperature disturbance can be observed in the north end of the model continuing approximately until 500 m in depth and continuing half way through the model in N-S direction.

Presenting 3D models in 2D, creates a challenge and therefore 2D serial section slicing is used to visualize the model. Location of the 2D slices relative to the Olkiluoto island can

be seen in Figure 45. The slices are generated with 300 m spacing resulting in five slices which are placed so that they cover the planned disposal tunnelling network (Figure 46). However, these slices only present the situation at each individual location and not any further. Therefore, especially the relation between the disposal tunnels and the fracture zones should not be over interpreted.

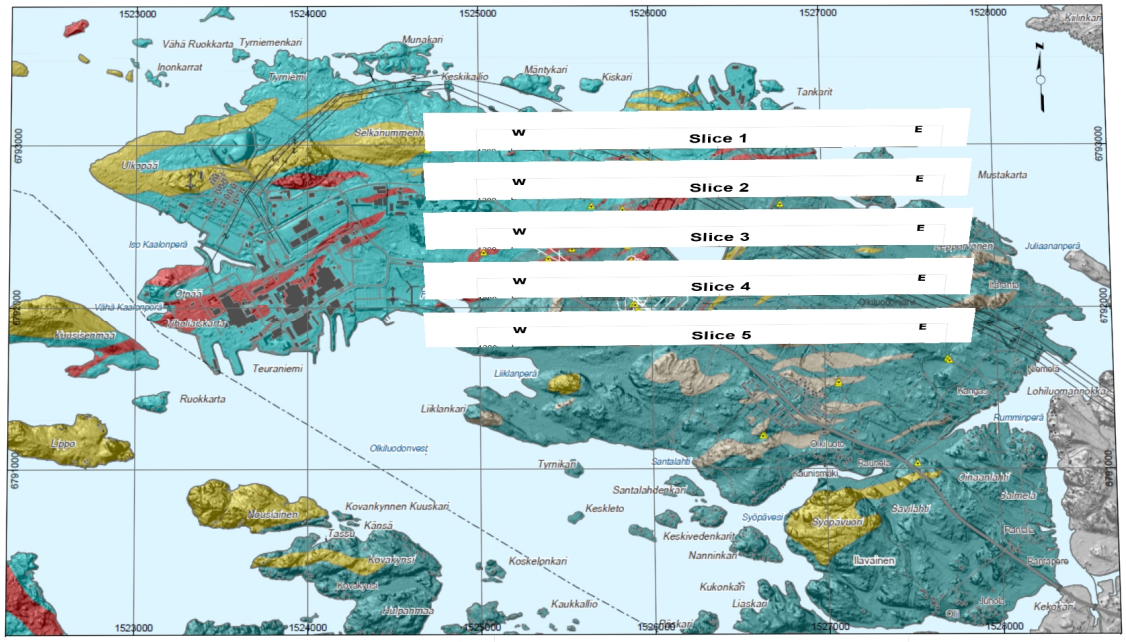

Figure 45. Location of the 2D slices relative to the Olkiluoto island.

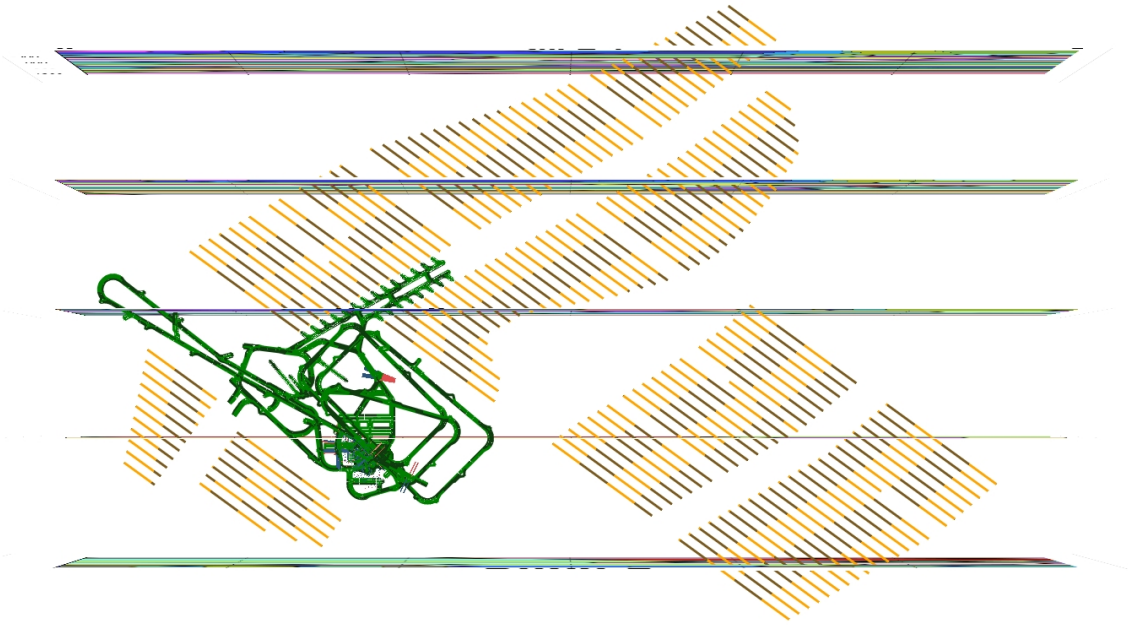

Figure 46. Location of the 2D slices relative to the planned tunnelling system. Slice one on top and rest respectively. Looking straight down and heading north.

Slice 1 (Figure 47) is located northernmost out of the 2D slices. The planned tunnelling network is located between the fracture zones OL-BFZ099 and OL-BFZ020A. The low temperature anomaly (Figure 41) can also be identified within the slice. Slice 2 (Figure 48) presents an area cut by two of the major fracture zones (OL-BFZ099 and OL-BFZ020A) with an appearance of fracture zone OL-BFZ020B. The cut is located at the same position where a low temperature anomaly is observed in Figure 41. Slice 3 (Figure 49) presents an area cut by all the fracture zones, OL-BFZ300 cutting the planned tunnelling network almost vertically. Directly on top of the slice is located the small lake of Olkiluoto island. Slice 4 (Figure 50) presents an area where the fracture zones OL-BFZ099 fades away and rest of the zones almost join. The planned tunnelling network is now located mainly on top of the fracture zones. Slice 5 (Figure 51) presents the southernmost cut. Fracture zone OL-BFZ099 is no longer visible and all the planned tunnelling network is located on top of the fracture zones. In large scale, temperatures at the disposal tunnel depth seem relatively homogenous (Figure 47, Figure 48, Figure 49, Figure 50 and Figure 51). However, almost all the tunnelling network parts which are visible in the slices are located at a border of a temperature interval. This indicates a situation where even bordering tunnels, or even further, bordering disposal holes could be located within a different initial bedrock temperature range. The area needs to be

inspected with model restricted just to the disposal depth in order to get better understanding of the temperature scale within the cuts. Nonetheless, these 2D slices provide a good insight to the location of the tunnelling network relative to the fracture zones.

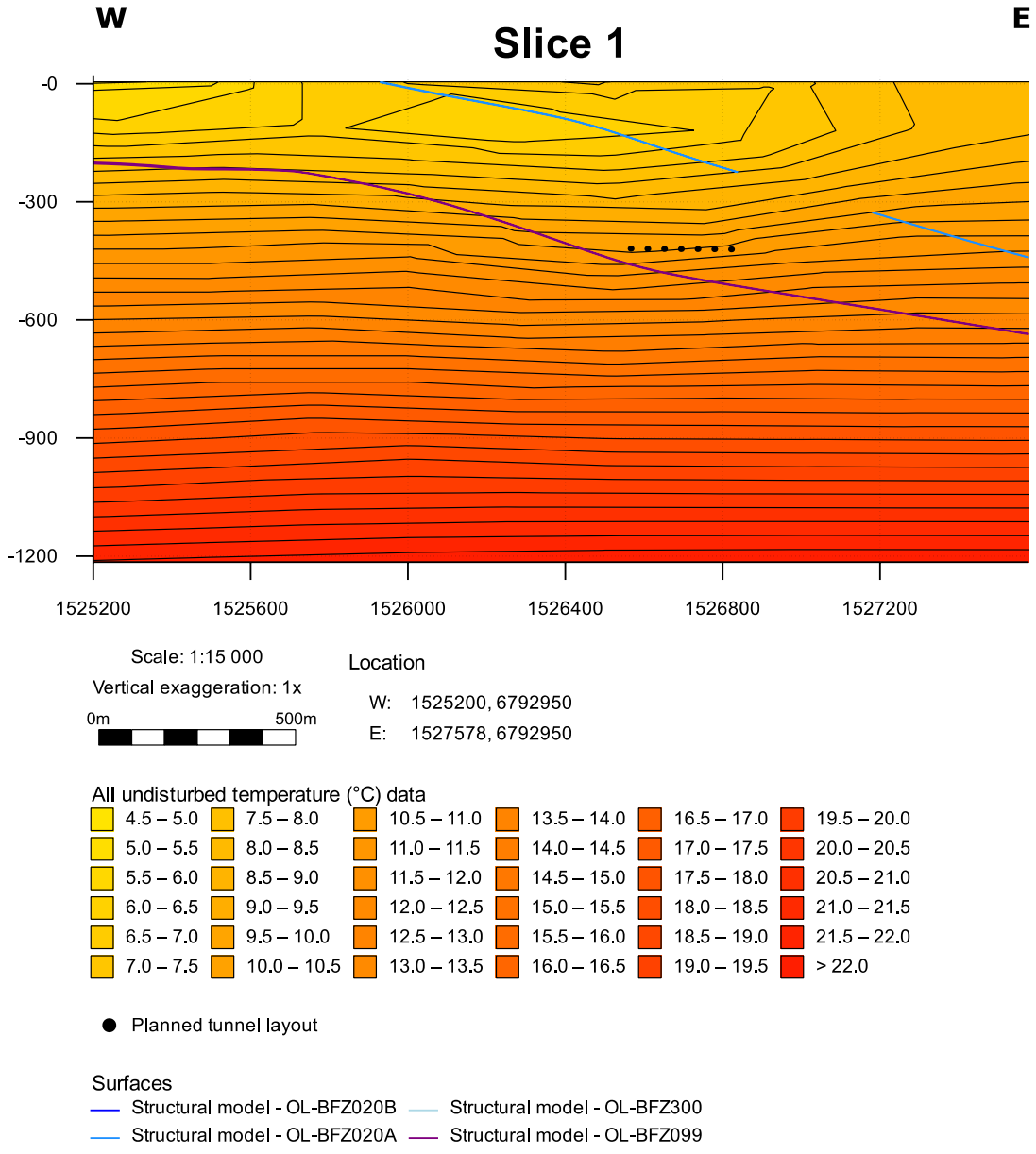

Figure 47. Slice 1 with maximum depth of 1200 m. Black dots show the location of the tunnelling system.

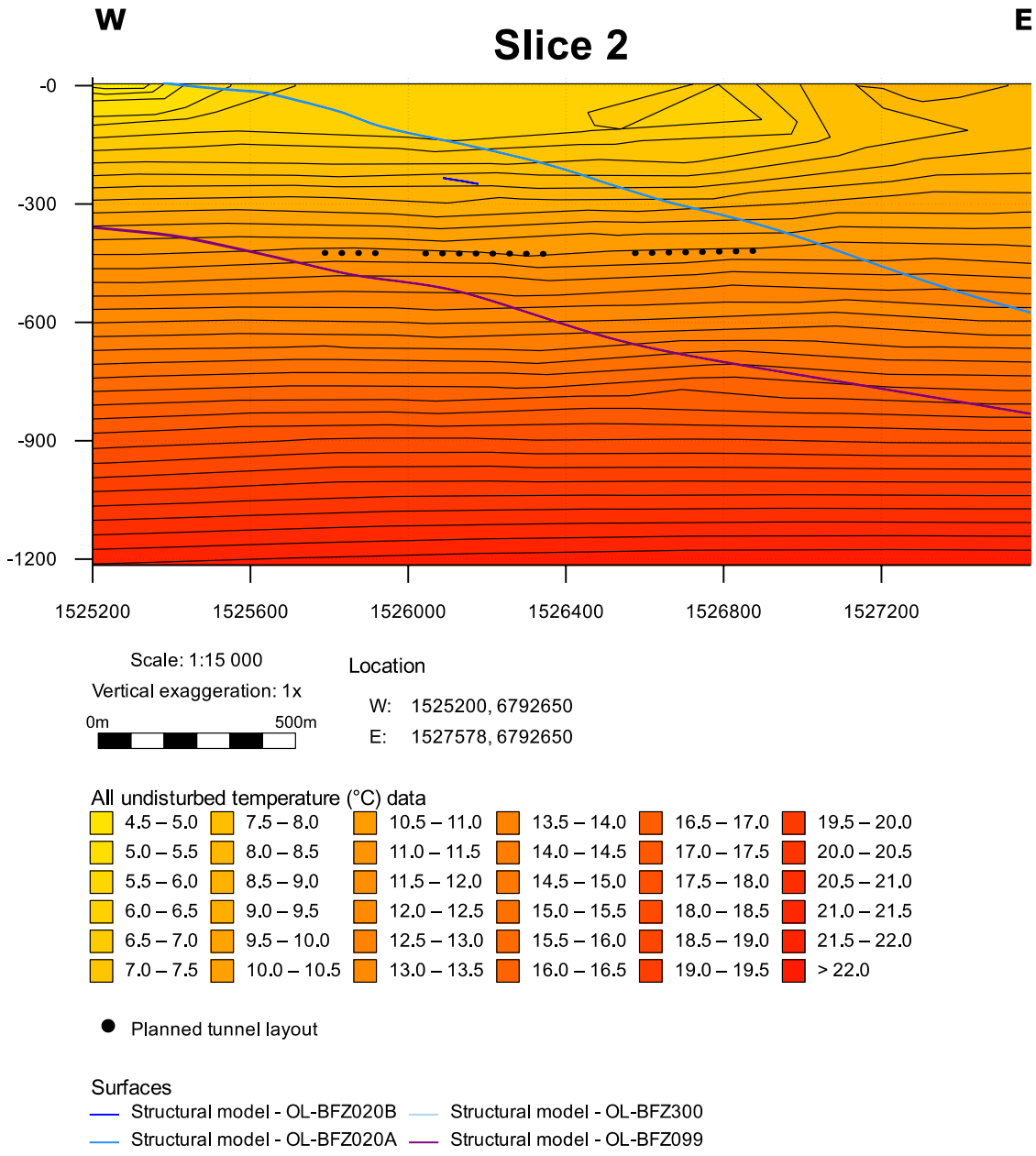

Figure 48. Slice 2 with maximum depth of 1200 m. Black dots show the location of the tunnelling system.

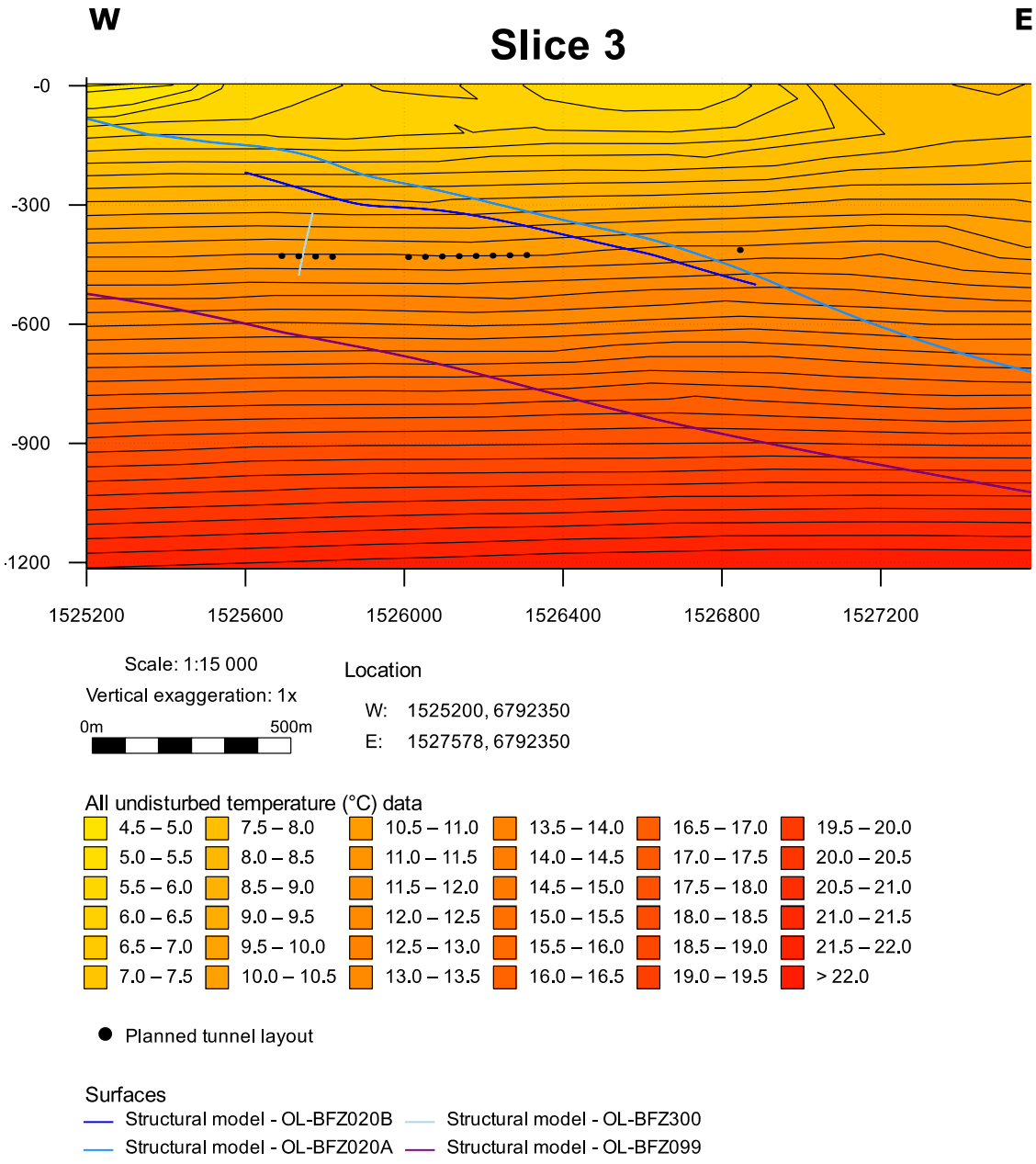

Figure 49. Slice 3 with maximum depth of 1200 m. Black dots show the location of the tunnelling system.

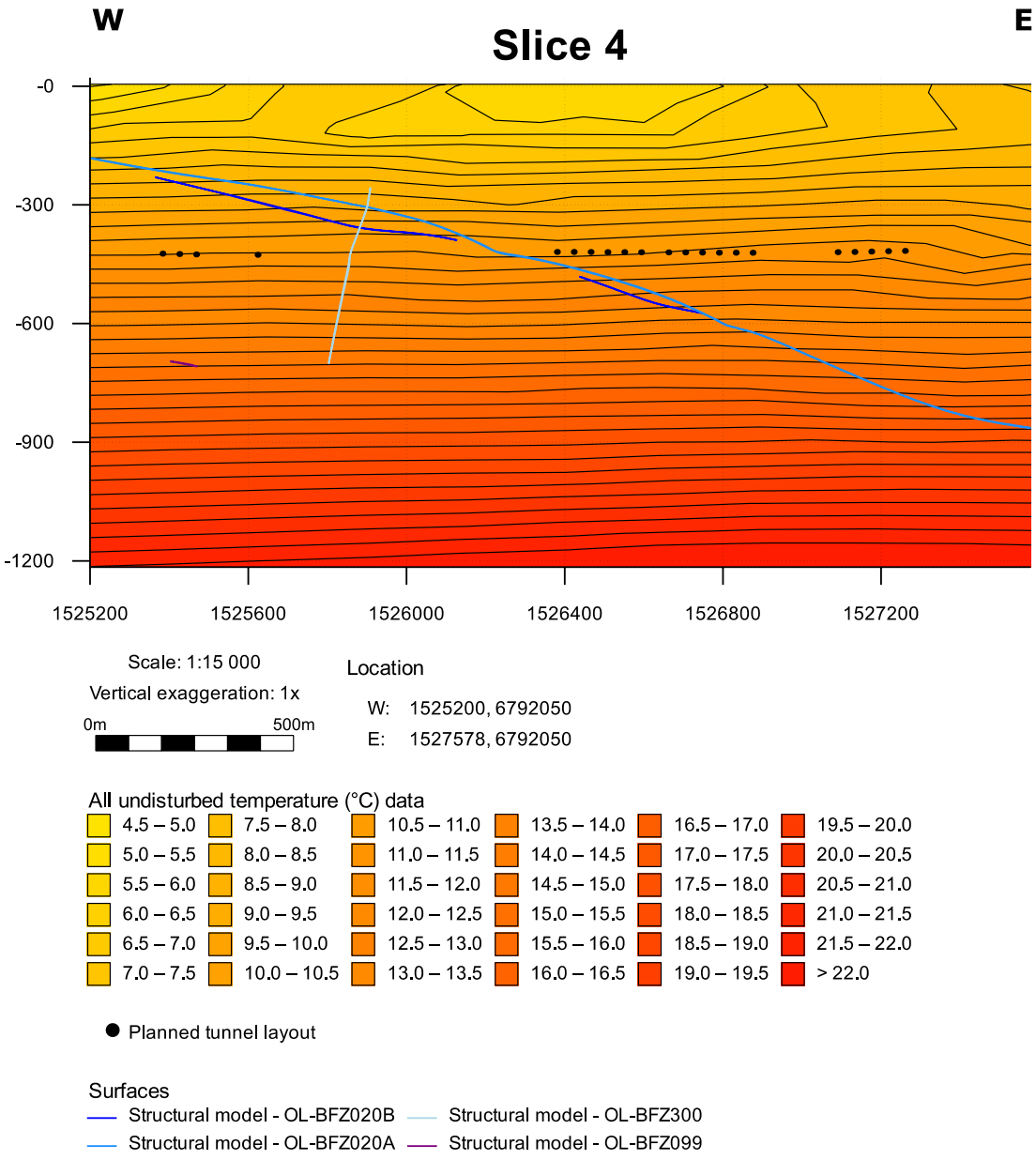

Figure 50. Slice 4 with maximum depth of 1200 m. Black dots show the location of the tunnelling system.

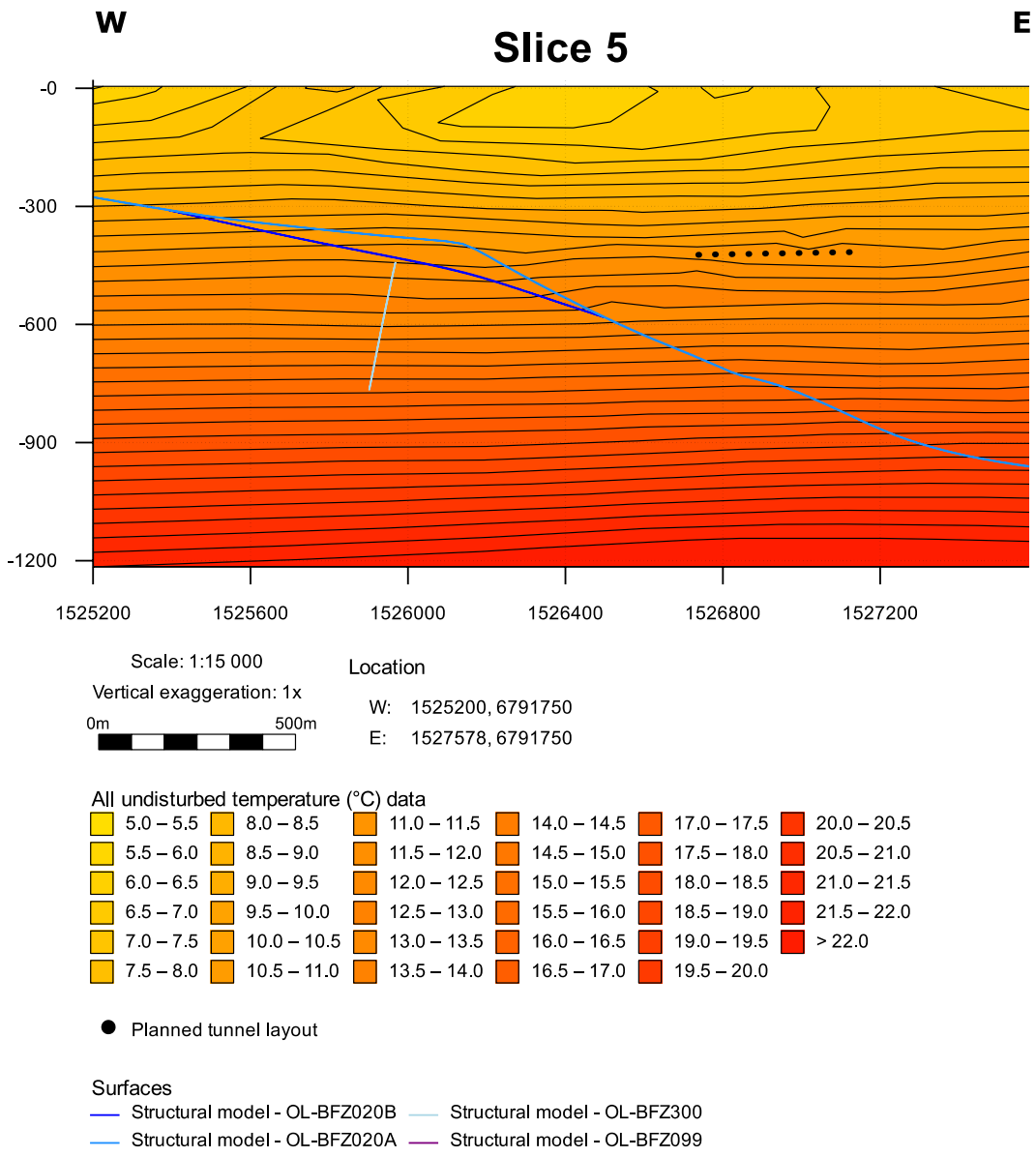

Figure 51. Slice 5 with maximum depth of 1200 m. Black dots show the location of the tunnelling system.

The temperature model restricted to the disposal depth of 412 – 432 m relative to the whole Olkiluoto island is presented in Figure 53. The ONKALO chain system, the planned tunnelling network and the data applied to the model can be seen in Figure 53. One large low temperature anomaly can be observed in the eastern parts of the model, two individual low temperature anomalies can be observed at the northern parts of the model and one large low temperature anomaly in the middle of the model (Figure 53). It is noticeable that the data which is used to create the model at this depth is relatively small group of points. Figure 54 shows the restricted temperature model relative to the

Olkiluoto island (Figure 4). When this is identified, it is important to remember the interpolation scheme behind the model.

When the fracture zones identifying the major brittle fault zones are plotted to the restricted model a correlation between them can be observed (Figure 55). The largest low anomaly observed in the eastern parts of the model is located right at the largest brittle fault zone (OL-BFZ020A). The two individual low anomalies located at the northern part of the model are also located on the second major brittle fault zone (OL-BFZ099). The absolute shape of the anomalies however might be over taken by the interpolation and should only be considered indicative.

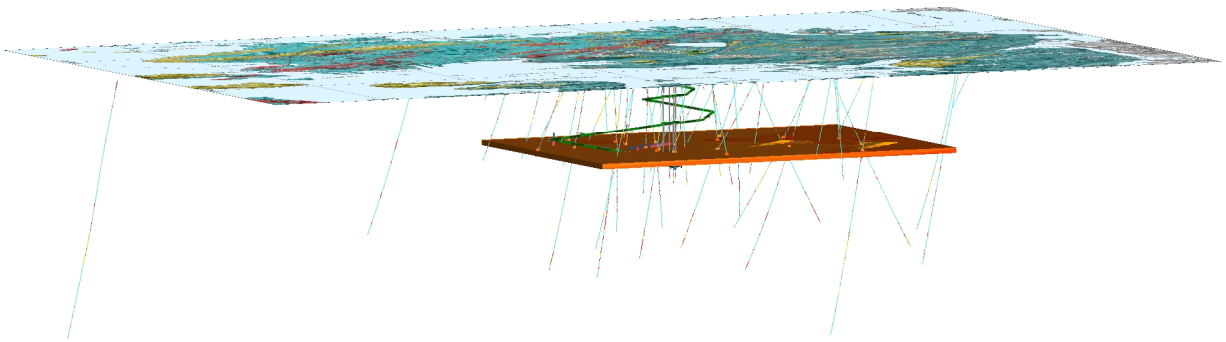

Figure 52. Resultant 3D model at the planned disposal depth. The area is restricted according to the planned disposal tunnel network to 412 – 432 m in depth. With the model are plotted Olkiluoto island rock type information and the projected map of the Olkiluoto island area.

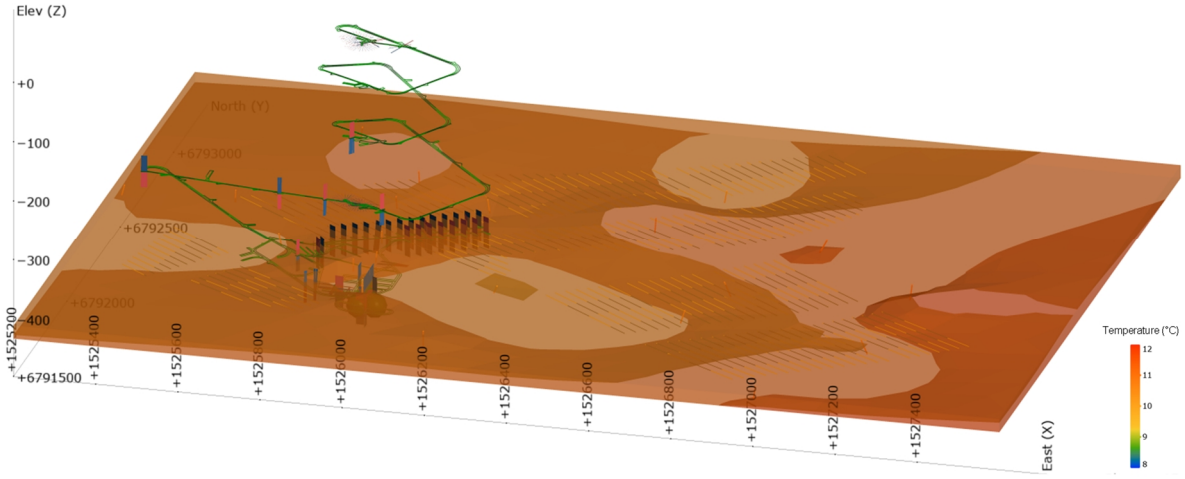

Figure 53. 3D temperature model for the planned disposal depth according to the ONKALO chain system and the planned disposal tunnels. Locations of the plotted drillholes show the data that is applied to create the model. Several low anomalies can be observed as well as an anomaly high at the east end of the model.

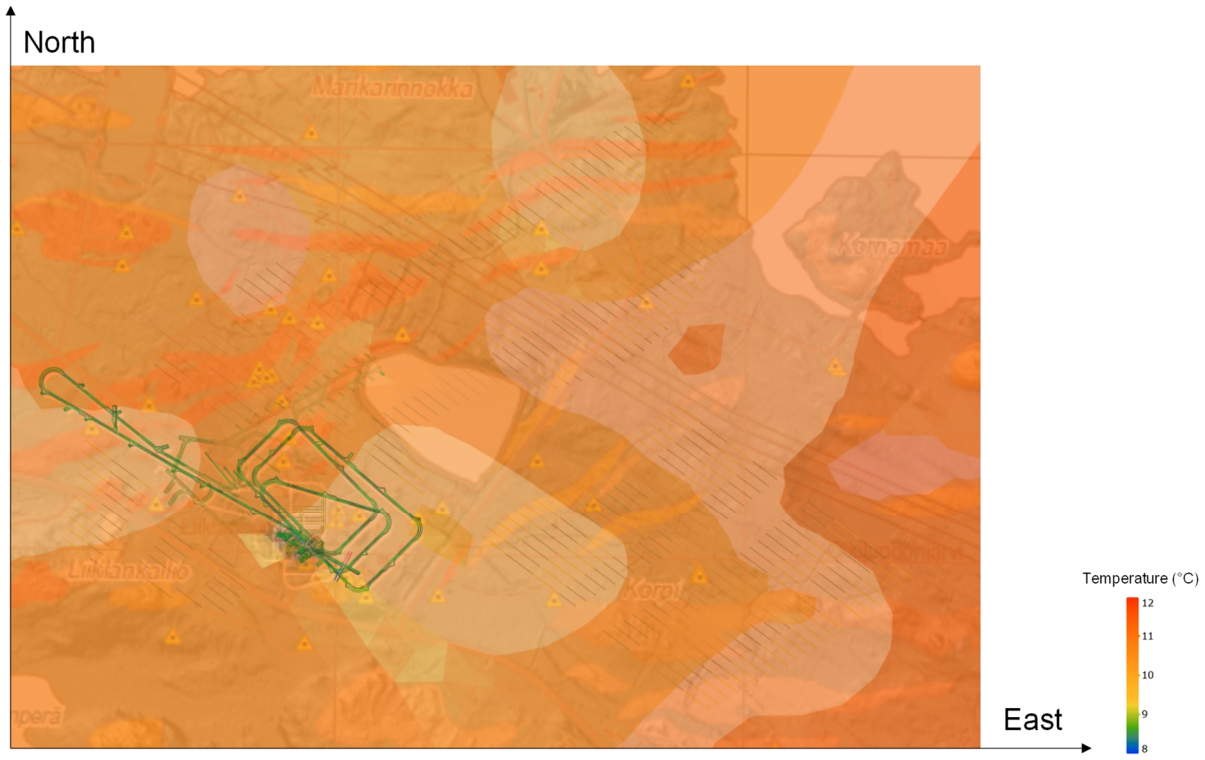

Figure 54. Looking straight down. 3D temperature model for the planned disposal depth according to the ONKALO chain system and the planned disposal tunnels plotted on top of the map of Olkiluoto island (Figure 4). Several low anomalies can be observed as well as an anomaly high at the east end of the model.

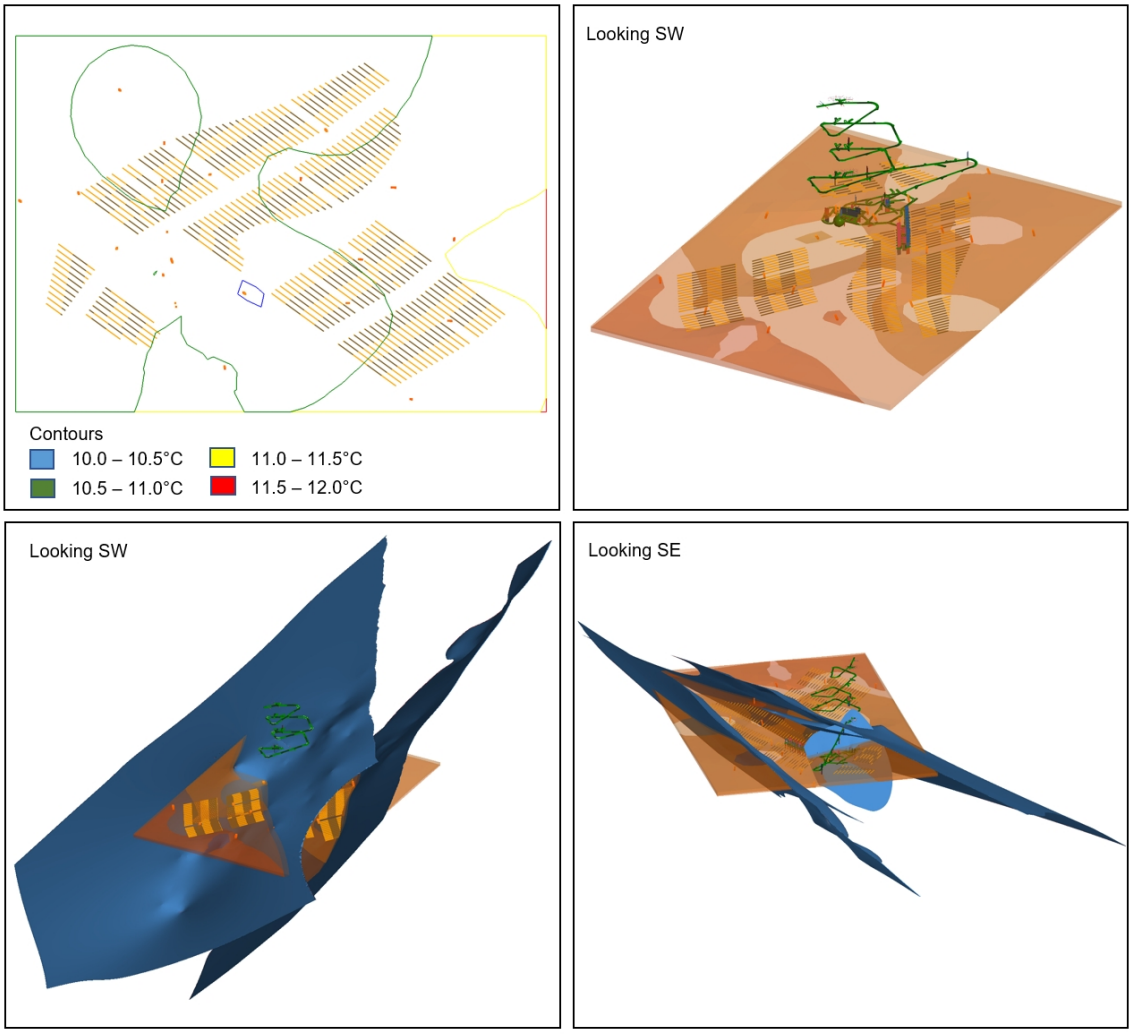

Figure 55. Top left: Contour lines for the restricted model. Temperatures encountered at the restricted depth are between 10.0°C – 12.0°C. Top right: 3D temperature model restricted to the planned disposal depth, ONKALO chain system and the planned location of the disposal tunnels, looking SW. Location of each data point is indicated with orange dots. Several temperature anomalies can be observed. Bottom left: Fracture structure models OL-BFZ020A, OL-BFZ020b, OL-BFZ099 and OL-BFZ300 (blue planes) indicate the major brittle fault zones relative to the temperature model, looking SW. Bottom right: Fracture structure models OL-BFZ020A, OL-BFZ020b, OL-BFZ099 and OL-BFZ300 (blue planes) relative to the temperature model, looking SE.

The restricted model is also presented in 2D through serial section slicing. The location of the slices relative to the tunnelling network can be seen in Figure 56. The slices are located with 300 m spacing resulting in five slices all together. The slicing is not completely the same as the slicing conducted for the model of the whole island.

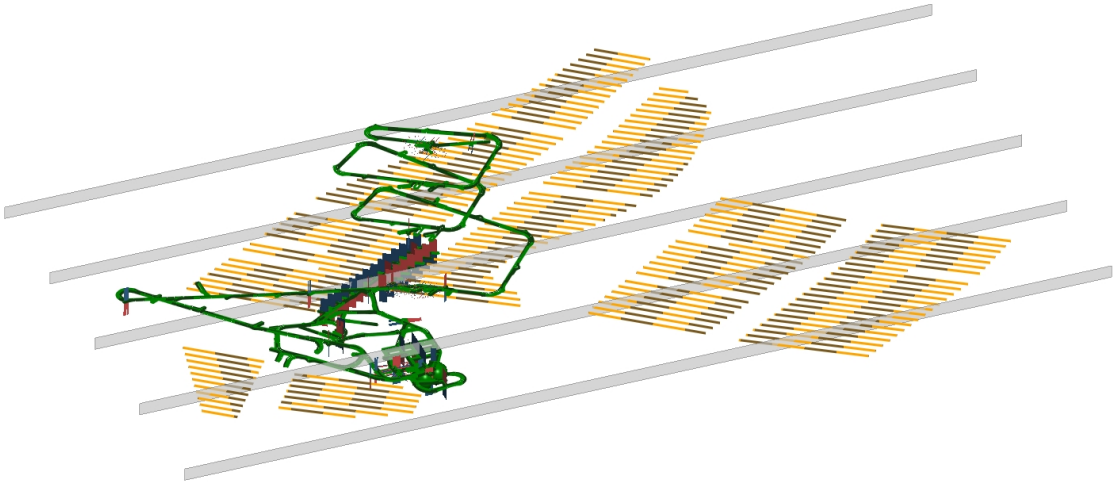

Figure 56. Location of the 2D slices (grey planes) according to the tunnelling system. Slice number 1 is the furthest one and rest respectively.

Slice 1 (Figure 57) is located northern most within the model. The planned tunnelling network is located fully in temperature range of 10.5°C – 11.0°C. Slice 2 (Figure 58) is located in relatively homogenous area. The planned tunnelling network is fully located in temperature range of 11.0°C – 11.5°C. Slice 3 and slice 4 are both located at the low temperature anomaly observed both in the model for the whole island and for the restricted model (Figure 59 and Figure 60). The planned tunnelling network is located in temperature range of 10.5°C – 11.5°C. Slice 5 (Figure 61) is the southernmost slice. The planned tunnelling network is fully located in temperature range of 11.0°C – 11.5°C. Slices 2 to 5 all point out the location of the eastern high temperature anomaly (Figure 58, Figure 59, Figure 60 and Figure 61). As the anomaly high cannot be correlated to any of the results presented in this study it should be considered with caution.

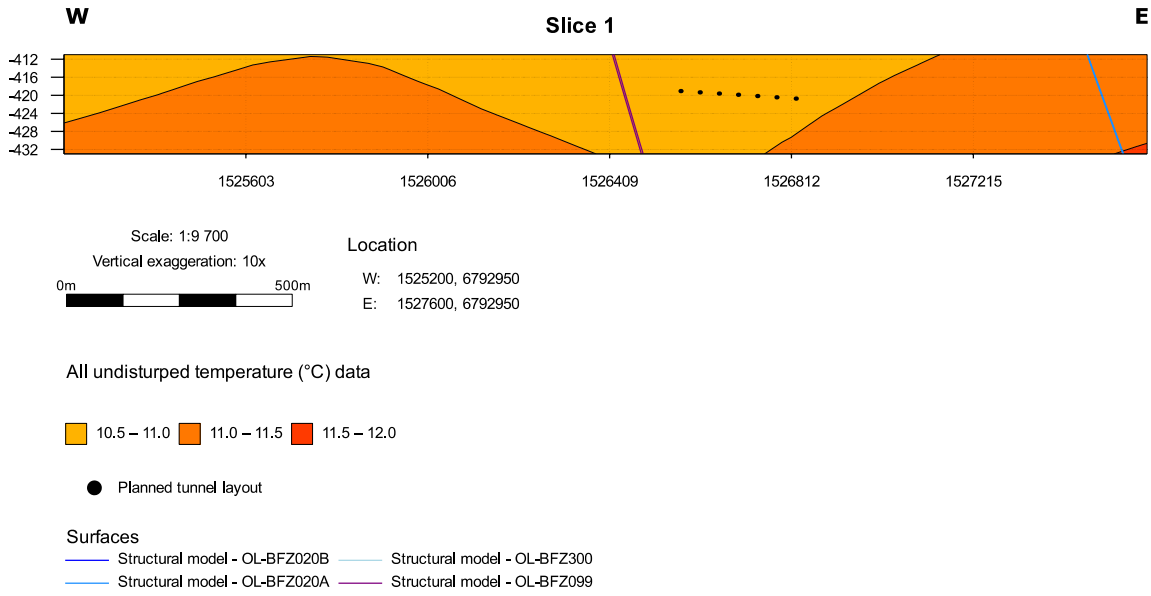

Figure 57. Slice 1 with maximum depth of 432 m. Black dots show the location of the tunnelling system lines show the location the fracture models.

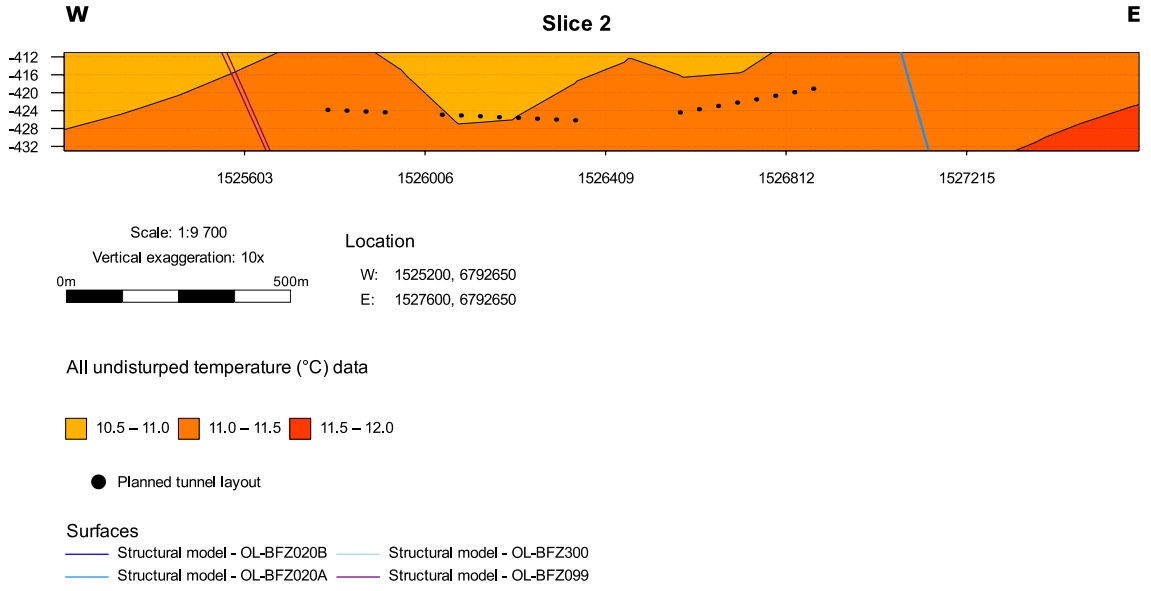

Figure 58. Slice 2 with maximum depth of 432 m. Black dots show the location of the tunnelling system lines show the location the fracture models.

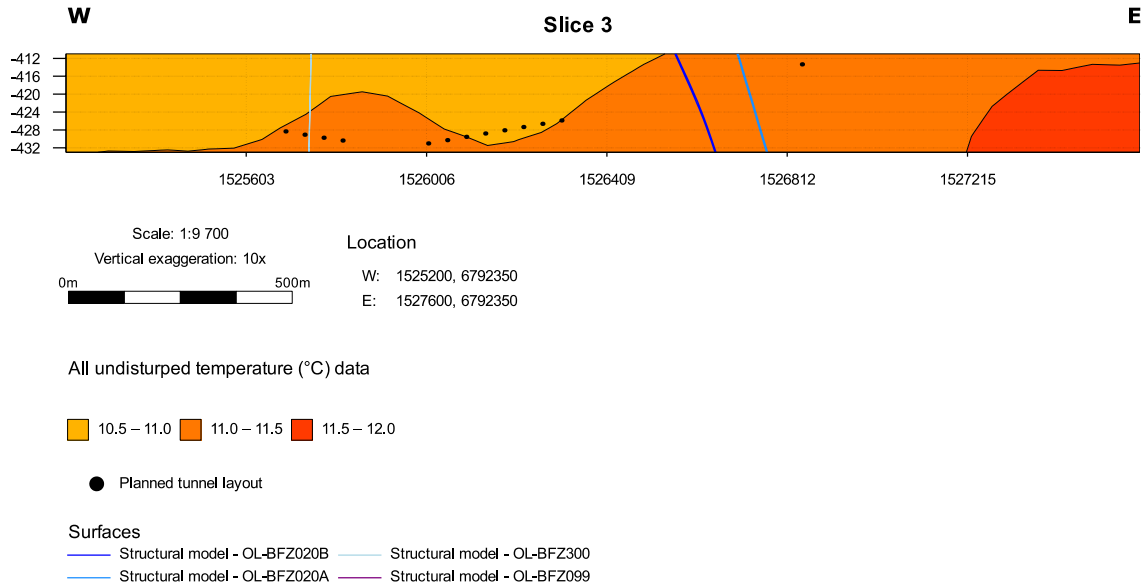

Figure 59. Slice 3 with maximum depth of 432 m. Black dots show the location of the tunnelling system lines show the location the fracture models.

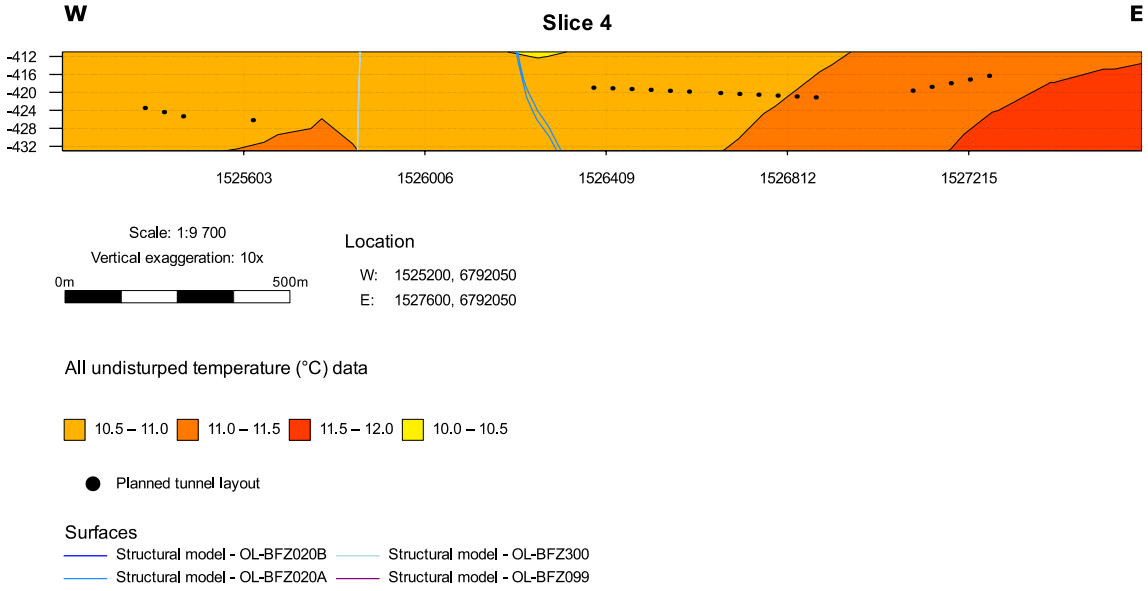

Figure 60. Slice 4 with maximum depth of 432 m. Black dots show the location of the tunnelling system lines show the location the fracture models.

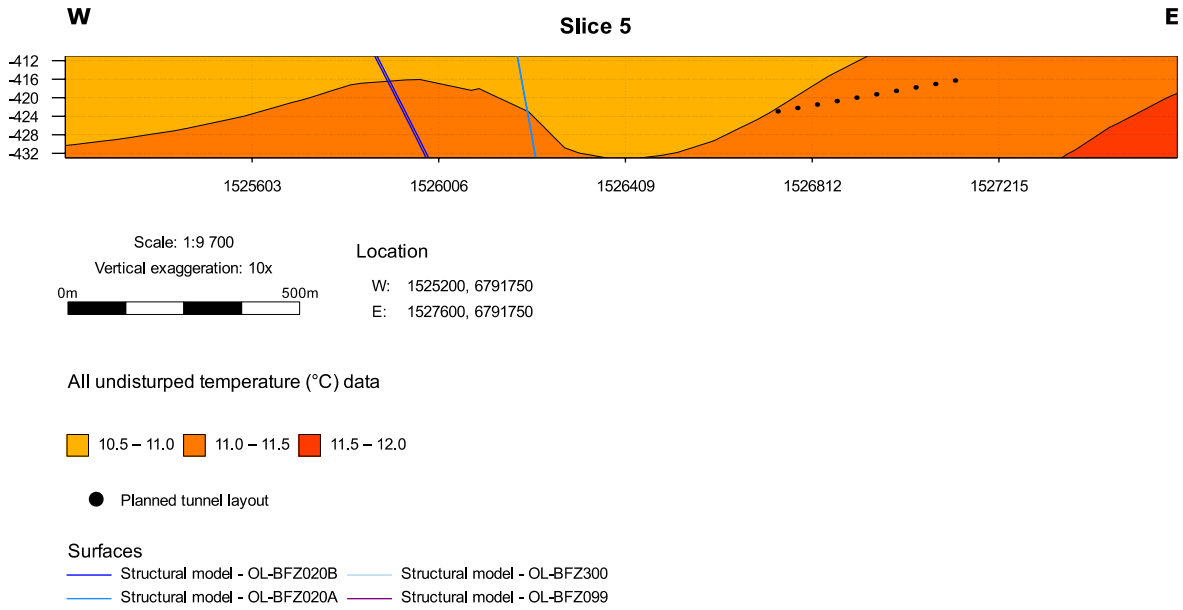

Figure 61. Slice 5 with maximum depth of 432 m. Black dots show the location of the tunnelling system and lines show the location the fracture models.

7. DISCUSSION

Modelling and quantifying the initial state of the bedrock in Olkiluoto is part of the thermal dimensioning project required in order to carry out the planned disposal of spent nuclear fuel in Olkiluoto, Finland. Previous estimates of the average bedrock temperature/depth profile, along with temperature gradients at the study location were carried out with temperature data which had not been inspected and classified according to the actual measurement specifics. The analysis carried out here demonstrates the need of a unifying data classification in order to create models or any further interpretations based on the temperature data that Posiva Oy has from Olkiluoto and ONKALO sites. When such a classification was carried out, the results indicated, that the 3D models created with the temperature data, could be used as a part the dimensioning of the Olkiluoto island by providing information through the observed temperature anomalies.

Applications for the temperature data sets presented in this study, are extensive. The measurements conducted between the main three methods and Antares configuration contain approximately > 500 individual measurements. It could be considered rare, to have such a large data set providing temperature information of bedrock, to exist in such

limited area. Most of the temperature data presented in this study are merely a byproduct of the actual measurements. This, along with other aspects such as unknown calibration history creates challenges within the analysis, classification and modelling phases. These aspects are discussed further in this section.

7.1 Reliability of the temperature data and the classification

All the main data sets have problems when considering the reliability and accuracy of the data. First of the geophysical multiparameter drillhole measurements were conducted 30 years ago and tracking back to the actual procedures while measuring remains challenging. This problem can be observed within all the four main methods excluding Antares (only one measurement occasion) during the early days of measuring. The geophysical, TERO and Antares measurements were designed to measure temperatures directly, whereas PFL measurements were not. This reflects especially to the early PFL measurements where there was no interest of recording or monitoring the temperature measurements. After the understanding of the usability of the acquired temperature data the reporting has been uniform and comprehensive, approximately since the 2000's. Out of all the data sets the measurements conducted with PFL are the most extensive and homogenous. This presents possibilities within the future measurements conducted with PFL regarding to the temperature data. However, with PFL, it is important to recognize that the recorded depth is not the absolute depth relative to the measured temperatures. There are two main reasons for a bias 1) error due to the location of the temperature sensor relative to the depth counter and, 2) the modifications done to the probe during the measurements conducted without pumping of water resulting in velocity error. The geophysical multiparameter drillhole loggings are still carried out in Olkiluoto and especially in ONKALO. These measurements also present an ideal way of expanding the temperature data sets presented in this study. TERO measurements are a relatively small data set when compared to the other main methods. Currently there are no plans on prospective measurements. However, the current TERO measurement package present, according to the classification, a worthy package where the main limitations are not problems in the measuring phase, but rather the extent of the data set. As Posiva Oy is moving on from the research phase to the actual construction phase, it must be considered what is the most efficient way to increase the temperature information from Olkiluoto.

Calibration of the measuring apparatuses varies. With PFL measurements there are clear procedures which have been followed and result in a relatively reliable outcome. The largest variation with calibration procedure can be observed with the geophysical drillhole loggings due the usage of several different measuring apparatuses. Calibrations might have been carried out with all the applicable procedures yet resulting in differences between the quality of the calibration, set by the available equipment. These problems within the data sets create a need for a unifying data classification frame. In order to such a frame to work it was built to be as transparent as possible. The usage of these data sets presented here is not only limited to this study and therefore the main features for useful classification are

- Clear
- Easy to follow and traceable
- Combine all the possible information available

For later use the frame could be stripped down not to contain as many criteria or not to be as strict. The qualification frame puts all the available data to a same starting point. This allows for comparisons to be done to data, measured with different configurations. Despite the frame, not all aspects of each individual dataset can be removed, neither would it be desirable. For example, the dataset containing all un-erroneous PFL measurements is noticeably larger than the data set containing all the TERO measurements. Therefore, it is ideal to use the sets together, at least in the light of this study. Certain patterns can be observed within the final data classification. Each individual data set has a certain reason for resulting in a particular class more often than others. For TERO it appears to be calibration, for geophysics measurements calibration and turnover with the measurement configurations and for PFL the drillhole environment. As these aspects can be recognized they can also be affected. In line with the hypothesis the results indicate that analysis and classification of the provided temperature data contributes to a clearer understanding of the measurement phase specifics and therefore builds a better base for future data usage.

7.2 On the initial bedrock temperature

In order to carry out estimates for the average bedrock temperature and for the temperature gradient in Olkiluoto the data needed to be vertically corrected to the true vertical depth. The measured data and depth were interpolated according to the known vertical deviation from initial drillhole dip. As the interpolation is done by iterating the same computing method for all the data, the possibility of an error remains relatively small. However, as the initial drillhole dip information are used as given, a possibility of an error must be recognized to exist within the dip measurements.

Measurements conducted in the deep drillholes with PFL and geophysical drillhole loggings both show indications on temperature disturbance. Drillholes OL-KR1 – OL-KR5 measured with geophysical drillhole logging between 1989 – 1990 show disturbance caused by the measuring practice. These measurements do not present the undisturbed bedrock temperature of a bedrock and are not used in this study. Measurements conducted with any of the Malå GeoScience's Wellmac/Li configurations show disturbances within the temperature profiles with no clear pattern. Flow of water and defective measurements can be interpreted to be the main reasons. Measurement conducted with the ELGI KTRMQ-3-120-43Y probe configuration does not indicate disturbance caused by the above-mentioned reasons. However, the recorded temperature range indicate disturbance. The ELGI configuration has been used only once for temperature measurements. Due to the lack of data with that configuration the deviating temperature range cannot be confirmed to be caused by the equipment itself. When compared to other measurements conducted with the geophysical drillhole loggings the data still settles in with the temperature range of the other measurements. Therefore, the data is interpreted to present the undisturbed temperature of the bedrock. Measurements conducted with the Mount Sopris configuration show disturbances within the temperature profiles without clear pattern. Disturbance caused by water flow and defective measurements are both present. Errors in the PFL temperature data are mainly caused by defective measurements. Some small disturbances caused by water flow are also present but are generally located within the first 50 m of the measurement which is in any case disturbed by the varying surface temperature. TERO or Antares measurements did not indicate disturbance within the measurements. However, as both data sets are relatively small the usage of them is tied to the usage of the other data sets. When the data with major disturbances is excluded from further use, the reliability of the estimated initial bedrock temperature is strengthened.

The results for the average bedrock temperature (at 412m in depth, geophysical: 10.93 ± 0.09°C, PFL: 10.85 ± 0.02°C, TERO: 10.60 ± 0.08°C and Antares: 10.75°C) and for the temperature gradient (Geophysics: 1.47°C/100m, PFL: 1.43°C/100m, TERO: 1.65°C/100m and Antares: 1.39°C/100m) define and reinforce the results conducted in a previous study by Sedighi et al. (2014). The result conducted in this study, unlike the previous results by Sedighi et al. (2014), used only the data that underwent the data classification and showed no large-scale disturbances in the temperature/depth profile. However, each measurement was not examined point by point and especially within the smaller datasets this might create relatively large bias to the average temperature and gradient estimates. The generalizability of the results is limited by the possible errors within the computing. These errors should be taken into account when considering the usage of the numerical average value in the thermal dimensioning of the repository.

The temperature data acquired from ONKALO with PFL and TERO measurements were not used for the calculations. However, the effects of tunnelling should be taken into consideration when discussing the temperature profile in ONKALO as it has an immediate effect on the disposal locations. The effect of long-term cyclic temperature variation is also present and should not be neglected. According to the literature, an effect of a such cycle was seen to have an influence over ~1000 m in depth, which is mostly beyond the depths of the drillhole data presented in this study. The effect cannot be directly observed form the presented temperature profiles but should still be taken into consideration.

7.3 On the temperature model

The 3D layer temperature models generated in this study display the temperature data acquired in Olkiluoto in a way that has not been applied to it before. Acknowledging the possibilities and limitations of the model creates a base for a plausible model. The base of the model comes from the input data and therefore reflects all the way back to the data classification created in this study. The model presents an excellent way of testing the data classification platform. Only the data that did not show major disturbance within the temperature/depth profile (category A or B) were used. What is considered major remains open to interpretations. Excluding too much data also creates a bias and therefore it might be beneficial not to cut down the data sets too harshly. At the same time this study

concerns specifically temperature data, which is easily influenced by the surrounding parameters and circumstances and therefore might include errors which are difficult to distinguish. These errors show as anomalies in the model and thus each observed anomaly needs to be considered thoroughly.

Several temperature anomalies were observed within the models created for the whole island of Olkiluoto and for the restricted depositional depth. The settings used in both models were the same except the areal extend. The biggest difference between the models is the used data. When the area is restricted, so is the amount of data. This might lead to differing results due to the interpolation function. However, when the two models were compared, they seemed to indicate anomalies to the same areas. The main difference is within the absolute shape of the anomalies.

A low temperature anomaly was observed in the layer model for the whole island of Olkiluoto. When the four major brittle fault zones were plotted to the model, it appeared that the observed anomaly is located right at the fracture zone OL-BFZ099. This could indicate that the anomalies are caused by the interference of water flow. The largest uniform low temperature anomaly was detected at the eastern parts of the restricted model. Several smaller individual low temperature anomalies were detected at the northern parts of the restricted model. All these anomalies showed connection with the major BF zones. The dot like smaller temperature anomalies might be one larger anomaly but due to the interpolation are plotted as two or wise versa for the largest anomaly. Temperature range according to the temperature model at the restricted depth is between 10.0°C – 12.0°C. Where the intervals are set to 0.5°C, meaning that the lowest values are between 10.0°C – 10.5°C and the highest values are between 11.5°C – 12.0°C. These values support the earlier results for the temperature gradient at the study location. The model is created in such a way that it is possible to track back each individual data point. As all the methods had varying temperature gradients the anomalies could also simply be produced by the uneven distribution of the methods within the model. For example, the eastern part of the model could only include data from geophysical measurements and therefore result in high temperature anomaly. However, the differences within the temperature gradients were found to be relatively small. And thus, even though the effect cannot be ignored, it can be considered to only cause relatively small errors.

The location of the brittle fault zones (OL-BFZ020a, OL-BFZ020b, OL-BFZ099 and OL-BFZ300), in both of the models, suggest that the low temperature anomalies could be caused by water flow within the fractures which has cooled down the surrounding bedrock at the location. However, the model should be inspected according to the hydraulic zone (HZ) models in order to confirm the connection between the observed anomalies and the possible water leakage. A present brittle fault zone does not automatically mean present hydraulic zone or vice versa.

Not all the anomalies can be tied into a possible cause. High temperature anomaly observed in the eastern parts of the restricted model cannot be explained with the aspects presented in this study. If the anomaly is not caused by problems within the modelling phase, a possible alternative explanation is needed. Now the model does not consider the geology of the area. By combining the model to the 3D geological model, a better understanding of rock variations within the bedrock could possibly be achieved. For example, variations in the rock types could indicate possible cause to the high temperature anomaly, or vice versa. If the temperature model presented in this study was combined with up-to-date geological model and with the hydraulic model of Olkiluoto area a better overall understanding of the study area could be achieved.

Further research is needed to determine the causes and relationships that the surrounding environment has on the temperature data. For example, the effect of the sea surrounding the island needs to be further studied. Sedighi et al. (2014) found that the temperatures were relatively higher at the southern parts of the Olkiluoto island and interpreted the difference to be caused by the adjacent sea. In this study such a correlation was not observed. However, it is beyond the scope of this study to exclude such an effect.

7.4 Recommendations for future work

Future studies should take into account the possibilities of expanding the temperature data sets with PFL and geophysical drillhole measurements. Aspects influencing the measured temperatures should be considered already in the planning phase of each measurement in the light of modelling the initial undisturbed bedrock temperatures. By proceeding in such manners, the resultant temperatures are more likely to present the undisturbed bedrock temperature without major disturbances.

The temperature models presented in this study are easy to modify and for example adding new data is straight forward. Creating parallel temperature models with differing base settings could lead in better understanding of the model specifics and the uncertainties within the model.

To better understand the implications of these results, future studies could address the relationship between the temperature model presented here, the hydraulic zones and a 3D geological model of the area. This could lead in a better understanding of the rock type variations within the bedrock regarding the observed temperature anomalies and in understanding the connections between the observed temperature anomalies and possible water interference.

The 3D layer models presented in this study are in no means a geothermal heat transfer model. In order to create a complete understanding of the geothermal state of the area a comprehensible and thorough 3D geothermal model is needed.

8. CONCLUSIONS

This research aimed to identify a unifying data classification platform for large and spread out data packages. The study clearly illustrates how such a classification improves the usability of data and leads into a better understanding of the possibilities and weaknesses within it. In conclusion according to the available temperature data, the initial bedrock temperature and the temperature gradient in Olkiluoto present thermally a relatively uniform bedrock. New estimates of the initial bedrock temperatures and the temperature gradient endorse the previous estimates. The 3D models presented here allocate a completely new manner to present the temperature data. A clear correlation between the fracture models indicating the major brittle fault zones (and possibly the hydraulic zones) and the temperature anomalies can be recognized with in the temperature models. Not all uncertainties within the generated models can be excluded and therefore, especially the absolute shape of the anomalies should only be considered indicative. The thermal models presented here yield the best results when combined with the major brittle fault zones. Therefore, combining the model together with the geological model of the area and the hydraulic model of the area could contribute in a clearer over all understanding of the

planned disposal location. The thermal related issues, which the repository will undergo once operating are significant and have fundamental contributions on the evolution of the repository. Therefore, future work regarding the thermal dimensioning of Olkiluoto island is still needed to ensure efficient and economical final solution for the spent nuclear fuel.

9. ACKNOWLEDGEMENTS

This thesis work was commissioned by Posiva Oy and conducted in collaboration with Geofcon. I would like to thank everyone, to mention Sophie Haapalehto, Pekka Kantia and Johannes Suikkanen, who made it possible for me to be part of this project. I have truly enjoyed working with the topic and could not have asked for better opportunity. As collecting of the material used in this study spreads out to over 30 years, I would like to address a special thank you, for everyone who helped me to get on track with the measurement specifics. I would like to thank my supervisors Ilmo Kukkonen and Risto Kiuru for their guidance throughout this work.

To my family and friends outside the University, who have never doubted me when I have. Lastly, I am forever thankful to my associates here at the University of Helsinki for your peer support and friendship.

REFERENCES

Aaltonen, I., Heikkinen, E., Paulamäki, S., Säävuori, S., Vuorinen, S. and Öhman, I. 2009. Summary of petrophysical analysis of Olkiluoto core samples 1990-2008. Posiva Oy, Working-report 2009-11, 239 pp.

Aaltonen, I. (ed.), Lahti, M., Engström, J., Mattila, J., Paananen, M., Paulamäki, S., Gehör, S., Kärki, A., Ahokas, T., Torvela, T. and Front, K. 2010. Geological Model of the Olkiluoto Site, Version 2. Posiva Oy, Working-report 2010–70, 580 pp.

Aaltonen, I. (ed.), Engström, J., Front, K., Gehör, S., Kosunen, P., Kärki, A., Paananen, M., Paulamäki, S., Mattila, J. 2016. Geology of Olkiluoto. Posiva Oy, POSIVA-report 2016-16, Eurajoki, Finland. 398 pp.

Balling, N. 2013. The lithosphere beneath Northern Europe: structure and evolution over three billion years. Aarhus University. (Doctoral thesis)

Beardsmore, G. R. & Cull, J. P. 2001. Crustal heat flow: A guide to measurement and modelling. Cambridge: Cambridge University Press.

Birch, F., Roy, R. and Decker, E. 1968. Heat flow and thermal history in New York and New England. Studies of Appalachian Geology: Northern and Maritime, 437-451.

Carslaw, H. and Jaeger, J. 1990. Conduction of heat in solids. 2nd edition. Oxford: Clarendon Press.

Fowler, C. 2005. The solid Earth: an introduction to global geophysics. Second edition Cambridge New York: Cambridge University Press.

GTK, 2019. Geological Map of Finland 1:5 000 000, Geological Survey of Finland (GTK) Hakku database.

Haapalehto, S., Malm, M., Saari, J., Lahtinen, S. and Saaranen, V. 2017. Results of Monitoring at Olkiluoto in 2016, Rock Mechanics. Posiva Oy, Working-report 2017-47, 108 pp.

Haapalehto, S. 2019. ONK-PP379-382 kuva. [Personal communication email 16.9.2019]

Hassinen, P. 1998. Pohjaveden suolaisuuden mittaukset Eurajoen Olkiluodon kairanrei'issä KR 1-KR4 ja KR9 vuonna 1997. Posiva Oy, Working-report 1998-14, 66 pp.

Heikkinen, E. 2019. [Personal communication email 12.2.2019]

Huotari, T. and Kukkonen, I. 2004. Thermal Expansion Properties of Rocks: Literature Survey and Estimation of thermal Expansion Coefficient for Olkiluoto Mica Gneiss. Posiva Oy, Working-report 2004-04 Eurajoki, Finland. 68 pp.

Ikonen, K. and Raiko, H. 2012. Thermal dimensioning of Olkiluoto repository for spent fuel. Posiva Oy, Working Report 2012-56, 76 pp.

Ikonen, K., Kuutti, J. and Raiko, H. 2018. Thermal Dimensioning for the Olkiluoto Repository − 2018 Update. Posiva Oy, Working-report 2018-26, Eurajoki, Finland. 130 pp.

Jaupart, C. and Mareschal, J., 2011. Heat generation and transport in the earth. Cambridge New York: Cambridge University Press.

Julkunen, A. 1989. Geofysikaaliset reikämittaukset Eurajoen Olkiluodossa, kairanreiät KR2 ja KR3. Suomen Malmi Oy, TVO/Paikkatutkimukset, Working-report 89-88, 29 pp.

Julkunen, A. 1990. Geofysikaaliset reikämittaukset Eurajoen Olkiluodossa, kairanreiät KR4 ja KR5. Suomen Malmi Oy, TVO/Paikkatutkimukset, Working-report 90-44, 31 pp.

Julkunen, A., Kallio, L. and Hassinen, P. 1995. Geofysikaaliset reikämittaukset Eurajoen Olkiluodossa 1995, kairanreiät KR2, KR3, KR4, KR6, KR7 JA KR8. TVO/Paikkatutkimukset, PATU-95-71, 116 pp.

Julkunen, A., Kallio, L. and Hassinen, P. 1996. Geofysikaaliset reikämittaukset Eurajoen Olkiluodossa 1996, kairareikä OL-KR9. Posiva Oy, PATU-report 1996-41, 40 pp.

Julkunen, A., Kallio, L. and Hassinen, P. 2000. Geofysikaaliset reikämittaukset Eurajoen Olkiluodossa 1999, kairanreikä KR11. Posiva Oy, Working-report 2000-02, 46 pp.

Julkunen, A., Kallio, L. and Hassinen, P. 2004. Geophysical Borehole Logging in Boreholes OL-KR23, OL-KR24, OL-KR25 and OL-KR25B at Olkiluoto, in Eurajoki,2003. Posiva Oy, Working-report 2004, 73 pp.

Kiviranta, L., Kumpulainen, S., Pintado, X., Karttunen, P. and Schatz, T. 2018. Characterization of Bentonite and clay materials 2012 - 2015. Posiva Oy, Working-report 2016-05, 164 pp.

Kjørholt, H. 1992. Thermal properties of rocks. Teollisuuden Voima Oy, TVO/Site investigations, Working-report 1992-56, 13 pp.

Korpisalo, A., Suppala, I., Kukkonen, I. and Koskinen, T. 2013. Thermal Conductivities and Diffusivities of Rocks in Four Shallow ONKALO Holes and Drillholes OL-KR46 and OL-KR56. Posiva Oy, Working-report 2013-36, 32 pp.

Komulainen, J. 2017. Posiva Flow Log (PFL), Tool for detection of groundwater flows in bedrock. Mine Water and Circular Economy IMWA 2017, 8 pp.

Komulainen, J. and Hurmerinta, E. 2018. Difference Flow and Electrical Conductivity Measurements at the Olkiluoto Site in Eurajoki Drillhole OL-KR58. Posiva Oy, Working-report 2017-19, 142 pp.

Komulainen, J., Vaittinen, T., Picken, P. and Heikkinen, E. 2018. Hydrogeological Bedrock Characterisation Based on Posiva Flow Log Measurement Data. Mine Water and Circular Economy IMWA 2018, 6 pp.

Kukkonen, I. 1987. Vertical variation of apparent and paleoclimatically corrected heat flow densities in the central Baltic shield. Journal of geodynamics, 8, 33-53.

Kukkonen, I. and Lindberg A. 1995. Thermal conductivity of rocks at the TVO investigation sites Olkiluoto, Romuvaara and Kivetty. Nuclear Waste Commission of Finnish Power Companies, Report YJT-98-08, 29 pp.

Kukkonen, I. & Lindberg, A. 1998. Thermal properties of rocks at the investigation sites: measured and calculated thermal conductivity, specific heat capacity and thermal diffusivity. Posiva Oy, Working-report 1998-09, 29 pp.

Kukkonen, I. 2000. Thermal properties of the Olkiluoto mica gneiss: Results of laboratory measurements. Posiva Oy, Working-report 2000-40, 28 pp.

Kukkonen, I., Suppala, I., Korpisalo, A. and Koskinen, T. 2005. TERO Borehole Logging Device and Test Measurements of Rock Thermal Properties in Olkiluoto. Posiva Oy, POSIVA-report 2005–09, 103 pp.

Kukkonen, I., Suppala, I., Korpisalo, A. and Koskinen, T. 2007. Drillhole Logging Device TERO76 for Determination of Rock Thermal Properties. Posiva Oy, POSIVA-report 2007-01, 43 pp.

Kukkonen, I., Kivekäs, L., Vuoriainen, S. and Kääriä, M. 2011. Thermal Properties of Rocks in Olkiluoto: Results of Laboratory Measurements 1994–2010. Posiva Oy, Working-report 2011-17, 96 pp.

Kukkonen, I., Korpisalo, A., Suppala, I., and Koskinen, T. 2014. In situ determination of thermal properties of rocks in crystalline rock drillholes with TERO56 and TERO76 devices. Posiva Oy, POSIVA-report 2013-06 Eurajoki, Finland. 63 pp.

Kukkonen, I. 2015. Thermal properties of rocks at Olkiluoto: results of laboratory measurements 1994-2015. Posiva Oy, Working-report 2015-30, 110 pp.

Kukkonen, I., Rath, V. and Korpisalo, A. 2015. Paleoclimatic Inversion of Ground Surface Temperature History from Geothermal Data on the Olkiluoto Drillhole OL-KR56. Posiva Oy, Working-report 2015-49, 72 pp.

Lachenbruch, A.H., 1968. Preliminary geothermal model of the Sierra Nevada. Journal of Geophysical Research, 73(22), 6977-6989.

Lahti, M., Tammenmaa, J. and Hassinen, P. 2001. Kairanreikien OL -KR 13 ja OL -KR 14 geofysikaaliset reikämittaukset Eurajoen Olkiluodossa vuonna 2001. Posiva Oy, Working-report 2001-30, 125 pp.

Lahti, M., Tammenmaa, J. and Hassinen, P. 2003. Kairanreikien Ol-KR19, Ol-KR19b, Ol-KR20, Ol-KR20b, Ol-KR22, Ol-KR22b ja Ol-KRB jatko-osan geofysikaaliset reikämittaukset Eurajoen Olkiluodossa vuonna 2002. Posiva Oy, Working-report 2003-05, 167 pp.

Lahti, M. and Heikkinen, E. 2005. Geophysical Borehole Logging of the Boreholes KR23 Extension, KR29 and KR29b at Olkiluoto 2004. Posiva Oy, Working-report 2005-17, 83 pp.

Laurila, T. and Tammenmaa, J. 1996. Geofysikaaliset reikämittaukset Eurajoen Olkiluodossa 1996, kairanreikä OL-KR 10. TVO/Paikkatutkimukset, PATU-96-14, 43 pp.

Leapfrog Geo User Manual. 2019. Webpage visited at 19.9.2019. Available at http://help.leapfrog3d.com/Geo/4.5/en-GB/LeapfrogGeoUserManual.pdf

Luukas, J., Kousa, J., Nironen, M. and Vuollo, J. 2017. Major stratigraphic units in the bedrock of Finland, and an approach to tectonostratigraphic division. GTK Spec Pap, 60, 9-40.

Mount Sopris. 2013. Fluid Resistivity/ Temperature Probe Models: 2PFA-1000, 2SFA-1000, 2SFB-1000, 2WQA-1000, 2WQB-1000, 2WQC-1000. Mount Sopris Instrument Co., Inc. Denver CO, U. S. A.

Niva, B. 1989. Geophysical borehole logging at Olkiluoto borehole OL-KR1. TVO/Paikkatutkimukset, Working-report 89-58, 13 pp.

Nordbäck, N. and Mattila, J. 2018. Brittle Fault System of the ONKALO Underground Research Facility. Posiva Oy, Working-report 2018-20, Eurajoki, Finland. 130 pp.

Okko, O., Front, K., Hassinen, P. and Vaittinen, T. 1990. Geofysikaalisten reikämittausten tulkinta Olkiluodon kairanreiät KR1, KR2 ja KR3. TVO/Paikkatutkimukset, Working-report 90-08, 98 pp.

Palomäki, J. and Ristimäki, L. 2013. Facility Description 2012 Summary Report of the Encapsulation Plant and Disposal Facility Designs. Posiva Oy, Working-report 2012-66, 142 pp.

Paulamäki, S., Paananen, M. and Elo, S. 2002. Structure and geological evolution of the bedrock of southern Satakunta, SW Finland. Posiva Oy, POSIVA 2002-04, Eurajoki, Finland. 128 pp.

Pollack, H., Hurter, S. and Johnson, J. 1993. Heat flow from the Earth's interior: analysis of the global data set. Reviews of Geophysics, 31(3), 267-280.

Posiva 2019a. Selecting the Site: The Final Disposal at Olkiluoto. Web page visited 21.5.2019 http://www.posiva.fi/loppusijoitus/paikanvalinta_olkiluoto

Posiva 2019b. Kuvapankki. Web page visited 21.5.2019 http://www.posiva.fi/media/kuvapankki

Posiva 2020. Rock mechanics of Olkiluoto. Posiva Oy, POSIVA-report 2020-xx, in press.

Pöllänen, J. and Rouhiainen, P. 2001. Difference flow and electric conductivity measurements at the Olkiluto site in Eurajoki, boreholes KR6, KR7 and KR12. Posiva Oy, Working-report 2000-51, 156 pp.

Schärli, U. and Rybach, L. 2001. Determination of specific heat capacity on rock fragments. Geothermics, 30(1), 93-110.

Schön, J. 2015a. Chapter 4 - Density. Developments in Petroleum Science, 65, 109-118

Schön, J. 2015b. Chapter 9 - Thermal Properties. Developments in Petroleum Science, 65, 369-414

Sedighi, M., Bennet, D., Masum, S., Thomas, H. and Johansson, E. 2014. Analysis of Temperature Data at the Olkiluoto. Posiva Oy, Working-report 2013-58, 86 pp.

Somerton, W. 1992. Thermal properties and temperature-related behaviour of rock/fluid systems. Developments in petroleum science, 37. Amsterdam, Netherlands: Elsevier Science publishers B.V. 257 pp.

Suppala, I., Kukkonen, I. and Korpisalo, A. 2013. Thermal diffusivity of a rock mass estimated from drillhole temperature monitoring in the ONKALO. Posiva Oy, Working-report 2013-35, Eurajoki, Finland. 50 pp.

Tarvainen, A-M. 2007. Geophysical Drillhole Logging of the Drillholes OL-KR40, OL-KR41, OL-KR41B, OL-KR42, OL-KR42B, OL-KR43 and OL-KR43B at Olkiluoto 2006 and 2007. Posiva Oy, Working-report 2007-38, 47 pp.

Tro, N. 2013, Chemistry: Pearson New International Edition, Pearson Education UK, Welwyn Garden City. Available from: ProQuest Ebook Central. [18 September 2019].

Ydinenergialaki 11.12.1987/990, 1987.

Öhberg, A. and Rouhiainen, P. 2000. Posiva Groundwater flow Measuring Techniques. Posiva Oy, POSIVA-report 2000-12 Eurajoki, Finland. 87 pp.

APPENDICES

1. WellCAD measured depth / temperature plots
2. WellCAD true vertical depth / temperature plots
3. Data classification for PFL measurements
4. Data classification for geophysical multiparameter drillhole loggings
5. Data classification for TERO and Antares measurements